Investigation into the source and variability of salinity in the Milk River, Alberta

In response to the winter limit exceedances under the South Saskatchewan Region-Surface Water Quality Management Framework

Alberta

Investigation into the source and variability of salinity in the Milk River, Alberta

In response to the winter limit exceedances under the South Saskatchewan Region-Surface Water Quality Management Framework

Brian Gaas and Natalie Kromrey

This publication can be found at: https://open.alberta.ca/publications/9781460151358

Comments or questions regarding the content of this document may be directed to:

Alberta Environment and Parks
Resource Stewardship Division
Air & Watershed Resource Management Branch
Email: aep.airshedws@gov.ab.ca

Recommended citation:

Gaas, B. and Kromrey, N. 2021 Investigation into the Source and Variability of Salinity in the Milk River, Alberta. In Response to the Winter Limit Exceedances Under the South Saskatchewan Region-Surface Water Quality Management Framework. Government of Alberta, Ministry of Environment and Parks. ISBN **978-1-4601-5135-8** Available at: https://open.alberta.ca/publications/9781460151358.

© 2021 Government of Alberta | August 24, 2021 | ISBN **978-1-4601-5135-8**

EXECUTIVE SUMMARY

Monthly measurements of water quality in the Milk River at the Hwy 880 bridge site revealed seasonal medians that exceeded the South Saskatchewan Region - Surface Water Quality Management Framework (SSR SWQMF) limit for total dissolved solids (TDS) in the winter (November to March) in 2015/2016, 2016/2017, 2017/2018 and 2018/2019 as well as specific conductance in the winter in 2017/2018 and 2018/2019. As a management response, an investigation was initiated that focused on three questions:

- Why do the SSR SWQMF exceedances for TDS in the Milk River at Hwy 880 only occur in the winter (November to March)?
- What is the primary source(s) of TDS to the Milk River during the winter?
- What are the main processes controlling variability in TDS concentrations during the winter?

The investigation consisted of an extensive literature review and data analysis on surface water and groundwater quality of the Milk River and surroundings. The results of the investigation suggest the following:

- Often water with a high dissolved ion concentration can have both high specific conductance and high TDS concentration, and the two measurements could be used interchangeably. Milk River samples for specific conductance and TDS concentrations were strongly, positively, and linearly correlated ($r^2=0.99$; $p<0.01$), for that reason the main focus was on TDS as a means to investigate both.

- Seasonal variability (open water versus winter) was primarily controlled by the input of relatively dilute water from the St. Mary River into the Milk River. During the open water season when diversion from the St. Mary River was active, TDS concentrations and composition matched the St. Mary River. In the winter, when the St. Mary River did not contribute to the Milk River flow, TDS concentrations and composition changed to reflect a different (high TDS) source.

- Framework exceedances in the Milk River did not occur in the open water season because the St. Mary River, which made up 94% of the North Milk River flow during the open water season, has relatively low TDS concentrations.

- A primary source of TDS to the Milk River in the winter was likely from groundwater input. This is suggested from: increasing downstream flows with no identified surface water input, a match between nearby groundwater chemistry with Milk River chemistry during the winter, the alignment of these results with previously established literature regarding the interaction of groundwater and the Milk River, and evidence of surface expressions of groundwater behavior (such as springs and soil piping).

- Trend analyses did not indicate a change over time in TDS or specific conductance since the framework was developed.

- Although data were generally not available to evaluate specific sources, road salt application, discharge from the town of Milk River, and petroleum/natural gas extraction did not appear to be major contributors to the TDS concentration in the Milk River.

- The range of variability in winter TDS concentrations in the Milk River was similar at both monthly and weekly scales. High resolution measures of specific conductance indicated that changes in salt concentration were related to changes in the volume of ice through the exclusion of salt ions.

The viability of salt exclusion controlling winter concentrations of TDS in the Milk River was confirmed using a physics-based ice volume model.

Data were generally not available to exclude specific human activities from impacting the surface water quality. However, with the exception of the influence of the St. Mary River diversion, the investigation did not find evidence of anthropogenic impacts on the concentration or variability of TDS concentrations. The cause of the framework exceedances could be explained through a combination of the seasonal diversion of the St. Mary River and natural processes (e.g., salt exclusion). Recommendations are provided for assessing the risk to aquatic life and other water uses, adjusting the SSR SWQMF to account for the timing of the influence of the St. Mary diversion, continuing regular time-series assessments, and identifying management actions to maintain or improve salinity in the Milk River.

TABLE OF CONTENTS

EXECUTIVE SUMMARY ii

TABLE OF CONTENTS v

LIST OF FIGURES vii

LIST OF TABLES ix

1 Introduction 1

1.1 The Surface Water Quality Management Framework and Report Objectives 1

1.2 Milk River Basin 1

1.3 Milk River Aquifer 5

1.4 Total Dissolved Solids 6

2 Methods 9

2.1 Data Compilation and Visualization 9

2.1.1 Surface Water Quality 9

2.1.2 Surface Water Flow 9

2.1.3 Groundwater Quality 11

2.1.4 Meteorology 11

2.2 Data Analysis 11

2.2.1 Specific Conductance to TDS Conversion 11

2.2.2 Trend Analysis 12

2.2.3 Geochemistry 12

2.2.4 Water Balance 13

2.2.5 Mixing Model 13

2.2.6 Ice Growth Model 14

3 Results 15

3.1 Trend Results 15

3.2 Investigation Question #1: Why do the Surface Water Quality Management Framework exceedances for total dissolved solids in the Milk River at Hwy 880 only occur in the winter (November to March)? 17

3.2.1 Results 17

3.2.2 Discussion 26

3.2.3 Question #1 Conclusion: 27

3.3 Investigation Question #2: What is the primary source(s) of total dissolved solids to the Milk River during the winter? 28

3.3.1 Results 28

3.3.2 Discussion 41

3.3.3 Question #2 Conclusion: 46

3.4 Investigation Question #3: What are the main processes controlling variability in total dissolved solids concentrations during the winter? 46

3.4.1 Results 46
3.4.2 Discussion 52
3.4.3 Question #3 Conclusion: 53
4 Overall Conclusions 54
5 Recommendations 55
6 References 56
6.1 Literature 56
6.2 Software 60
6.3 Websites 60
Appendix A 61
Ancillary information for Investigation Question #1: 61
Appendix B 68
Ancillary information for Investigation Question #2: 68
Appendix C 86
Ancillary information for Investigation Question #3: 86
Appendix D 90
Ice Volume Model 90
Appendix E 94
Ice Volume Model R Code 94
Appendix F 98
Appendix F-1 (Excel file): Raw datasonde and meteorology data 98
Appendix F-2 (Excel file): Raw flow rates 98
Appendix F-3 (Excel file): Raw groundwater well depths 98
Appendix F-4 (Excel file): Raw Milk River area water quality (AEP) 98
Appendix F-5 (Excel file): Raw Milk River water quality (AAF) 98
Appendix F-6 (Excel file): Raw St. Mary River water quality 98

LIST OF FIGURES

Figure 1: Google Earth image of the Milk River, focused on Alberta. 4
Figure 2: Google Earth image with the approximate boundaries of Milk River Aquifer 6
Figure 3: Processes identified in the literature review that can contribute to the magnitude or variation in total dissolved solids concentrations. 7
Figure 4: Google Earth image of station locations 10
Figure 5: Relationship between observed specific conductance (measured in the laboratory) and observed total dissolved solids concentrations for monthly samples (open water and winter) in the Milk River at Hwy 880. 12
Figure 6: Median concentrations of monthly total dissolved solids in the Milk River, as measured at the Highway 880 bridge. 17
Figure 7: Median monthly total dissolved solids concentrations in the Milk River, measured at Hwy 880, 2011-2016. 18
Figure 8: Median surface water flow (from daily averages; Environment Canada hydrometric station EC 11AA005) and total dissolved solids concentrations (monthly) from the Milk River at the town of Milk River, 2011-2016. 19
Figure 9: Median total dissolved solids concentrations (monthly) and corresponding flow rate (daily average; Environment Canada hydrometric station EC 11AA005) from the Milk River at the town of Milk River, 2011-2016. 20
Figure 10: Median monthly total dissolved solids in the St. Mary and Milk rivers, 2011-2016. 21
Figure 11: Piper plot of monthly surface water samples from the St. Mary River (at Cardston, AB) and the Milk River (at Hwy 880), 2011-2016. 22
Figure 12: Ion ratio versus total dissolved solids concentration for the St. Mary River. 23
Figure 13: Monthly total dissolved solids concentration versus flow rate in the St. Mary River between 2011-2016. 24
Figure 14: Monthly total dissolved solids concentration versus flow rate in the Milk River between 2011-2016. 25
Figure 15: Molar ion ratio versus total dissolved solids concentration for the Milk River. Monthly measurements at Hwy 880 between 2011-2016. 26
Figure 16: Flow balance (outflow at Milk River minus inflow from North Fork and South Fork) for the winter season.. 28
Figure 17: Flow balance and flow in the North Fork (station EC 11AA001) in the winter, 1931-2017. 29
Figure 18: Flow balance and flow in the South Fork (station EC 11AA025) in the winter, 1931-2017. 30
Figure 19: Flow balance and flow in the Milk River at the town of Milk River (station EC 11AA005) in the winter, 1931-2017. 31
Figure 20: Snow pack versus flow balance, winter 2013 to 2017. 32
Figure 21: Pearson cross-correlation of snow melt and the Milk River flow balance (outflow minus inflow). 33
Figure 22: Piper plot for surface waters collected during the winter at the Hwy 880 bridge. 36
Figure 23: Piper plot of groundwater chemistry from the Groundwater Observation Well Network (GOWN). 38
Figure 24: Piper plot of groundwater chemistry from the Groundwater Observation Well Network (GOWN). 39
Figure 25: Annual seasonal median differences in well water depth. 40
Figure 26: Annual range of winter total dissolved solids concentration (maximum monthly TDS- minimum monthly TDS); 2004-2017 from the Milk River at Hwy 880. 47
Figure 27: Absolute value of the difference in total dissolved solids concentrations between subsequent winter months, Milk River at Hwy 880, 2003-2017.. 48
Figure 28: Ten days of data used to test the hypothesis that salt exclusion affects TDS concentrations.. 49

Figure 29: Relationship between air temperature (measured at the town of Milk River) and total dissolved solids concentration (measured as specific conductance in the Milk River by a datasonde at the Hwy 880 bridge). 50
Figure 30: Observed (A) and modeled (B) water temperature at the Hwy 880 bridge, January 2 through 11, 2012. 51
Figure 31: Observed (A) and modeled (B) total dissolved solids concentrations from a datasonde at the Hwy 880 bridge, January 2 through 11, 2012. 51
Figure 32: Observed and modeled total dissolved solids concentrations from a datasonde at the Hwy 880 bridge, January 2-11, 2012. 52
Figure A-1: Total dissolved solids concentrations observed in the Milk River at the Hwy 880 sampling station. 61
Figure A-2: Milk River flow rates and total dissolved solids (TDS) concentrations measured in 2010. 62
Figure A-3: Milk River flow rates and total dissolved solids (TDS) concentrations measured in 2011. 63
Figure A-4: Milk River flow rates and total dissolved solids (TDS) concentrations measured in 2014. 64
Figure A-5: Flow rates of the North Milk River (North Fork) from Environment Canada hydrometric station EC 11AA001, “North Milk Near Boundary.” 65
Figure A-6: Flow rates of the Milk River (South Fork) from Environment Canada hydrometric station EC 11AA025, “Milk River at West Crossing.” 66
Figure A-7: Flow rates of the Milk River from Environment Canada hydrometric station EC 11AA005, “Milk River at Milk River.” 67
Figure B-1: Milk River flow rates measured at the town of Milk River in 2012. 68
Figure B-2: Upstream to downstream changes in major ion content. 74
Figure B-3: Ratio of alkalinity (carbonates) to silica (clay) for winter samples taken at Hwy 880. 75
Figure B-4: Ratio of alkalinity (carbonates) to (SO_4 + Cl) for monthly winter samples taken at Hwy 880. 76
Figure B-5: Ratio of (Ca + Mg) to alkalinity (carbonates) for monthly winter samples taken at Hwy 880. 77
Figure B-6: Ratio of calcium to magnesium for monthly winter samples taken at Hwy 880. 78
Figure B-7: Ratio of calcium to sulphate for monthly winter samples taken at Hwy 880. 79
Figure B-8: Ratio of sodium to chloride for monthly winter samples taken at Hwy 880. 80
Figure B-9: Ratio of (Na - Cl) to silicate for monthly winter samples taken at Hwy 880. 81
Figure B-10: Ratio of (Na - Cl) to sulphate for monthly winter samples taken at Hwy 880. 82
Figure B-11: Ion exchange plot. 83
Figure B-12: Change in proportion of calcium with changes in non-halite sodium (Na - Cl). 84
Figure B-13: Change in proportion of sulphate with changes in non-halite sodium (Na - Cl). 85
Figure C-1: Datasonde time-series from Writing-on-Stone Provincial Park, from December 14, 2010 to March 11, 2011. 86
Figure C-2: Datasonde time-series from Hwy 880, from December 18, 2008 to February 24, 2009. 87
Figure C-3: Datasonde time-series from Hwy 880, from December 13, 2011 to January 20, 2012. 88
Figure C-4: Datasonde time-series from Hwy 880, from January 24, 2012 to February 16, 2012. 89

LIST OF TABLES

Table 1: Status of trend assessments for TDS and specific conductance in the Milk River at Hwy 880. ..16
Table 2: Ion chemistry and mixing model results for the North Fork, South Fork, and Milk River mainstem. 34
Table 3: Results of the mass balance calculation. 41
Table A-1: Dates when the St. Mary River diversion was active. 61
Table B-1: Mineral saturation index (SI) for calcite and gypsum for monthly water samples taken during the winter at the Hwy 880 bridge, 1986-1988 and 2003-2017. 80
Table B-2: Properties of the Groundwater Observation Well Network (GOWN) sites near the Milk River. 85
Table B-3: Major ion chemistry for GOWN Well #101. 85

Acknowledgements

This document was made possible by the joint effort of many people. Thanks go out to the Alberta Environment and Parks (AEP) field staff (Ray Walker, Rachel Morse, Jon Pedlar, Kate Forbes, Salina Perry, Mark Potvin, Ryan Martin, Meghan Anderson, Tori Slobodzian, Dennis Rollag, Jim Zettel, Jay Parsons, James Rogans, Joanna Borecki and Scott Campbell) for collecting the Milk River and St. Mary River water quality samples. Additional data were collected by the field crews of the AEP Groundwater Well Observation Network and Alberta Agriculture and Forestry (AAF). The Milk River Watershed Council Canada (MRWCC) shared Milk watershed water quality data they had collected and AAF also granted access to data they collected on Milk River water quality. Tim Romanow, Mary Lupwayi, and Kandra Forbes (MRWCC), Cecilia Chung, Wendell Koning (AEP), and the residents of the Milk River basin provided useful insight and hospitality during the site visit. This document was improved by the thoughtful comments of the Water Quality Management Framework-Milk River Investigation Science Team, comprised of AEP (Dr. Jason Kerr, Dr. Cynthia Mcclain, Muhammed Sabur, Jeff Gutsell, Wendell Koning, Brian Hills, Emily Taylor, Rob Simieritsch and the authors), Alberta Energy Regulator (Chris Teichreb), AAF (Janelle Villenueve, Evan Hillman) and the MRWCC (Tim Romanow).

Abbreviations

≈: approximately

°C: degrees Celsius

<, >: less than, greater than

%: percent

↔: reversible chemical reaction

AAF: Alberta Agriculture and Forestry

AEP: Alberta Environment and Parks

AER: Alberta Energy Regulator

Ca: calcium

Cl: chloride

CO_3: carbonate

EC: Environment Canada

ESRD: Alberta Environment and Sustainable Resource Development (predecessor to Alberta Environment and Parks)

F: fluoride

GOWN: Groundwater Observation Well Network

HCO_3: bicarbonate

H_2O: water

K: potassium

km, km^2: kilometer, square kilometer

K_{sp}: solubility constant

m: metre

m/s, m^3/s: metres per second, cubic metres per second

m^3/yr: cubic metres per year

Mg: magnesium

mg/L: milligrams per litre

MRWCC: Milk River Watershed Council Canada

n: sample size

Na: sodium

p: probability

r^2: coefficient of determination

SI: saturation index

SO_4: sulphate

SWQMF: Surface Water Quality Management Framework

(t), (t+1): current time step of model, next time step in model

TDS: total dissolved solids

µS/cm: microsiemens per centimetre

USGS: United States Geological Survey

W m^{-2}: watts per square metre

1 Introduction

1.1 The Surface Water Quality Management Framework and Report Objectives

The South Saskatchewan Region - Surface Water Quality Management Framework (SSR SWQMF; AESRD 2014) is one of the environmental management frameworks developed under the South Saskatchewan Regional Plan (SSRP; GOA 2017) and came into effect September 2014. The plan was developed by the Government of Alberta (GOA) under the Land-use Framework (LUF; GOA 2008) and is given legislated authority under the *Alberta Land Stewardship Act* (ALSA; Statutes of Alberta 2009). The SSR SWQMF focuses on the mainstem Bow, Milk, Oldman and South Saskatchewan rivers and Alberta Environment and Parks (AEP) is the lead department. The framework includes a set of 15 primary and 6 secondary parameters which are evaluated as indicators each year against seasonal triggers (statistically derived using historical data) and limits (derived from published water quality guidelines) to determine whether a change in water quality is occurring toward a less desirable state (triggers) and if water uses are being protected (limits).

Water quality parameters are monitored monthly at nine Long-term River Network (LTRN) monitoring sites and are evaluated each year against the triggers and limits for each indicator at each site in both the open water (April- October) and winter (November- March) seasons. A full description of the process is provided in the SSR SWQMF (AESRD 2014). Briefly, a trigger is exceeded if data are statistically significantly different (in an undesirable direction) from their historical data and a limit is exceeded if a median surpasses its limit. A management response is required if a trigger or limit is exceeded at a site and an investigation is required if a limit is exceeded at a site. In the Milk River at the Hwy 880 site (Figure 1), the results of the assessments for total dissolved solids (TDS) in 2015/2016, 2016/2017, 2017/2018 and 2018/2019 and specific conductance in 2017/2018 and 2018/2019 revealed the winter median values exceeded their limits (Kerr et al. 2018a; Kerr et al. 2018b; Chung et al. 2019; Taube and Kerr 2020).

As a result of the limit exceedances, AEP initiated a scientific investigation to understand the behavior of TDS and specific conductance in the Milk River. The goal of this investigation was to determine whether anthropogenic activities were responsible for the exceedances, and whether it was appropriate to identify management actions to mitigate environmental impacts. The investigation focused on three questions:

1) Why do the SWQMF exceedances for TDS in the Milk River at Hwy 880 only occur in the winter (November to March)?

2) What is the primary source(s) of TDS to the Milk River during the winter?

3) What are the main processes controlling variability in TDS concentrations during the winter? This question addresses why winter exceedances are observed in some years and not others.

Answers to these questions will inform recommendations for management actions (if any) and adjustments to the management framework to ensure its process is achieving the intended outcome.

1.2 Milk River Basin

The headwaters of the Milk River are in Montana (United States), originating from springs at the toe slopes of Glacier National Park, north of Two Medicine drainage. The headwaters flow northward and cross the Canadian border in two places, the North Fork and South Fork of the Milk River, and make the larger Milk River after their confluence (Figure 1). The South Fork is also called the Milk River or the South Milk River, and the North Fork is sometimes identified as the North Milk River. In this report, “North

Fork" and "South Fork" will be used to identify the portions of the Milk River upstream of the confluence of these two watercourses, and "Milk River" for the portion downstream of the confluence and/or the river as a whole. The South Fork of the Milk River gains volume from two tributaries (Dry, and Middle Fork) before crossing into Alberta, Canada (east of Del Bonita on the Twin River Provincial Grazing Reserve). The North Fork of the Milk River originates on the Blackfeet Indian Reservation; it receives augmented flow through an interbasin transfer from the St Mary River drainage. This United States Bureau of Reclamation (USBR) Milk River project starts with the Sherburne Reservoir, on Swift Current Creek above the St Mary River, and diverts water from the Lower St. Mary Lake and St. Mary River near Babb, Montana over the continental divide and into the North Milk River. A number of engineering structures (dams, canals, siphons and drop structures) create this St. Mary diversion system, which diverts the water every year into the North Milk River during the summer months (April-September) under the apportionment of the 1909 Boundary Waters Treaty. After crossing into Alberta, the Milk River flows around 200 km to the east before crossing eastern Alberta's Canada-USA border back into Montana and entering the Fresno Reservoir near Havre, Montana. The Milk River continues to flow southeast (710 km) until it eventually joins the Missouri River. Extensive background information about the Milk River and its geography is available in the Milk River Transboundary State of the Watershed (MRWCC 2013).

The Milk River basin is covered by glacial sediment deposited during the Laurentide glaciation event (Beaney 2002). Although most of the surficial geology is ice moraine, the area around the Milk River also includes preglacial fluvial deposits, glaciolacustrine deposits, and glacial moraines (Pétré and Rivera 2015). Glaciation altered the flow path of the ancestral Milk River, which originally flowed to the northeast into the South Saskatchewan River but currently flows south into the Missouri/Mississippi River system (Beaty 1990; Beaney 2002). Restricted inflow to the old South Saskatchewan drainage system resulted in a limited period where most of the surface waters in southern Alberta fed into the Milk River, creating a much wider river valley than would be expected for the current size of the Milk River (Beaty 1990).

Most of the soils in the Milk River basin are Chernozemic or Solonetzic (MRWCC 2013), and have high exchangeable sodium content (Miller and Brierley 2011). Saline seepage from groundwater reaching the surface is the primary source of soil salinization. Poor drainage, snow accumulation, overwatering, and crop fallowing can create higher water tables and enhance seepage, increasing the risk of salinization (Salama 1999). Soil salinity in southern Alberta was linked with the clay content of the soil (Chang et al. 1985), and also with surface topography (Florinsky et al. 2000). Irrigation did not significantly affect the salinity of Solonetzic soils in southern Alberta beyond what could be attributed directly to the quantity and quality of the irrigation water (Bennett and Entz 1990; Bennett et al. 2000). However, a study by Kerr (2017) in the South Saskatchewan River basin (also in southern Alberta) found that the proportion of salt-affected soil in a watershed can increase the salt concentration and change the salt content in surface runoff.

The Milk River basin experiences chinooks, episodic periods of above freezing air temperatures, that occur multiple times during winter. During chinooks, large snow packs can melt over the period of a few days. Winter flow in many of the Milk River tributaries is limited to these melting periods, thereby linking changes in tributary flow rates to changes in the snowpack in the tributary catchment areas.

The St. Mary River in Alberta also originates in Montana and flows northward, passing to the west of the Milk River. During irrigation season (approximately April to September), natural flow in the Milk River is augmented by water diverted from the St. Mary River. The St. Mary River diversion canal combines with the North Fork of the Milk River, and greatly enhances flow rates along the Milk River. The additional water from the St. Mary diversion increases flow in the Milk River by approximately 20 times, from 2-10 m^3/s to near 20 m^3/s (Maclean and Beckstead 1985). The diversion of the St. Mary River into the Milk River occurs south of the border between Alberta and Montana (see Figure 1). Flow in the South Fork is unaffected by the St. Mary diversion. Flow rates in the St. Mary River diversion canal, and hence those of the Milk River, are controlled by the United States. Flow apportionment of the Milk River between Canada

and the United States is legislated by the Boundary Waters Treaty of 1909 and subsequent clarification in the 1921 Order of the International Joint Commission.

The flow added to the Milk River from the St. Mary River diversion led to a large increase in the channel width of the Milk River (AMEC 2008). Bank erosion is especially prevalent in the sand reach of the Milk River, which starts near Writing-on-Stone Provincial Park and extends downstream (east) to the Alberta-Montana border. Erosion is still present, but reduced, in the upstream gravel bed reach. Erosion rates range from 0.2 m to over 1 m per year (AMEC 2008), with erodability perhaps related to the percent silt-clay in the streambank (Simpson and Smith 2001). Localized erosion of the river valley, especially in the eastern badlands section, contributes to a high suspended sediment load (Ashmore 1993; AMEC 2008). Milk River sediments include bentonite (smectite) clays, which have high ion exchange capacities for calcium, magnesium, and sodium (Armstrong et al. 1998). Ion exchange with these bentonite clays were associated with changes in groundwater chemistry, especially after a long contact time (Armstrong et al. 1998).

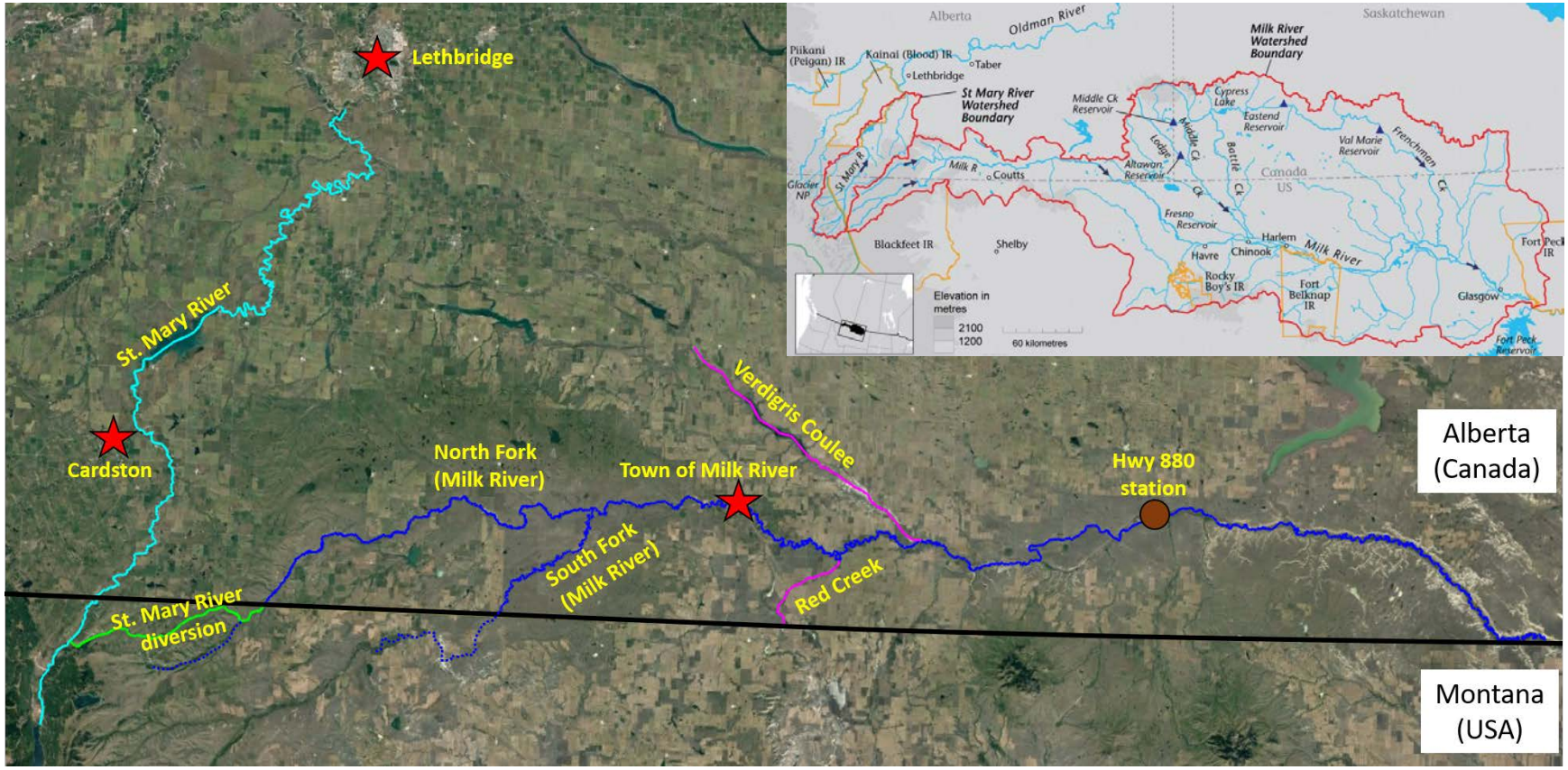

Figure 1: Google Earth image of the Milk River, focused on Alberta. The Milk River consists of the North Fork, South Fork, and mainstem (dark blue solid lines). The river enters Alberta from Montana in the west (dark blue dotted lines; full extent not shown). Also indicated is the St. Mary River (light blue line), the St. Mary diversion into the Milk River (green line), and municipalities (red stars). The long-term water quality monitoring station for the Milk River (brown circle) is located at the Hwy 880 bridge; the station is operated by Alberta Environment and Parks. Inset – location of the Milk River within Canada (Alberta and Saskatchewan) and the United States (Montana).

1.3 Milk River Aquifer

An aquifer is a natural geologic unit that can store and transmit water in sufficient quantities to be economical. It acts as an underground reservoir that can contain substantial amounts of groundwater. The groundwater resides in the spaces (pores) between rock particles, or in larger spaces like cracks or voids. Where there are pressure differences that result in varying water levels across the aquifer, a gradient is created. If a gradient is present, and the rock particles have enough open pore space between the soil or rock particles, and the pores are interconnected with each other, groundwater can move through these spaces. Confined aquifers are aquifers that are bounded on the top and bottom by less permeable layers of soil (e.g., clay) or rock material. The water in this type of aquifer is under pressure and will rise above the top of the aquifer if a well is drilled into this unit. In contrast, unconfined (water table) aquifers have high permeability materials that extend to the ground surface and interact with the atmosphere.

Extensive research has been done on the Milk River Aquifer starting in the 1960s (Schwartz and Muehlenbachs 1979; Hendry et al. 1991). A comprehensive summary was created as part of the development of a unified aquifer model by Pétré and Rivera (2015), Pétré et al. (2016), Rivera et al. (2017), and the references therein.

The Milk River Aquifer is a confined sandstone aquifer that extends over both Canada and the United States (Figure 2). The surficial sediments overlying the bedrock formations are usually less than 25 m thick (Rivera et al. 2017). The Virgelle member of the underlying Milk River Formation is often considered to be the Milk River Aquifer (Pétré and Rivera 2015). Both the Sweet Grass Hills (south of the Milk River) and Cypress Hills (northeast of the Milk River) are areas of groundwater recharge. The Milk River Aquifer outcrops along the Milk River for approximately 70 km between the town of Milk River and the Hwy 880 sampling station.

The Milk River Aquifer flows radially from recharge areas in the Sweet Grass Hills and north of Cut Bank. Stable isotope mapping suggests a travel time of ≈14,000 years from the Sweetgrass Hills recharge area north to the Milk River, and a minimum flow rate of 1-1.5 m per year (Drimmie et al. 1991). This matches the estimated flow rate provided by Golder (2004). The Milk River Aquifer extends past the north side of the Milk River, though groundwater flows and ages in the north are an order of magnitude slower and older than on the south side (Drimmie et al. 1991; Hendry et al. 1991).

The Milk River intersects the Belly River Group/Judith River Formation, an aquifer that lies above the Milk River Aquifer, near the North Fork. The river also intersects the Milk River Aquifer near Hwy 880, and may be incised into the Pakowki formation in the eastern side of the study area (Pétré et al. 2016; Rivera et al. 2017). The Milk River Aquifer partially discharges into the Milk River (Drimmie et al. 1991; Hendry et al. 1991; Rivera et al. 2017), and up to 96% of the Milk River Aquifer flow may be intercepted by the Milk River (Pétré and Rivera 2015; Pétré et al. 2016; Rivera et al. 2017). The amount of water intercepted by the Milk River is estimated at 8.6 million m^3/yr, or 0.3 m^3/s (Rivera et al. 2017). Flow interception may be augmented by the Whiskey Valley Aquifer (Rivera et al. 2017), which lies under a small portion of the Milk River near the town of Milk River. There may also be an upward flow from the Milk River Aquifer into the Whiskey Valley Aquifer (Pétré et al. 2016). There is likely a connection between the Milk River Aquifer, the Whiskey Valley Aquifer, and the Milk River itself (Golder 2004). In addition, enhanced summer flows in the Milk River from the St. Mary River diversion recharges part of

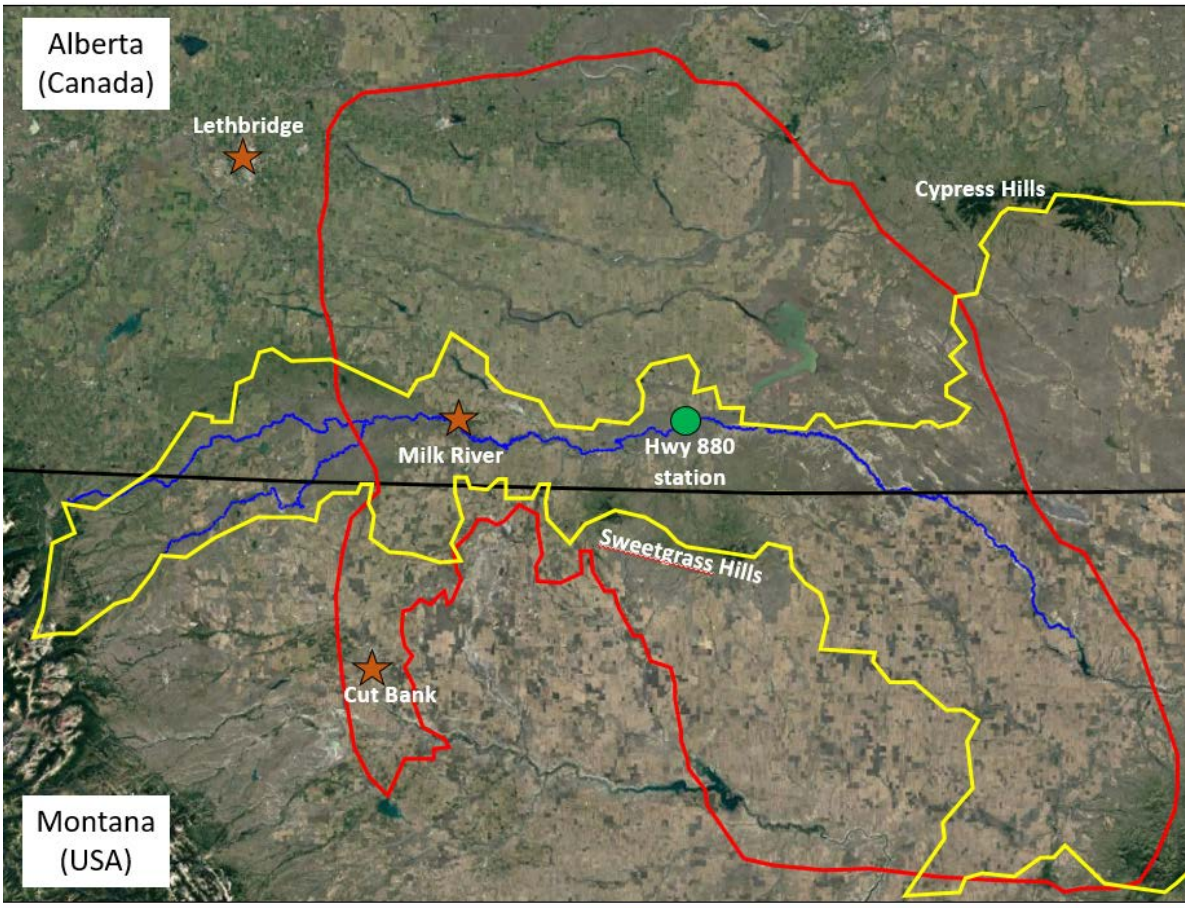

Figure 2: Google Earth image with the approximate boundaries of Milk River Aquifer (red line), associated area of the Milk River watershed (yellow), the Milk River (blue line), municipalities (orange stars), and the Hwy 880 water quality sampling station (green circle). The watershed continues to the east, and the Milk River continues to the southeast. The North Fork of the Milk River receives water from outside the watershed, from the St. Mary River diversion. Aquifer and watershed delineation from Pétré and Rivera (2015).

the surficial alluvium, which then discharges back into the Milk River in the winter when the diversion stops (Thompson 1986).

There are multiple surface expressions of groundwater influence in the Milk River basin. The southwest part of the Milk River Aquifer, near Cut Bank, has many artesian wells, springs, and seeps. The expansion and contraction of bentonite clays creates natural underground tunnels (soil piping) that transport large amounts of sediment to the floor of the Milk River valley (Barendregt and Ongley 1977). Extensive soil piping exists in the easily erodible bedrock in the eastern portion of the Milk River, which also contributes to the relatively large size of the Milk River valley compared to the size of the Milk River (Beaty 1990).

1.4 Total Dissolved Solids

Total dissolved solids is not a specific compound, but is defined methodologically. Total dissolved solids is the mass of salt that remains after water is filtered and dried (APHA 1999). The filtering step isolates the dissolved fraction, and the drying step removes water from the total mass.

Total dissolved solids concentrations are often estimated using specific conductance. In general, water with a high dissolved ion concentration will have both a high TDS concentration and high specific conductance. In many waters, the specific conductance is proportional to the concentration of TDS, and the two measurements can be used interchangeably. This report will mainly focus on TDS as a means to investigate both TDS and specific conductance winter limit exceedances of the SSR-SWQMF.

A literature review identified eight potential processes that could modify TDS concentrations in the Milk River during the winter (Figure 3): mainstem effects, ice scouring, groundwater flow, tributary effects, non-erosional overland flow, erosional overland flow, salt exclusion, and aerial deposition. Specific human activities are included in the list of processes based on how the TDS would enter the Milk River system. For instance, the direct discharge of TDS into the Milk River would be observed as a mainstem effect. Human activities are dealt with in this way because the information required to evaluate specific inputs (e.g., direct release of salts into the Milk River) were generally not available. Each of the eight processes were evaluated as a potential answer to the three investigation questions and are described in more detail here.

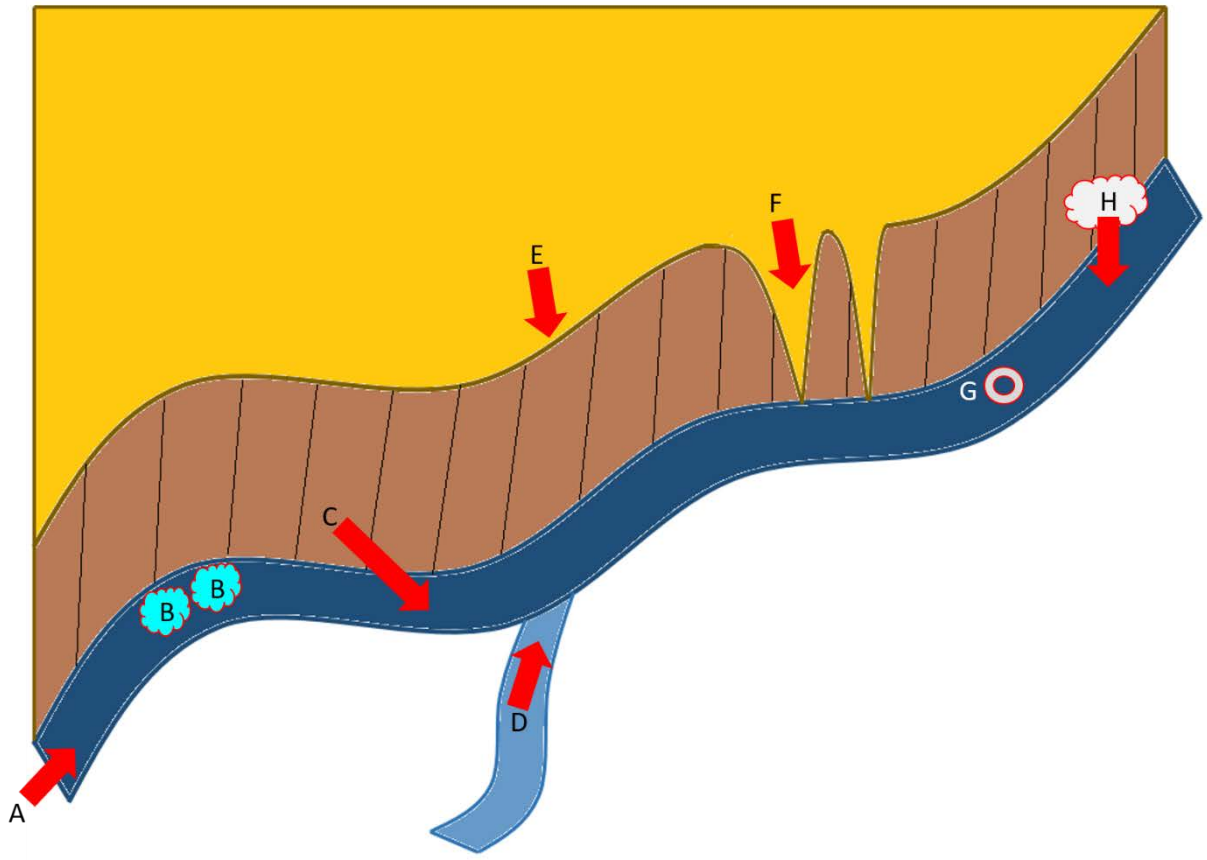

Figure 3: Processes identified in the literature review that can contribute to the magnitude or variation in total dissolved solids concentrations. A: mainstem effects; B: ice scouring; C: groundwater flow; D: tributary effects; E: non-erosional overland flow; F: erosional overland flow; G: salt exclusion; H: aerial deposition.

Mainstem effects (Figure 3, A) refers to processes driven by the transport of water from the North Fork/St. Mary River diversion, and/or the water from the South Fork. Concentrations of TDS downstream of the confluence of the two branches would be related to the proportional mixing of TDS from the two forks. Direct releases of TDS into the Milk River from human activities are also characterized as mainsteam effects.

Ice scouring (Figure 3, B) is the erosion of the streambank or streambed by chunks of ice. Ice jams are a regular occurrence in the Milk River, and a combination of local scouring, bank destabilization, and erosion could contribute to the load of total solids (Smith and Pearce 2002; AMEC 2008). The concentration of TDS would change depending whether ice is present, whether ice is moving, and the amount of ice. The impact of ice scouring on TDS would likely be episodic.

Groundwater flow (Figure 3, C) is the addition of TDS to the Milk River by groundwater. The groundwater could originate from infiltration of Milk River water into the alluvium during high river flow, which is subsequently released back into the Milk River when the river flow rates are low (Thompson 1986). It could also be from stored precipitation, subsurface water flowing through the glacial till that covers the Milk River area, or from either the Milk River or Whiskey Valley aquifers. The potential importance of groundwater to the Milk River is suggested by the presence of springs and through extensive soil piping in the streambanks. Changes in groundwater withdrawal could alter the quantity or source of groundwater entering the Milk River, leading to changes in surface water chemistry.

Tributary effects (Figure 3, D) are similar to mainstem effects, but with TDS loads originating from one or more of the tributaries to the Milk River. During the winter, many of the tributaries dry up and are usually considered a minor source of flow. However, TDS concentrations are often very high in the tributaries (MRWCC 2013), so even a small flow could contribute substantial amounts of TDS to the Milk River. Human activities occurring in the catchment areas of a tributary (e.g., road salting) are characterized in this report as tributary effects. Similarly, snowmelt and groundwater additions that add to tributary flow are considered tributary effects, as the effects would be identified in data originating from the tributary flow rates and water chemistry samples.

Non-erosional overland flow (Figure 3, E) involves the transport of TDS along the land surface. During chinooks, snowmelt could transport salts that accumulated on the surface during irrigation periods. They may also originate from water flowing through Solonetzic soils (Miller and Brierley 2011), or manure-fertilized fields (Hao and Chang 2003). Runoff of salts from road deicers is also documented (Kerr 2017). Significant TDS input from non-erosional overland flow would likely be episodic, potentially with the magnitude of the changes decreasing over the course of a single winter as the salt source was leached.

Erosional overland flow (Figure 3, F) could transport salts from the land surface. However, instead of transporting salts that were deposited on the surface (as a result of irrigation, or vertical transport from salty soils), the TDS load would come from the erosion of surficial sediment and soil. This process would also likely be episodic, occurring during chinooks when sufficient meltwater was available to provide erosional force.

Salt exclusion (Figure 3, G) is the concentration (increase) of salts in a volume of water after part of the volume has been frozen. The formation of ice “kicks out” salt ions, which concentrate in the unfrozen water. The process is similar to the concentration of salts from evaporation, except the removal of water occurs by ice formation.

Aerial deposition (Figure 3, H) is the direct addition of salts from the atmosphere through dust, rain, or snow to the water surface. This can be an important pathway for some ions, such as potassium, sulphate, and chloride (Grasby and Hutcheon 2000). Biomass burning or other sources of aerial emissions could increase the deposition rate of TDS. The surface area of the Milk River and its tributaries are relatively small, suggesting the effects of direct deposition would likely be minimal.

2 Methods

2.1 Data Compilation and Visualization

Multiple datasets were used and analysed to evaluate the eight processes potentially contributing TDS to the Milk River. The datasets included surface water quality, surface water quantity, groundwater quality, and meteorological data. The sources of the data are identified in parentheses, and sampling locations are presented in Figure 4.

2.1.1 Surface Water Quality

- Water quality grab sample data were manually collected from the safely wadeable portion of the streamflow as described in Alberta Environment (2006).
- Grab samples were collected at least monthly from March 1985 to June 1988, and April 2003 to December 2017 from the LTRN station Milk River at Hwy 880 (AEP).
- Additional grab samples were collected along the Milk River and tributaries (AEP; MRWCC). These data were collected inconsistently, and primarily from the open water season.
- Grab samples were collected monthly from 2011 to 2016 from the St. Mary River at Cardston, AB (AEP).
- Monthly grab samples were collected along a four location, downstream transect (stations MST_A through MST_D) of the Milk River between April and August 2012 (AAF). All samples were collected when diversion flow from the St. Mary River was active. A total of 14 analytes were measured: pH, electrical conductance, major ions (calcium, magnesium, sodium, potassium, sulphate, chloride, bicarbonate, carbonate), TDS, sodium adsorption ratio, total suspended solids, and total phosphorus.
- Six deployments of a datasonde (temperature, pH, dissolved oxygen, specific conductance) occurred in the Milk River (AEP). The deployments occurred at Writing on Stone Provincial Park (December 14, 2010 to March 11, 2011), at Hwy 880 during the open water season (July 16, 2008 to September 4, 2008; July 21, 2010 to September 16, 2010), and Hwy 880 during the winter (December 18, 2008 to February 24, 2009; December 13, 2011 to February 16, 2012 with a gap between January 20-24, 2012).

2.1.2 Surface Water Flow

- Daily flow rates of the North Fork in Alberta near the border (1909-2017), South Fork at west crossing (1931-2017), and the Milk River at the town of Milk River (1909-2017) were available (Environment Canada). Additional limited flow data were available from the Milk River near Writing-on-Stone Provincial Park, Milk River at Hwy 880, Red Creek, and Verdigris Coulee (Environment Canada).
- Daily flow rates were available at the head of the St. Mary canal in Montana (1918-2017)(Environment Canada)
- Daily flow rates of the St. Mary River were available at the international boundary (1902-2017)(Environment Canada)

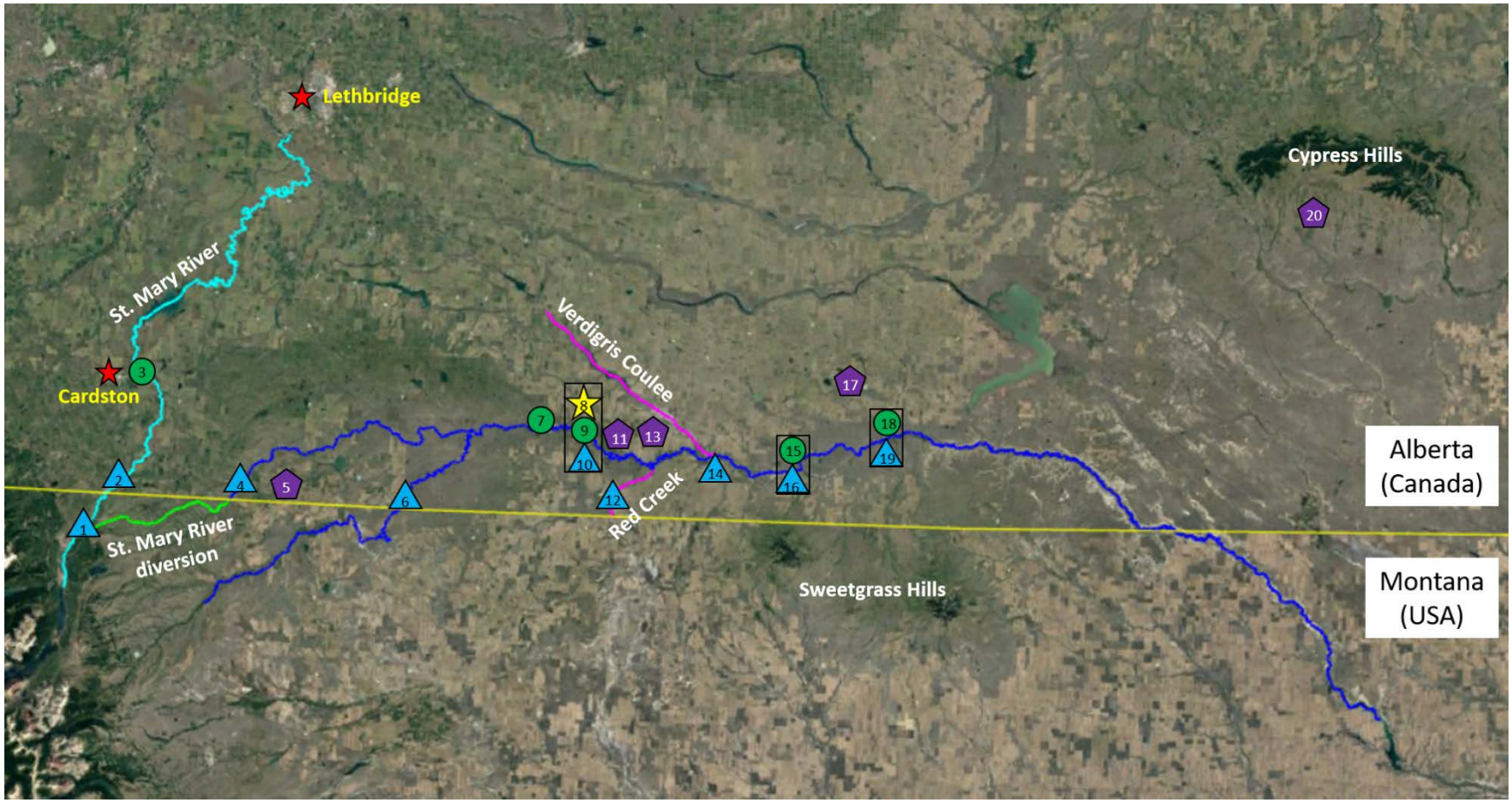

Figure 4: Google Earth image of station locations for water quantity (blue triangles), groundwater quality (purple pentagons), surface water quality (green circles), and meteorology (yellow star). Yellow line indicates the boundary between Canada (north) and United States (south); red stars indicate municipalities. AEP = Alberta Environment and Parks; AAF = Alberta Agriculture and Forestry; EC = Environment Canada; GOWN = Groundwater Observation Well Network. The sites are: 1 = St. Mary canal at St. Mary crossing (EC 05AE029); 2 = St. Mary River at international boundary (EC 05AE027); 3= St. Mary River at Cardston (AEP); 4 = North Milk River near international boundary (EC 11AA001); 5 = GOWN well #101; 6 = Milk River at western crossing of international boundary (EC 11AA025); 7 = MST_A (AAF); 8 = town of Milk River (AAF); 9 = MST_B (AAF); 10 = Milk River at Milk River (EC 11AA005); 11 = GOWN well #260; 12 = Red Creek at Hwy 4 (EC 11AA037); 13 = GOWN wells #103,212,213; 14 = Verdigris Coulee near the mouth (EC 11AA038); 15 = Writing-on-Stone Provincial Park (AEP) and MST_C (AAF); 16 = Milk River near Writing-on-Stone Provincial Park (EC 11AA034); 17 = GOWN well #211; 18 = Hwy 880 (AEP) and MST_D (AAF); 19 = Milk River at Hwy 880 (EC 11AA036); 20 = GOWN well #106.

There is no flow gauging station at the Hwy 880 bridge where the LTRN surface water quality monitoring samples are taken; the discontinued Environment Canada station at Hwy 880 measured water level instead. The closest upstream station on the Milk River with flow data available after 2002 (when monitoring for the SWQMF began) is at the town of Milk River, ≈100 km upstream of the Hwy 880 bridge. Flow rates between the town of Milk River and the Hwy 880 bridge are not necessarily expected to be equal: flow rates in the Milk River increased steadily downstream in the winter, though they were constant over much of the distance between the town of Milk River and Hwy 880 during the summer (MacCulloch and Wagner-Watchel 2010, 2011). Although the flow rates between locations may differ, the relative proportions of flow during the year are assumed to be similar; and, the hydrograph from the town of Milk River should be a good approximation of how flows change at Hwy 880 for the water balance and ice formation model described later. For trend analysis of TDS and specific conductance in the Milk River at Hwy 880, flow rates were modelled by AEP hydrologists using distance weighted and correlation methods (Linsley 1975; Capesius et al. 2009).

2.1.3 Groundwater Quality

- Three to five samples were taken at each of seven wells located near the Milk River, within the approximate horizontal boundary of the Milk River Aquifer (Groundwater Observation Well Network). The wells had variable depths and did not necessary penetrate the Milk River Aquifer. At each location, groundwater samples were taken in different years, and included both open water and winter seasons.
- Daily water depth at Well #101, Well #103, and Well #260 were measured from 1988-2001 (Groundwater Observation Well Network)

2.1.4 Meteorology

- Daily average air temperature, snow depth on ground, and radiance were measured at the town of Milk River (AAF)

Hydrology and meteorology data were accessed online; websites are presented in the References section. Figures and statistical tests (other than trends described in 2.2.2) were created using R (R Core Team 2018) and Microsoft Excel. Piper plots were generated using an Excel module created by the Nevada branch of the United States Geological Survey (Nevada Water Science Center).

2.2 Data Analysis

2.2.1 Specific Conductance to TDS Conversion

Specific conductance and TDS concentrations were strongly, positively, and linearly correlated (r^2=0.99; p<0.01) in Milk River samples taken monthly throughout the year (open water and winter) at the Hwy 880 bridge (Figure 5). The resulting regression equation was: TDS (mg/L) = 0.66(±0.004) * Specific conductance (uS/cm) - 25.6(±2.4). The slope of the regression increased slightly (3%) during the winter only and was marginally significant (*p*=0.046; n=229). For consistency, the regression equation using the entire dataset was used to convert specific conductance to TDS concentration.

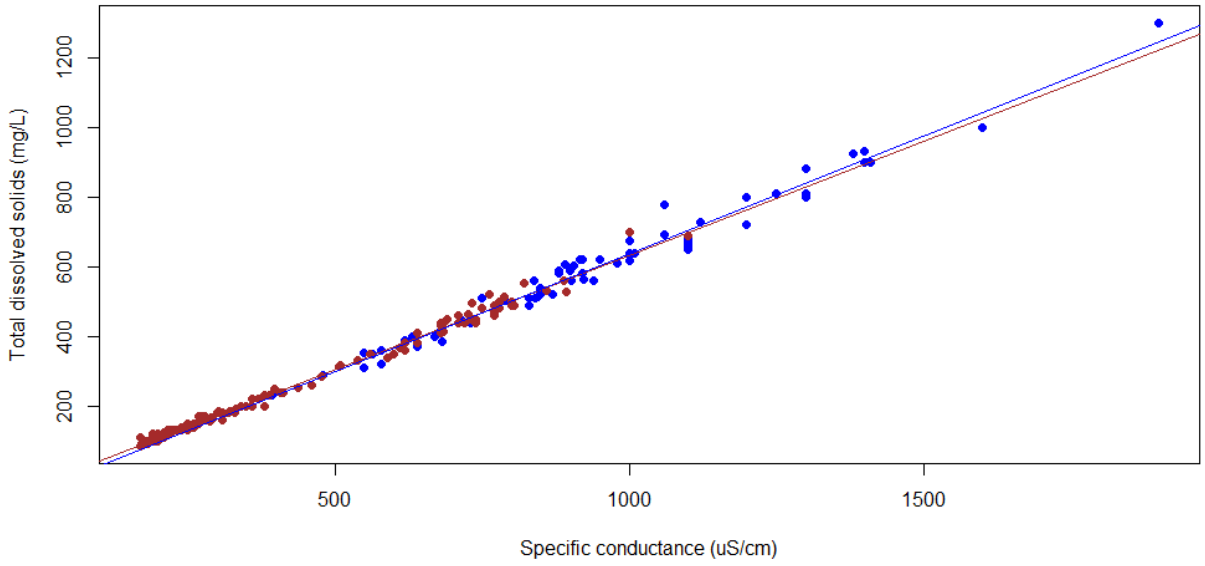

*Figure 5: Relationship between observed specific conductance (measured in the laboratory) and observed total dissolved solids concentrations for monthly samples (open water and winter) in the Milk River at Hwy 880. The overall relationship can be described as: TDS (mg/L) = 0.66(±0.004) * Specific conductance (µS/cm) - 25.6(± 2.4). r^2=0.99; p<0.01; n=229. Brown points are samples taken during the open water season (April to October); blue points were taken during the winter (November to March). Brown and blue lines indicate the season-specific regression lines for summer and winter data, respectively.*

2.2.2 Trend Analysis

Trend assessments were completed to determine whether TDS and specific conductance have changed over time and followed the approach outlined in HDR (2012) and Helsel and Hirsch (2002). Analyses were completed in the AEP HDR companion software and JMP® 15.1.0 (2019). Each year a limit was exceeded, trends were completed for three different time frames. The full dataset available (2003 to the year of limit exceedance) was explored to gain an understanding of long term status, the dataset of the last decade (10 years prior to the year of limit exceedance) was examined to understand recent conditions, and the post WQMF dataset (2009 to year of limit exceedance) was examined to understand conditions since the WQMF was developed. α = 0.05 for all these trend analyses. Results will help to direct the pace at which any management action recommendations may be developed and implemented.

2.2.3 Geochemistry

The relative concentrations and ratios of dissolved ions can provide important insights into the interactions between water sources, surficial geology, bedrock geology, and receiving waters like the Milk River. The major ion composition of the St. Mary River, Milk River, and groundwater wells were examined using Piper plots. Piper plots are standard ways of graphically displaying and comparing ion chemistry of different water samples (Hounslow 1995). The location of a sample (point) on the Piper plot creates a kind of geochemical “fingerprint.” If samples had a “fingerprint” similar to a particular TDS source, this would provide evidence that the two are related. In general, a line of points in the Piper plot indicates a mixing or exchange reaction, and a cluster of points occurs when the samples have the same composition.

Some of the samples had missing analyte concentrations. In the case where only one analyte was missing, the missing value was imputed using the charge balance: the sum of cation charges should

equal the sum of anion charges, and the residual was assigned to the missing analyte. Samples that were missing more than one analyte were excluded from analysis.

Potential source materials for the major ions in the Milk River were derived from specific ion ratios. The following ion ratios based on equivalents (moles of charge) were used to infer rock sources that could potentially contribute to the TDS load of the Milk River:

- Alkalinity to silica: differentiates between primarily carbonate versus silicate rocks (clays)
- Alkalinity to (SO_4 + Cl): differentiates between carbonates versus other minerals
- (Ca + Mg) to alkalinity: whether calcium and/or magnesium are primarily from carbonates
- Calcium to magnesium: whether most carbonates are calcium, magnesium, or both
- Calcium to sulphate: whether calcium and/or sulphate is likely to come from gypsum/anhydrite ($CaSO_4$)
- Sodium to chloride: whether sodium comes from halite (NaCl)
- (Na - Cl) to silicate: whether sodium comes from silicates

Mineral saturation indices were calculated for calcite and gypsum for monthly water samples taken during the winter at the Hwy 880 bridge, 1986-1988 and 2003-2017. Solubility constants, log(K_{sp}), were -8.4 and -4.6 for calcite and gypsum, respectively (Visconti et al. 2010).

2.2.4 Water Balance

A water balance was calculated to determine whether the North Fork and South Fork were the main contributors to the total water volume in the Milk River during the winter. Daily winter discharge rates from March 1931 to March 2017 were acquired for the “North Milk near international boundary” [North Fork] (station EC 11AA001), “Milk River at western crossing of international boundary” [South Fork] (EC 11AA025), and “Milk River at the town of Milk River” (EC 11AA005) Environment Canada hydrometric stations (Figure 4). The town of Milk River station was used instead of a further downstream station because the Milk River station had a substantially longer dataset than either the Writing-on-Stone Provincial Park or Hwy 880 stations.

A lagged Spearman rank correlation was run between the North Fork and Milk River flow sites, and between the South Fork and the Milk River flow sites to estimate the travel time between stations. The Milk River time-series (the downstream site) was lagged behind the North/South Fork time-series between zero and five days. The lag period with highest correlation was selected to correspond to the number of whole days it took for water to flow from the North or South Fork to the downstream Milk River station (Menke and Menke 2016).

The winter flow balance between the three stations was calculated as the outflow minus inflow:

Outflow: Milk River (lagged relative to the North Fork station)

Inflow: North Fork (no lag); South Fork (lagged relative to the North Fork station)

The flow balance may be affected by snow melt. Daily snow depth was measured by AAF at the town of Milk River from November 2012 to December 2017. Snowmelt was estimated as the change in snowpack depth between consecutive days. The potential for a delayed effect in snowmelt was explored using the cross-correlation function. A maximum of 60 days lag in both directions (snow melt lagging flow balance, and flow balance lagging snow melt) was tested, and the pattern between the change in snow depth and flow balance visually compared to ensure non-linearity was not decreasing the (Pearson) correlation of otherwise coherent data.

2.2.5 Mixing Model

A two-component mixing model was used to calculate the relative proportion of the North Fork and South Fork’s contributions to the total TDS in the Milk River. Water chemistry data came from the North Milk

River near the international boundary (North Fork), the Milk River at the western crossing of the international boundary (South Fork), the mainstem Milk River upstream of the town of Milk River, and the Milk River at Hwy 880. Data were available from each location on March 14, 2017. The direction of flow is from the North and South forks of the Milk River, to the station upstream of the town of Milk River, to the Hwy 880 station. For a conservative analyte (an analyte with no major loss mechanisms such as sinking or biological uptake), the relative proportions of TDS from the North Fork and South Fork contributing to the downstream sites can be calculated from two equations:

Equation 1: Downstream concentration = North Fork proportion * North Fork TDS concentration + South Fork proportion * South Fork TDS concentration

Equation 2: North Fork proportion + South Fork proportion = 1

Solving these equations for the North Fork proportion results in:

North Fork proportion = (Downstream concentration - South Fork concentration) / (North Fork concentration - South Fork concentration)

A three-component mixing model was used to calculate the proportion of TDS originating from the North Fork, South Fork, and groundwater. The groundwater chemistry from GOWN Well #101 was used since it most closely matched the cation and anion distributions of the Hwy 880 samples. The most recent groundwater sample (November 2012) from Well #101 was used assuming it would be representative of the March 2017 surface water samples. A Piper plot representing the Hwy 880 winter data (see Figure 22) suggests that calcium-sodium ion exchange processes may be active, and that these two analytes may not behave conservatively. Although sulphate may behave conservatively, the anomalously low value of sulphate in the North Fork (3 mg/L; see Table 2) may not be representative (median winter SO_4 = 55 mg/L; n = 7). Magnesium, alkalinity, and chloride were used as conservative tracers. The combination of three potentially contributing fractions (North Fork, South Fork, and groundwater), and three analytes permits an exact solution for the three proportions. The addition of a conservation equation (North Fork proportion plus South Fork proportion plus groundwater proportion equals one) results in an overdetermined system that was solved using singular value decomposition with respect to the Milk River at the town of Milk River, as well as the Milk River at Hwy 880.

2.2.6 Ice Growth Model

A physical ice growth model was developed to explain how changes in air temperature, water temperature, and radiance may interact to control ice volume and hence TDS concentrations. The model is briefly described below, with more in-depth information and the model code (written in R; R Core Team 2018) provided in Appendix D and Appendix E.

The ice volume model is effectively a two-component box model consisting of a water component and an ice component. Energy flows between these two boxes, with external inputs from a fixed time-series of air temperature and radiance. Energy transfer is balanced in the water and ice components, but is not balanced in radiance or air temperature; these last two are strictly used to force changes in the model. The overall approach is similar to the ice growth and decay processes described in Lil and Shen (1993).

The ice volume model considers a fixed and arbitrary volume of water. For each time step, the amount of energy in the water is calculated from heat capacity (which converts temperature into energy), energy gain from radiance, and energy loss/gain from the air depending on the relative difference in temperature between the water and the air. Energy gained by the water component from the air and/or radiance first goes into melting existing ice, then to warming up the water. Conversely, energy lost by the water first lowers the water temperature to the freezing point before increasing the ice volume. The model tracks the total volume of ice at each time step, and assumes the amount of ice in the model is proportional to the

amount of salt (TDS) excluded. TDS was treated as a homogenous substance with constant ion proportions (Iwanyshyn et al. 2009).

Two time-series were used in the ice volume model. Air temperature, in degrees Kelvin, was acquired from a meteorological station in the town of Milk River operated by AAF. The second time-series is for radiance (in units W/m^2), taken from the same station. The model was calibrated to match the specific conductance measured at 15 minute intervals between January 2, 2012 and January 12, 2012 by a datasonde in the Milk River at the Hwy 880 bridge. This time period was chosen because it included multiple large changes in specific conductance, and included fine scale, daily features.

3 Results

3.1 Trend Results

With two exceptions (of unadjusted TDS), the results of unadjusted and flow-adjusted trend analysis indicate no trend or a negative trend in TDS and specific conductance in the Milk River at Hwy 880 (Table 1). For the two increasing trend results of unadjusted TDS, the same was not found in the corresponding flow-adjusted assessment, indicating a driving relationship of flow on water quality. The trend results indicate that the TDS and specific conductance concern has not become worse over time and that the current investigation and management actions can focus on the existing state of water quality.

Table 1: Status of trend assessments for TDS and specific conductance in the Milk River at Hwy 880. NT indicates no trend, + indicates significant ($p<0.05$) increasing trend, - indicates significant ($p<0.05$) decreasing trend. *Caution should be used when interpreting trend results with shorter timeframes. ^ In lieu of flow-adjusted trend due to the lack of validated flow data.

Milk River at Hwy 880 Trend Results							
		Flow-adjusted Trend			Unadjusted Trend (Concentration)		
	Season	Full dataset	Post WQMF dataset	10 year dataset.	Full dataset	Post WQMF dataset	10 year dataset.
Year of Limit Exceedance 2015/2016		2003-2016	2009-2016*	2006-2016	2003-2016	2009-2016*	2006-2016
Total Dissolved Solids Median (Winter only) Milk Hwy 880	Open Water	NT	NT	NT	NT	NT	NT
	Winter		NT	NT	+	NT	NT
Year of Limit Exceedance 2016/2017	Season	2003-2017	2009-2017*	2007-2017	2003-2017	2009-2017*	2007-2017
Total Dissolved Solids Median (Winter only) Milk Hwy 880	Open Water	NT	NT	-	+	NT	NT
	Winter	NT	-	NT	NT	NT	-
Year of Limit Exceedance 2017/2018	Season	2003-2018	2009-2018*	2008-2018	2003-2018	2009-2018*	2008-2018
Total Dissolved Solids Median (Winter only) Milk Hwy 880	Open Water	NT	-	-	NT	NT	NT
	Winter	NT	NT	NT	NT	NT	NT
Specific Conductance Median (Winter only) Milk Hwy 880	Open Water	NT	-	-	NT	NT	NT
	Winter	NT	NT	NT	NT	NT	NT
		Seasonally-adjusted Trend ^			Unadjusted Trend (Concentration)		
Year of Limit Exceedance 2018/2019	Season	2003-2019	2009-2019	←	2003-2019	2009-2019	←
Total Dissolved Solids Median (Winter only) Milk Hwy 880	Open Water	NT	NT	←	NT		←
	Winter				NT	NT	
Specific Conductance Median (Winter only) Milk Hwy 880	Open Water	NT	NT	←	NT		←
	Winter				NT	NT	

3.2 Investigation Question #1: Why do the Surface Water Quality Management Framework exceedances for total dissolved solids in the Milk River at Hwy 880 only occur in the winter (November to March)?

3.2.1 Results

Concentrations of TDS in the Milk River have been measured monthly at the Hwy 880 bridge since 2003. Between 2010 and 2017, median winter TDS concentrations exceeded the SWQMF limit (500 mg/L) in every year except 2015, and exceeded the trigger (606 mg/L) once (Figure 6; see also Figure A-1). The difference in median TDS concentrations between the open water and winter seasons ranged from 150 to 650 mg/L, averaging 381 mg/L. The higher median open water concentrations in 2010, 2011, and 2014 appeared to be related to the amount of flow in the Milk River (see Figure A-2 to A-4).

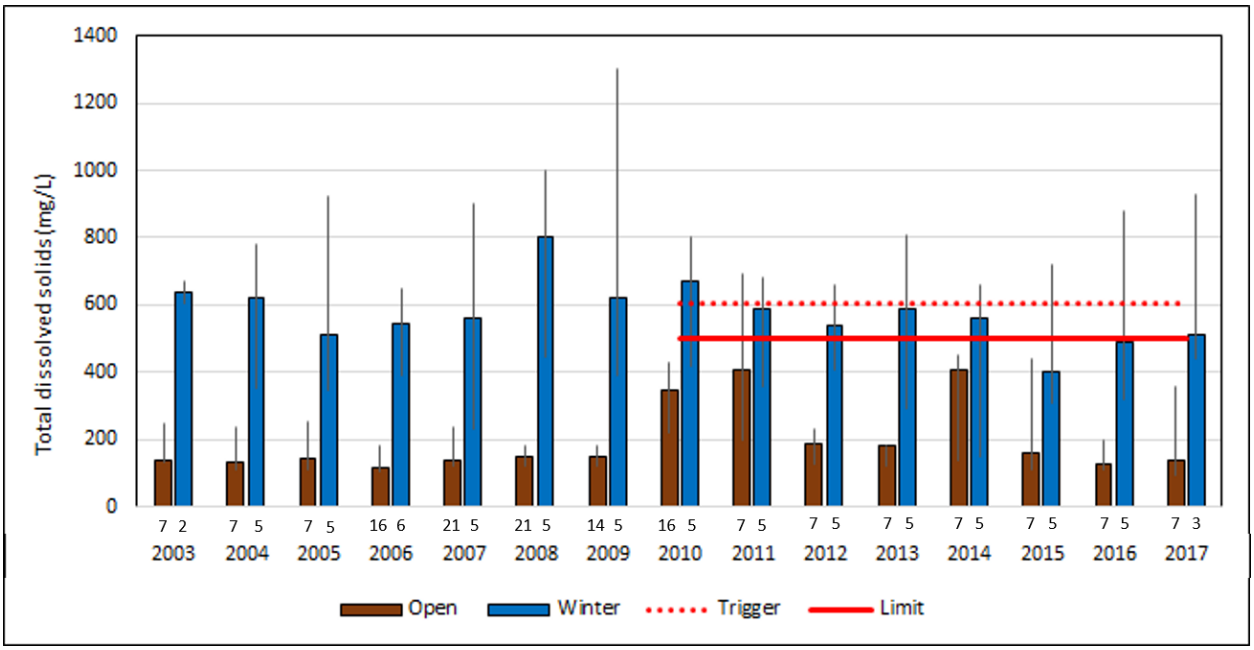

Figure 6: Median concentrations of monthly total dissolved solids in the Milk River, as measured at the Highway 880 bridge. open water season = April to October; winter season = November to March. The winter trigger (606 mg/L) and limit (500 mg/L) values refer to the thresholds identified in ESRD (2014). Note that the winter trigger concentration is greater than the limit concentration. The thresholds were applied beginning in 2014. Error bars are the 95% bootstrapped confidence interval on the median; numbers directly below each bar are the number of samples.

Although October is classified as part of the open water season, these samples were usually collected after diversion flow had stopped. The TDS concentration in October samples from the Milk River were more similar to winter (post-diversion) concentrations than open water concentrations (Figure 7).

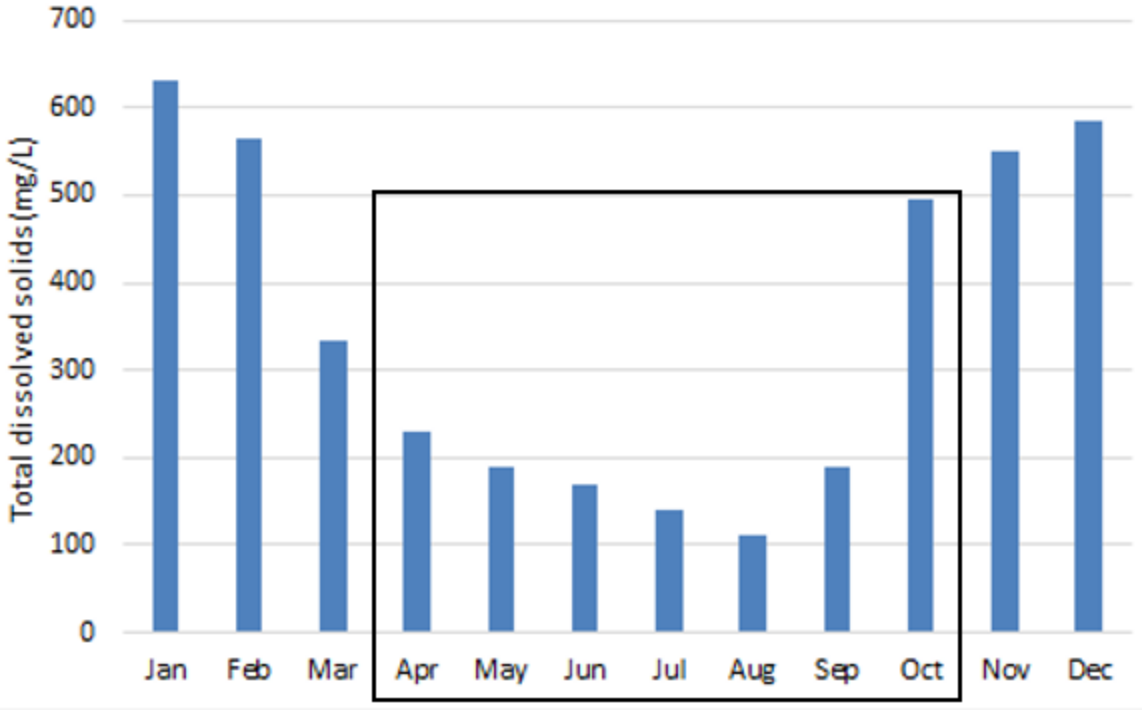

Figure 7: Median monthly total dissolved solids concentrations in the Milk River, measured at Hwy 880, 2011-2016. The black box indicates the months included in the open water season.

During the open water season when diversion is active (see Table A-1), the Milk River receives supplemental flow from the St. Mary River via the North Fork. Between June and August 2003 to 2016, the St. Mary diversion flow accounted for 94% of the flow in the North Fork (based on the median daily difference in flow rates). Hydrographs from the North Fork, South Fork, and town of Milk River are presented in Figure A-5 to A-7. The diversion plus baseflow represents a three-fold increase over winter (base) flow in the North Fork. Flow rates in the North Fork generally increased in April and remained steady until mid-September when water from the St. Mary River was no longer diverted into the Milk River. Flow rates at the town of Milk River, which is downstream of the confluence of the North Fork and South Fork, are also dominated by the diversion flow. Flow in the South Fork is not modified by the St. Mary River diversion. Flow increased sharply during the spring melt (February to March), varied from April to June as a result of local precipitation, and then decreased to base flow around August. Although the amount and duration of the flow varied from year to year, the overall pattern of near-baseline flows after summer precipitation was common.

The amount of flow was inversely related to the TDS concentration (Figure 8). When the diversion was not active and flow rates in the Milk River were low (<5 m^3/s), TDS concentrations were relatively high. When the diversion was active and flow rates were above 5 m^3/s, TDS concentrations were low. The relationship was not linear, however; a decrease in flow did not lead to a proportional increase in TDS concentration (Figure 9). Rather, high flows (>5 m^3/s) had TDS concentrations <250 mg/L, whereas low flows (<5 m^3/s) had TDS concentrations >250 mg/L.

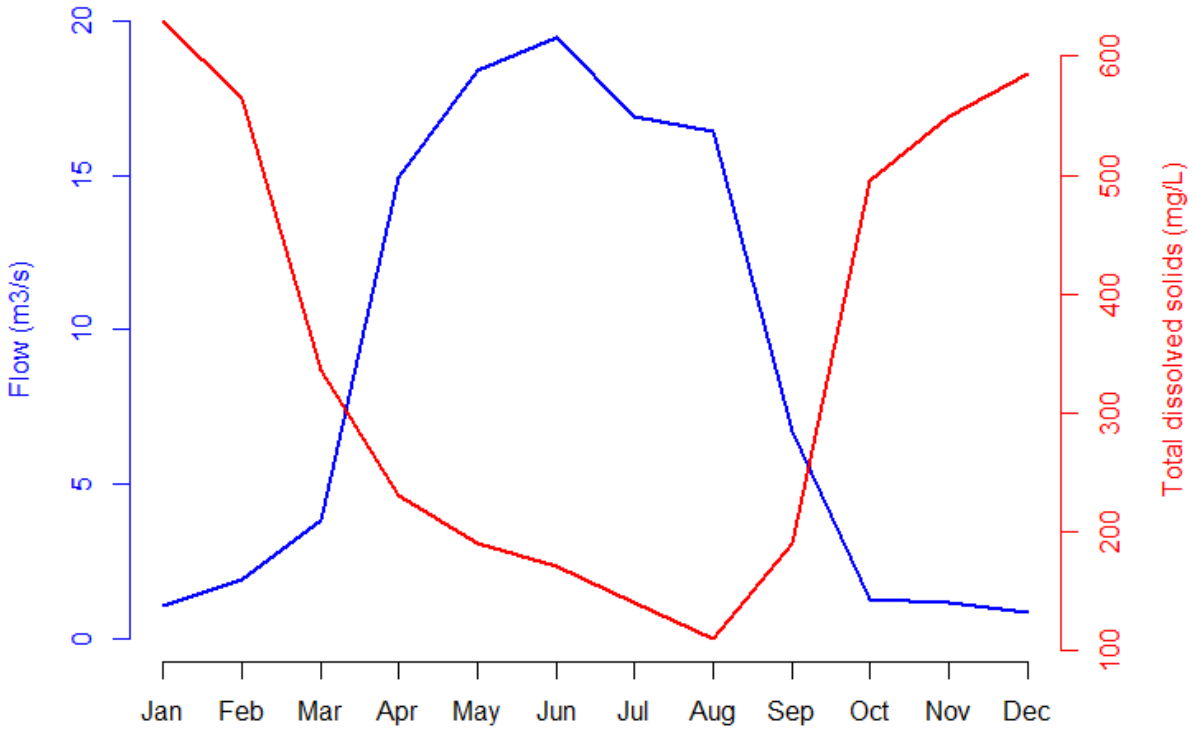

Figure 8: Median surface water flow (from daily averages; Environment Canada hydrometric station EC 11AA005) and total dissolved solids concentrations (monthly) from the Milk River at the town of Milk River, 2011-2016.

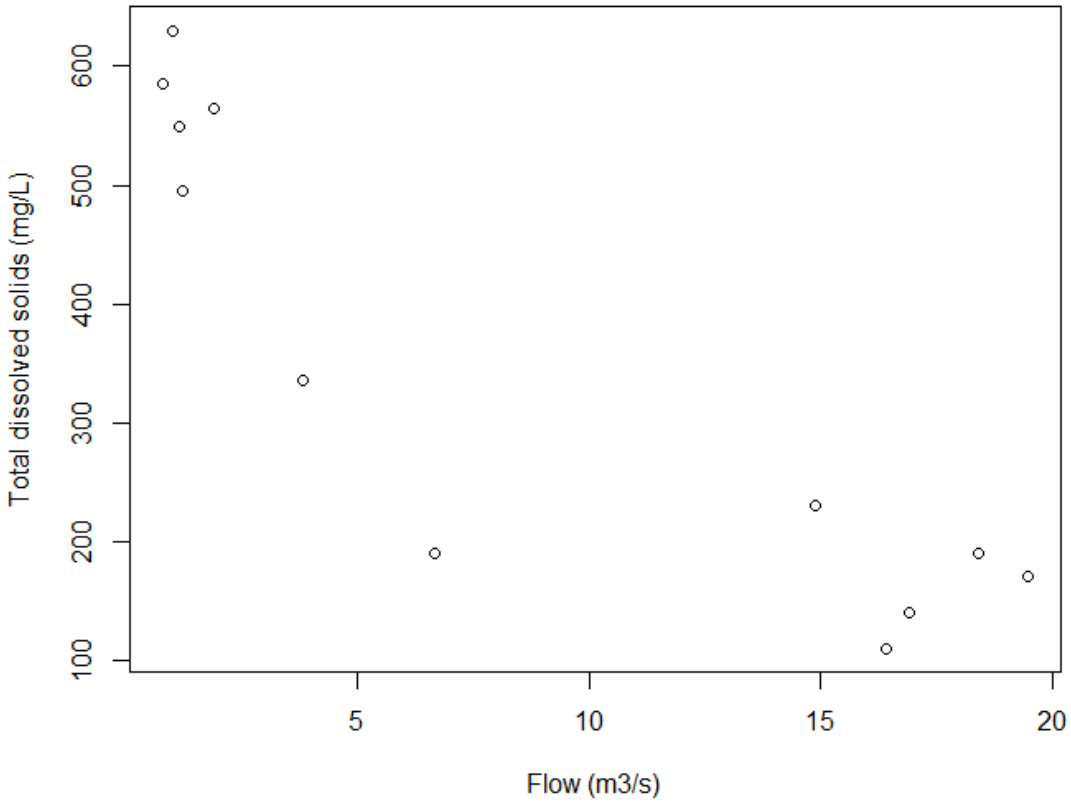

Figure 9: Median total dissolved solids concentrations (monthly) and corresponding flow rate (daily average; Environment Canada hydrometric station EC 11AA005) from the Milk River at the town of Milk River, 2011-2016.

Measurements of TDS concentrations in the St. Mary River at Cardston, AB (downstream of the diversion) were available between 2011 and 2016, and were compared to the TDS concentrations in the Milk River at Hwy 880 (Figure 10). Overall, there was little change (30 mg/L increase) in median TDS concentrations in the St. Mary River between the open water and winter seasons. Concentrations of TDS in the Milk River during the open season were also similar (15 mg/L higher) to those in the St. Mary River. However, TDS concentrations in the Milk River more than doubled (365 mg/L increase) in the winter season compared to the St. Mary River or the Milk River itself during the open water season.

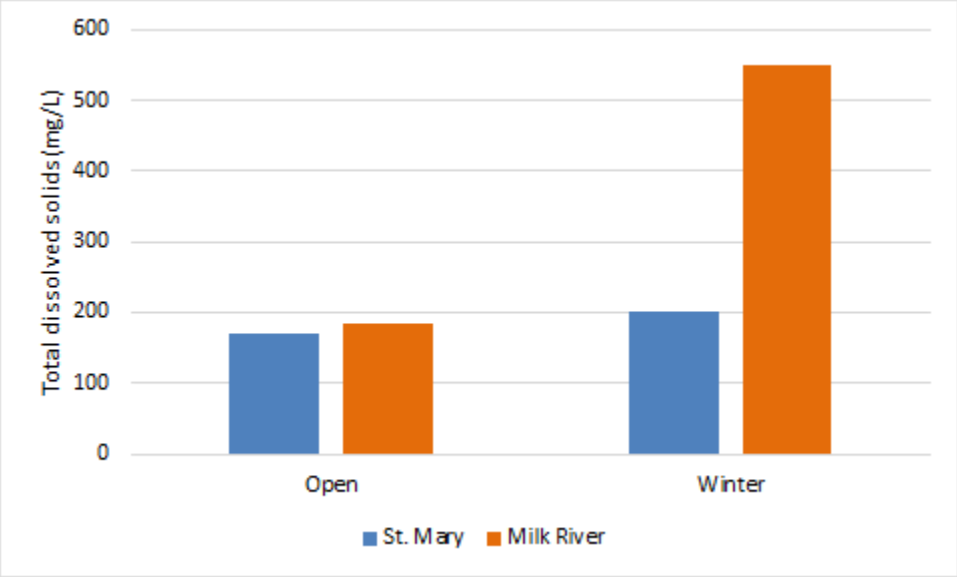

Figure 10: Median monthly total dissolved solids in the St. Mary and Milk rivers, 2011-2016. The St. Mary River was sampled at Cardston, AB; the Milk River was sampled at Hwy 880.

There was a limited change in ion composition in the St. Mary River between seasons, though winter samples tended to have lower proportions of calcium and bicarbonate, and correspondingly higher proportions of sodium and sulphate (Figure 11). There were, however, linear trends in the cation and anion proportions. Calcium (Ca) was the dominant cation in all the St. Mary River samples. The proportion of magnesium (Mg) was nearly constant (~30%), while the proportions of calcium and sodium (Na) + potassium (K) were inversely related. This suggests a potential exchange reaction between calcium and sodium.

Bicarbonate (HCO_3) + carbonate (CO_3) were the primary anions in the St. Mary River. However, some of the samples approached a 50% split between bicarbonate/carbonate and sulphate (SO_4). The proportion of chloride (Cl) + fluoride (F) was consistently low, with changes in bicarbonate/carbonate offset by changes in sulphate. The proportion of sulphate tended to increase in the winter, indicating a difference in the source rock contributing to the ion load, or a non-weathering input of sulphate (e.g., sulphide oxidation).

The St. Mary River samples had one characteristic water type (geochemical endmember) in the (Ca + Mg) (HCO_3 + CO_3) corner of the central diamond, suggesting a calcium carbonate (limestone) source. There was potentially also a source of calcium-magnesium-carbonates (dolomite). Magnesium carbonates (e.g., magnesite) are relatively insoluble and are hence unlikely to be an important contributor to the water quality. The changes in St. Mary River chemistry point to a second characteristic water type consisting of ~70% (Ca + Mg)/30% (Na + K) and 40% (HCO_3 + CO_3)/60% (Cl + F + SO_4). The water quality samples were collected at the same place in the St. Mary River between 2011 and 2016, so the water types are not affected by sampling location.

There was also a linear trend in the central diamond of the Piper plot for the Milk River samples. The leftmost endmember matched the (Ca + Mg)(HCO3 + CO3) endmember of the St. Mary River during the open water season. This result is consistent with a majority of the Milk River flow consisting of St. Mary River water during the open water season: both the Milk River and St. Mary River had similar total TDS concentrations, and similar ion compositions.

The winter endmember, and the mixing line between the two endmembers, were different than the St. Mary River samples. The Milk River samples taken during winter had a lower proportion of calcium, slightly less magnesium, and more sodium than the St. Mary River samples. There was some overlap between the Milk River samples taken during the open water and winter seasons, though the winter samples cluster more tightly towards the low (Ca + Mg)/high (Na + K) and low (HCO_3 + CO_3)/high (Cl + F + SO_4) axes. Most of the overlap occurred in late September and October, when flow from the St. Mary diversion had stopped. Similar to TDS concentrations, the ion composition of the Milk River during October was more representative of the Milk River during the winter, despite October being categorized as open water in the SWQMF.

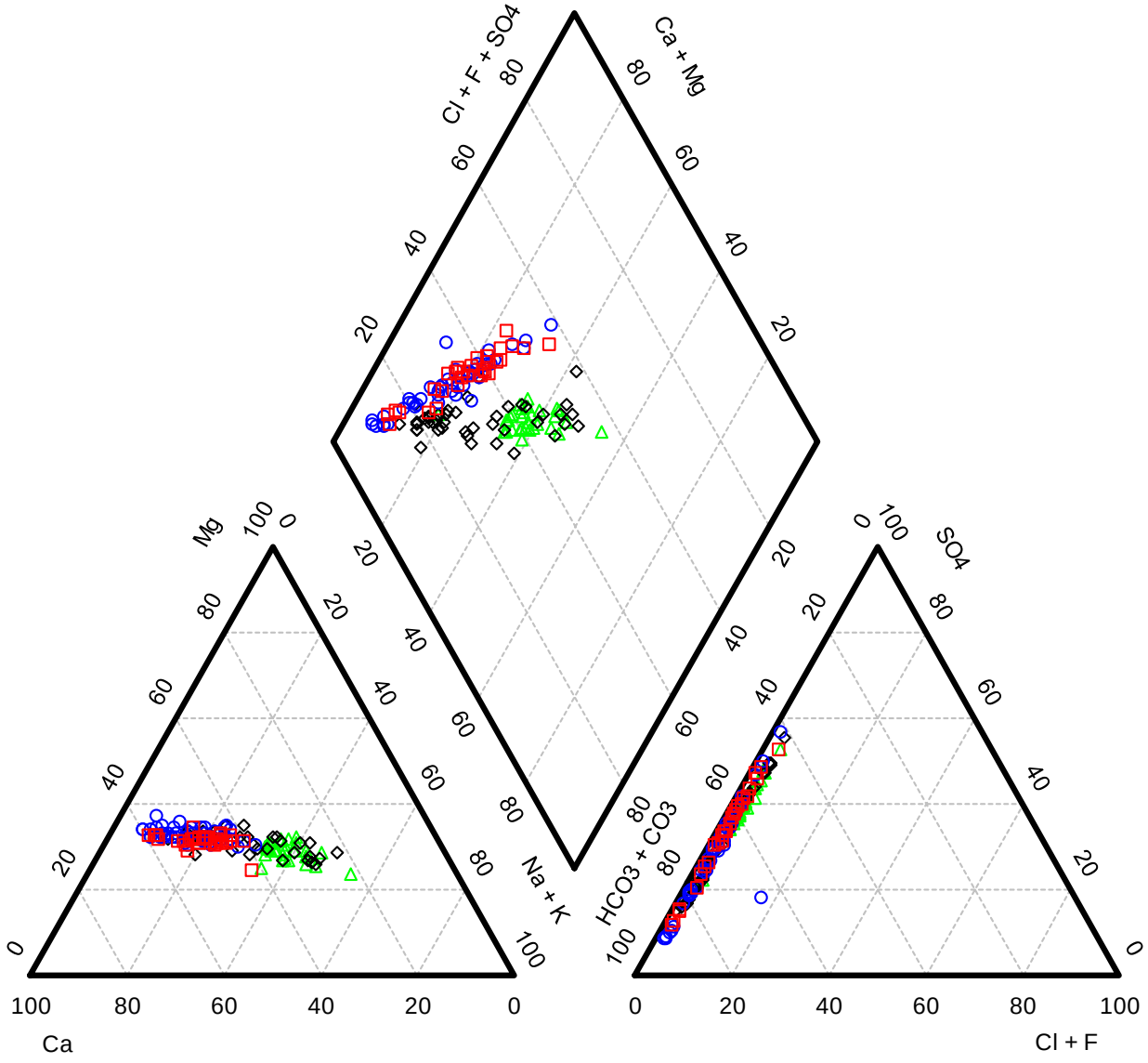

Figure 11: Piper plot of monthly surface water samples from the St. Mary River (at Cardston, AB) and the Milk River (at Hwy 880), 2011-2016. Left figure is the "cation" triangle; right figure is the "anion" triangle; central figure is the "diamond." Blue circle = St. Mary River during open water; red square = St. Mary River during winter; black diamond = Milk River during open water; green triangle = Milk River during winter. Ion proportions based on equivalents.

The molar ratio of (Ca + Mg) to (Cl + F + SO_4) in the St. Mary River was used to characterize points along the mixing line of the diamond (Figure 12). As the concentration of total ions (TDS) increased, the relative proportions of calcium and magnesium decreased. This means that the calcium carbonate endmember had lower TDS concentrations, and the mixing line in the diamond portion of the Piper plot is likely related to the total amount of TDS. There was no relationship between the ion ratio and water temperature or air temperature, with the exception that an ion ratio above four only occurred at temperatures above 0°C (data not shown).

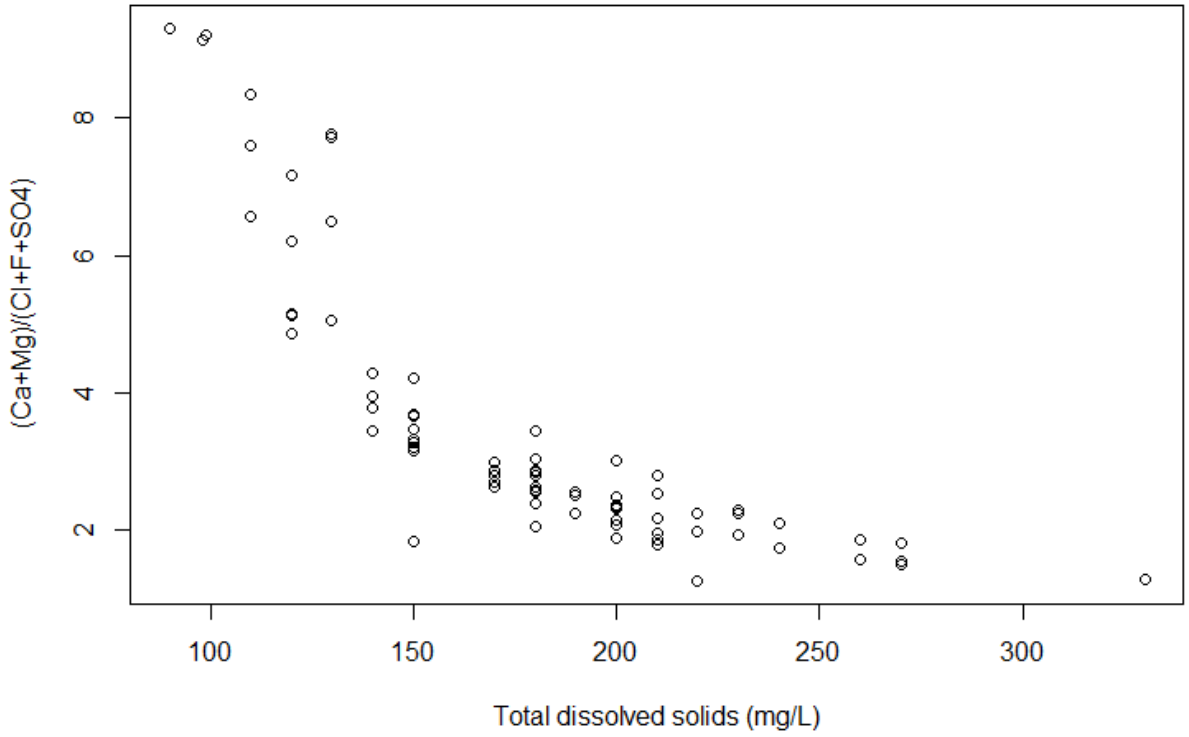

Figure 12: Ion ratio versus total dissolved solids concentration for the St. Mary River. Monthly measurements at Cardston, AB between 2011-2016. Ion concentrations were measured in moles.

There was a weak relationship between flow rate and TDS concentration in the St. Mary River, where the highest flow rates were found with relatively low TDS concentrations (Figure 13). High flow rates (>50 m^3/s) in the St. Mary River were only observed between May and July. Data collected in 2015 had consistently low monthly TDS concentrations.

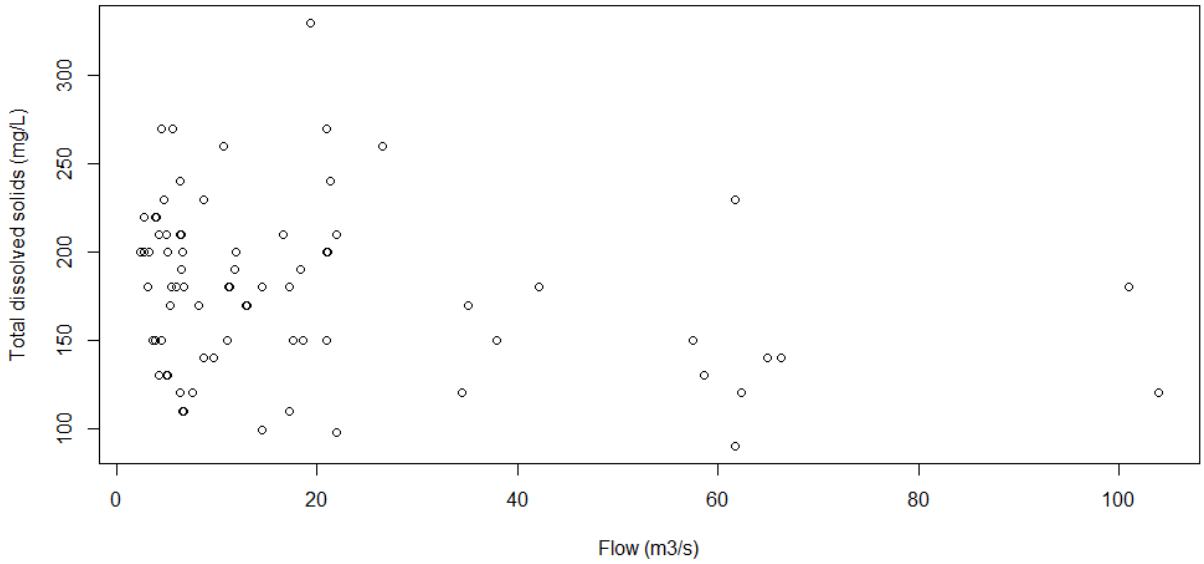

Figure 13: Monthly total dissolved solids concentration versus flow rate in the St. Mary River between 2011-2016. Concentrations were measured at Cardston, AB and flow was measured at Environment Canada hydrometric station EC 05AE027 ("St. Mary at International Boundary").

Many of the same patterns observed in the St. Mary River were also present in the Milk River. Concentrations of TDS decreased consistently but nonlinearly with increasing flow (Figure 14). The relationship between TDS concentration and flow was more pronounced in the Milk River compared to the St. Mary River, perhaps because the range of TDS values in the Milk River was almost three times that of the St. Mary River. The ion ratio in the Milk River was highest when TDS concentrations were low, with a higher proportion of sulphate and lower calcium at higher TDS concentrations (Figure 15).

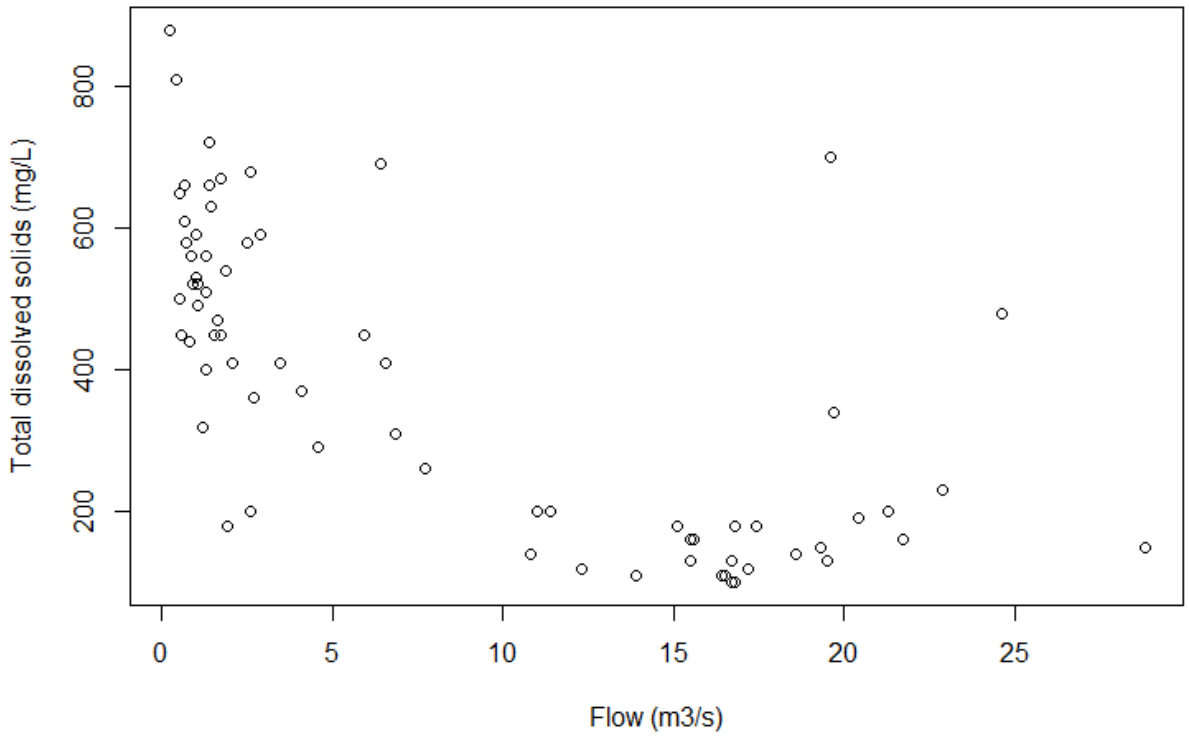

Figure 14: Monthly total dissolved solids concentration versus flow rate in the Milk River between 2011-2016. Concentration was measured at Hwy 880, while flow was measured at Environment Canada hydrometric station EC 11AA005 ("Milk River at town of Milk River").

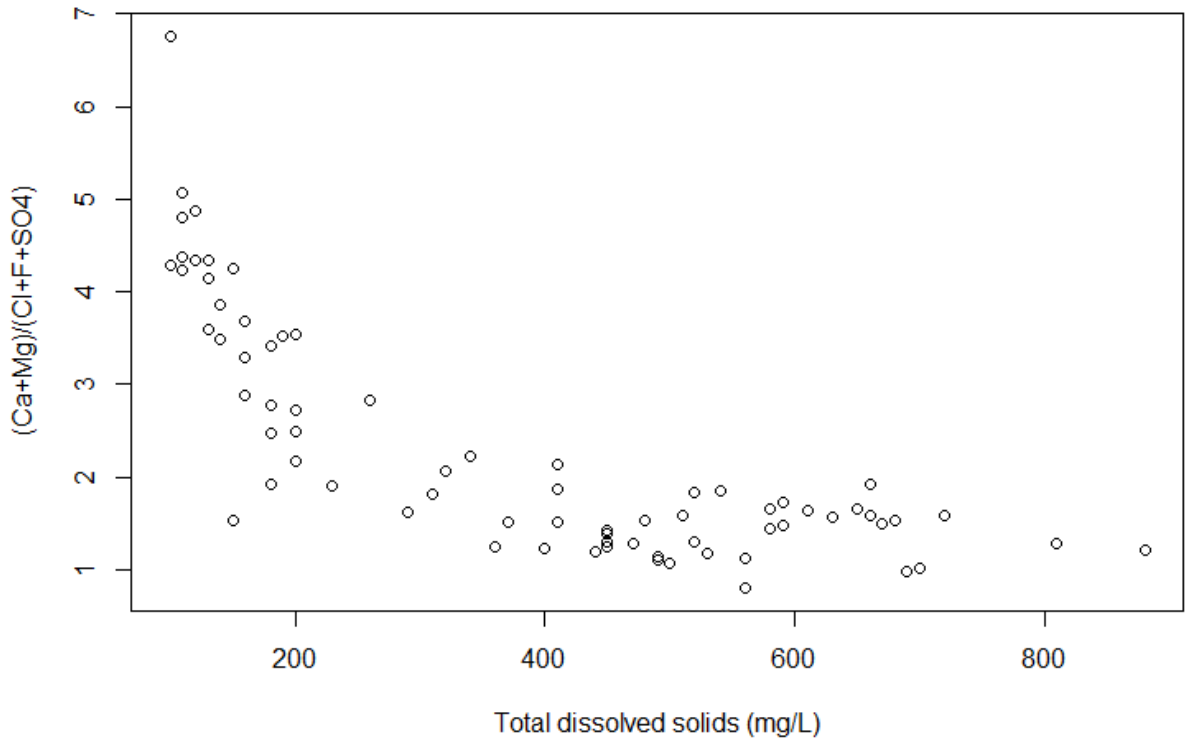

Figure 15: Molar ion ratio versus total dissolved solids concentration for the Milk River. Monthly measurements at Hwy 880 between 2011-2016.

3.2.2 Discussion

Overall, the results of trend analyses indicate TDS and specific conductance have not become worse since the management framework was developed and that management decisions could be made considering current conditions.

Seasonal changes in TDS concentration in the Milk River appeared to be due to the diversion of St. Mary River water that had relatively low TDS concentrations. This is supported by:

- The flow pattern of the Milk River downstream of the confluence of the North Fork and South Fork was dominated by the diversion flow. This implies that on a volumetric basis, input from the St. Mary River was more important during the open season, but not during the winter (when there was no diversion).

- Flow in the Milk River and TDS concentrations were inversely correlated. Flows were high when there was a lot of input from the St. Mary River through the diversion, and a larger proportion of the flow was from low TDS water. When flows were low, a larger proportion of the total flow in the Milk River (up to 100% when diversion is no longer active) was from the higher TDS Milk River.

- When Milk River flows were dominated by the St. Mary River diversion, TDS concentrations in the Milk River were nearly equal to TDS concentrations in the St. Mary River. The Milk River had a higher TDS concentration in the winter when the St. Mary River diversion was not active.

- The TDS concentration in October samples were more similar to winter (post-diversion) concentrations than open water concentrations. Although October is classified as part of the open water season, these samples were usually collected after diversion flow has stopped.

- The ion composition of the Milk River was the same as the ion composition of the St. Mary River during the open water season. The ion composition of the Milk River changed during the winter, after diversion flow stopped.

The patterns in the hydrographs highlight the importance of the St. Mary River diversion on the total flow in the Milk River between the open water and winter seasons. Variability in precipitation drives the differences between the magnitude and timing of peak flows. These are layered on top of an overall consistent pattern: low flow until the spring melt, an increase in flow from the diversion after the spring melt has ended, high and stable flow during the open water season when the diversion is active, a sudden decrease in flow after the diversion (that occurs faster than the flow increase), and a low and steady flow during winter. The influence of season cannot be easily differentiated from the influence of diversion flow; the two overlap with the exception of October, which is classified as open water but occurs after the diversion flow stops.

Lower flow rates in the Milk River generally had higher TDS concentrations and an ion composition with less calcium and magnesium, and more chloride and sulphate. The observed relationship between flow (from the diversion) and the ion ratio describes one endmember representing the St. Mary River water during the open water season, and a different endmember that was dominant during the winter season when surface flows were at a minimum.

Many rivers have concentration versus discharge relationships for major ions similar to the St. Mary River and Milk River (Godsey et al. 2009), including the Bow River in southern Alberta (Grasby and Hutcheon 2000). However, different physical mechanisms could explain the underlying power law type relationship. These include mixing between waters with different chemistry, the effects of water storage and transport in the catchment, and changes in the reactive surface area of minerals and/or mineral dissolution rates (Godsey et al. 2009). The shape of the concentration-discharge relationships can provide information on the relative balance between hydrologic controls and biogeochemical controls in catchments (Bieroza et al. 2018). A negative relationship for salts is often associated with dilution (Rose et al. 2018). Common to the interpretation of concentration-discharge relationships is the idea that the flow comes from natural processes like baseflow and precipitation. In the Milk River, flow rates are controlled by the St. Mary River diversion. High flow rates occur when the diversion is active during the irrigation season, and most of the Milk River flow consists of water from the St. Mary River (e.g., 94% in the North Fork). In the winter, the St. Mary diversion is not active and flow rates are low. This results in a confounding of flow rate and chemistry that falls outside the interpretation of concentration-discharge plots.

The evidence suggests that the Milk River normally has high TDS concentrations, and open water TDS concentrations in the Milk River are decreased by mixing with low TDS water from the St. Mary River. As a result, the SWQMF limit exceedances only occurred in the winter because that is the period when Milk River TDS concentrations are not diluted by St. Mary River water.

3.2.3 Question #1 Conclusion:

The SWQMF exceedances for TDS in the Milk River at Hwy 880 only occur in the winter (November to March) because most of the water in the Milk River is made up of dilute (low TDS) St. Mary River water during the open water season. In the winter, the flow in the Milk River comes from a different source, which increases the TDS concentration as well as changes the ion composition of the river water.

3.3 Investigation Question #2: What is the primary source(s) of total dissolved solids to the Milk River during the winter?

3.3.1 Results

The flow balance looking at the contributions from the North Fork and the South Fork showed that the Milk River hydrometric station experienced a one day lag during the winter compared to the North Fork station, and no lag (less than one day) compared to the South Fork. The Spearman correlation result matched a qualitative assessment that compared the time it took for sudden changes in winter flow rates in the North and South Fork stations to appear at the downstream Milk River station.

The median difference between the outflow (at the town of Milk River) and inflow (from the North and South Forks) was 0.59 m^3/s. The net positive flow indicates a source of ungauged water entered the Milk River upstream of the town of Milk River (Figure 16). Although the flow imbalance was small, the magnitude of the ungauged flow was greater than the site-to-site and/or person-to-person variability observed in the winter along a single cross-section of the Milk River (MacCulloch and Wagner-Watchel 2010).

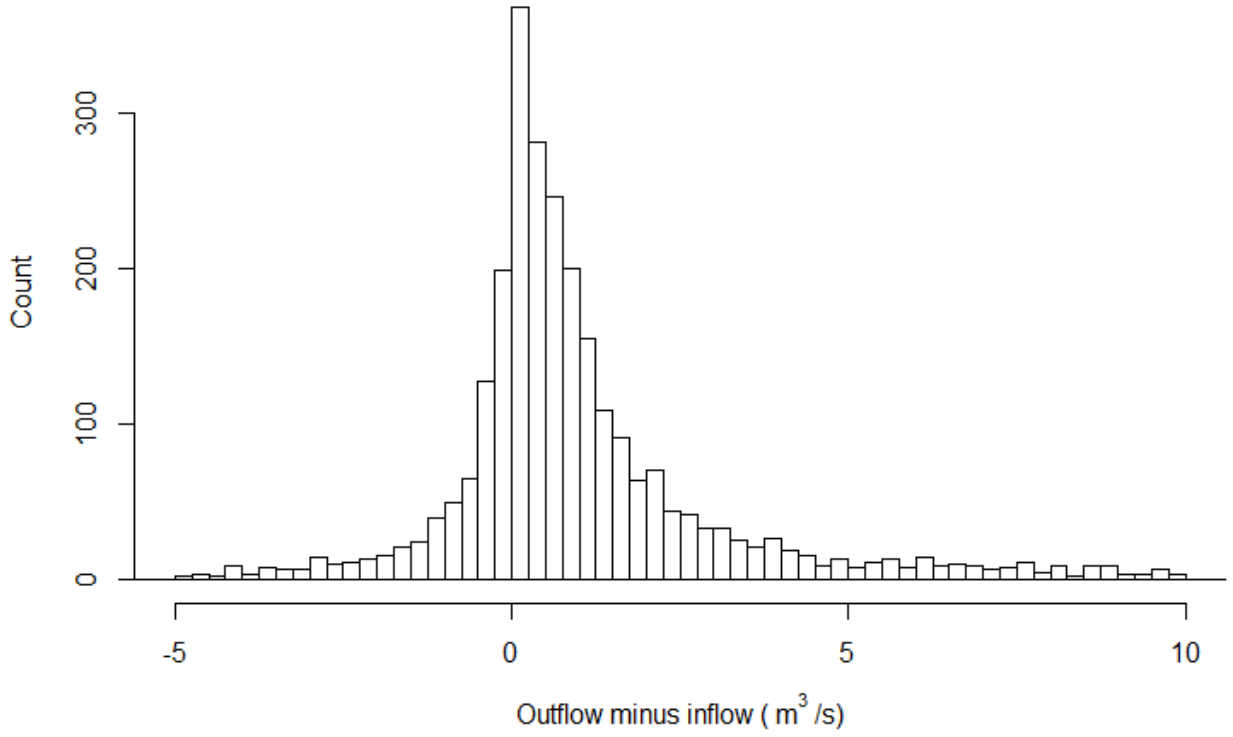

Figure 16: Flow balance (outflow at Milk River minus inflow from North Fork and South Fork) for the winter season. The flow axis has been shortened; the minimum flow balance was -82.5 m^3/s, and the maximum flow was 52.2 m^3/s. Extreme values occurred when flow in the North Fork was substantially different than the flow in the South Fork. The bars are in 0.25 m^3/s increments.

Flow in the North Fork was related to the flow balance (Figure 17). When flows were very low in the North Fork, there could be a substantial positive flow balance. As flows increased above 5 m^3/s, there was usually no difference between inflow and outflow. This pattern is consistent with a seasonal, ungauged flow source. When gauged flows were above 5 m^3/s, the effect of the ungauged source was small relative to the total flow balance. However, when flows in the North Fork were low, the ungauged flow was more

important to the flow balance. In contrast, there was no apparent relationship between the flow in the South Fork of the Milk River and the flow balance (Figure 18). There was an overall pattern of a greater flow difference with higher flow rates at the town of Milk River (Figure 19). This relationship is expected, as the “outflow” component of the flow balance is defined as the flow at the town of Milk River.

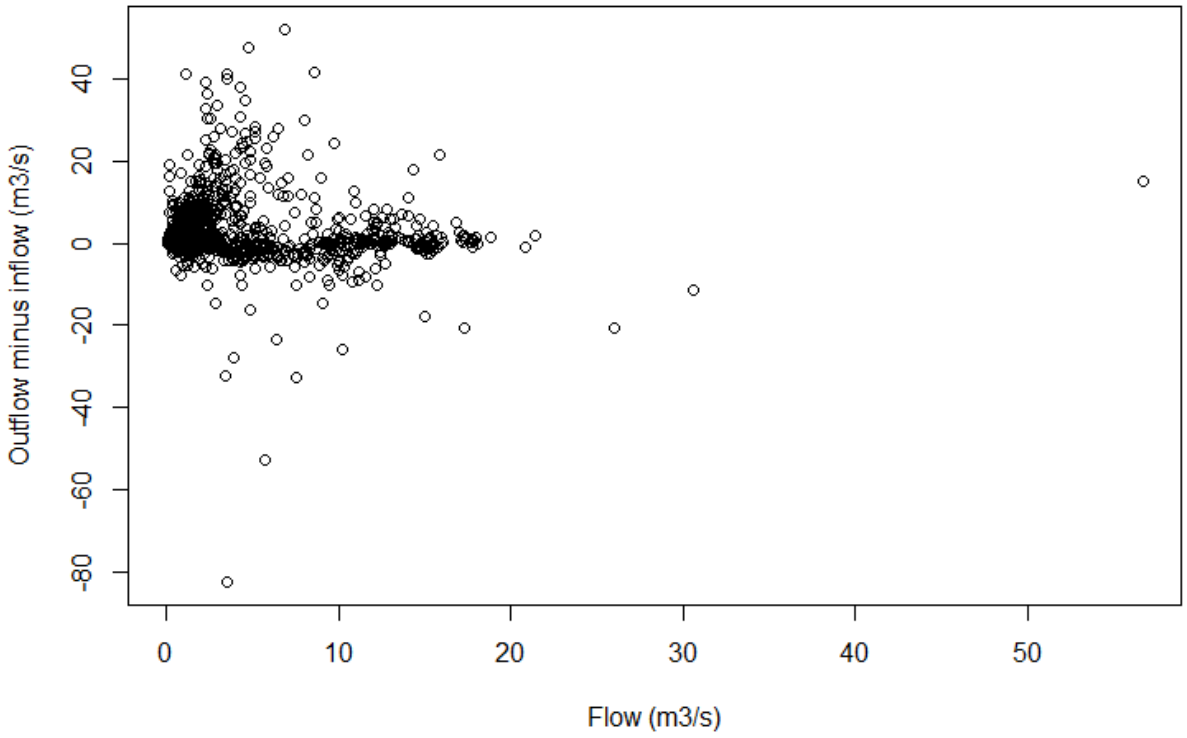

Figure 17: Flow balance and flow in the North Fork (station EC 11AA001) in the winter, 1931-2017.

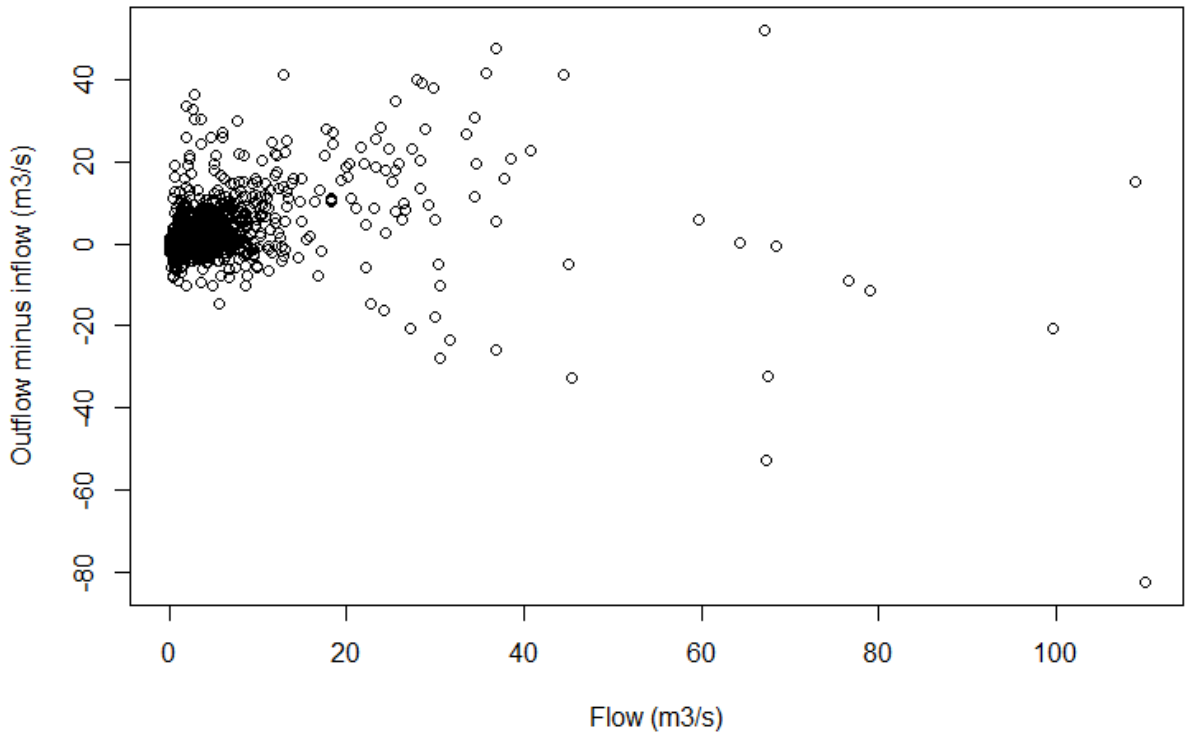

Figure 18: Flow balance and flow in the South Fork (station EC 11AA025) in the winter, 1931-2017.

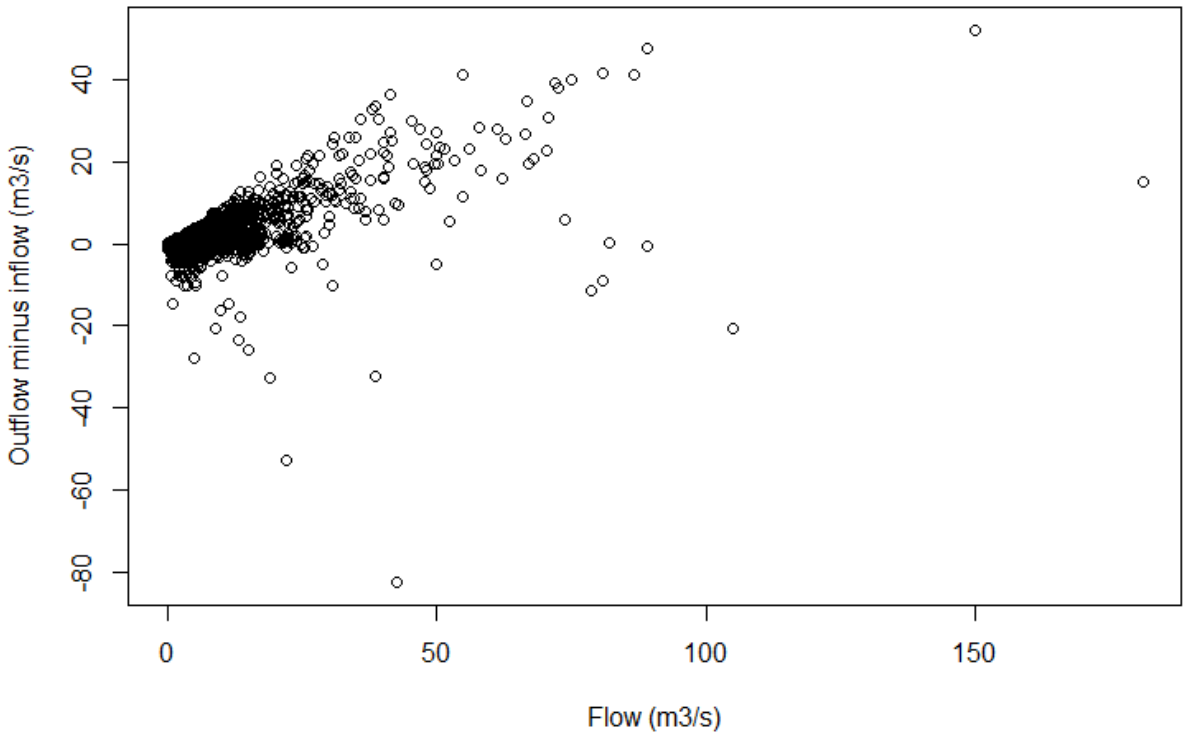

Figure 19: Flow balance and flow in the Milk River at the town of Milk River (station EC 11AA005) in the winter, 1931-2017.

There was no structured relationship between snowmelt and the flow balance (Figure 20). Moreover, the maximum range of variability in snow depth occurred with no change in flow; similarly, the maximum range of variability in flow occurred with no change in snow depth. The largest periods of both snowmelt as well as snow accumulation had no apparent effect on the flow balance. Likewise, the largest changes in flow balance occurred when there was minimal change in snow cover. Considering a 1 to 5 day lag between the flow balance and snowmelt improved the relationship, though the overall correlation was still poor (Figure 21). The highest correlations were for negative lags, indicating the effect of snowmelt preceded the flow balance. The lags were negatively correlated (i.e., higher snowmelt was associated with a more negative flow balance), which is the opposite of the expected relationship if snowmelt volume was contributing to the ungauged inflow volume. The overall pattern shown in Figure 20 was consistent across all the lags, with the largest changes in snow depth occurring with a minimal difference between outflow and inflow.

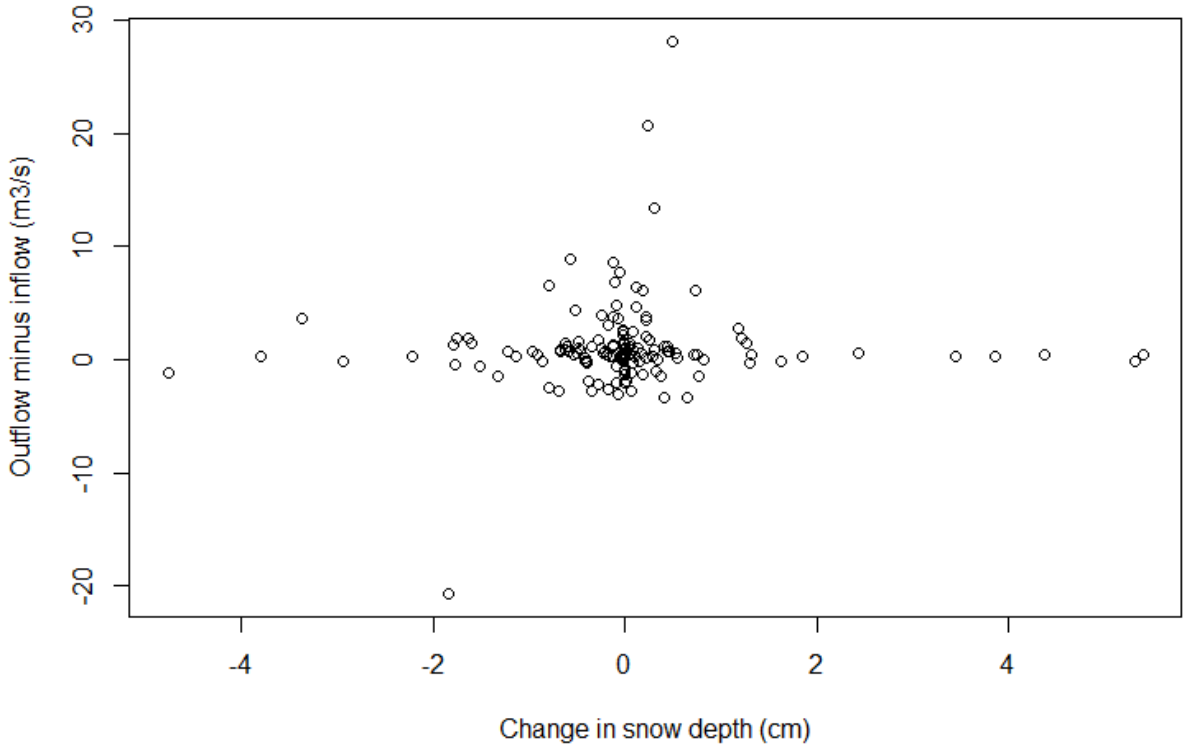

Figure 20: Snow pack versus flow balance, winter 2013 to 2017. Change in snow depth measured by Alberta Agriculture and Forestry at the town of Milk River. The flow balance (outflow minus inflow) was calculated as described in Section 2.2.

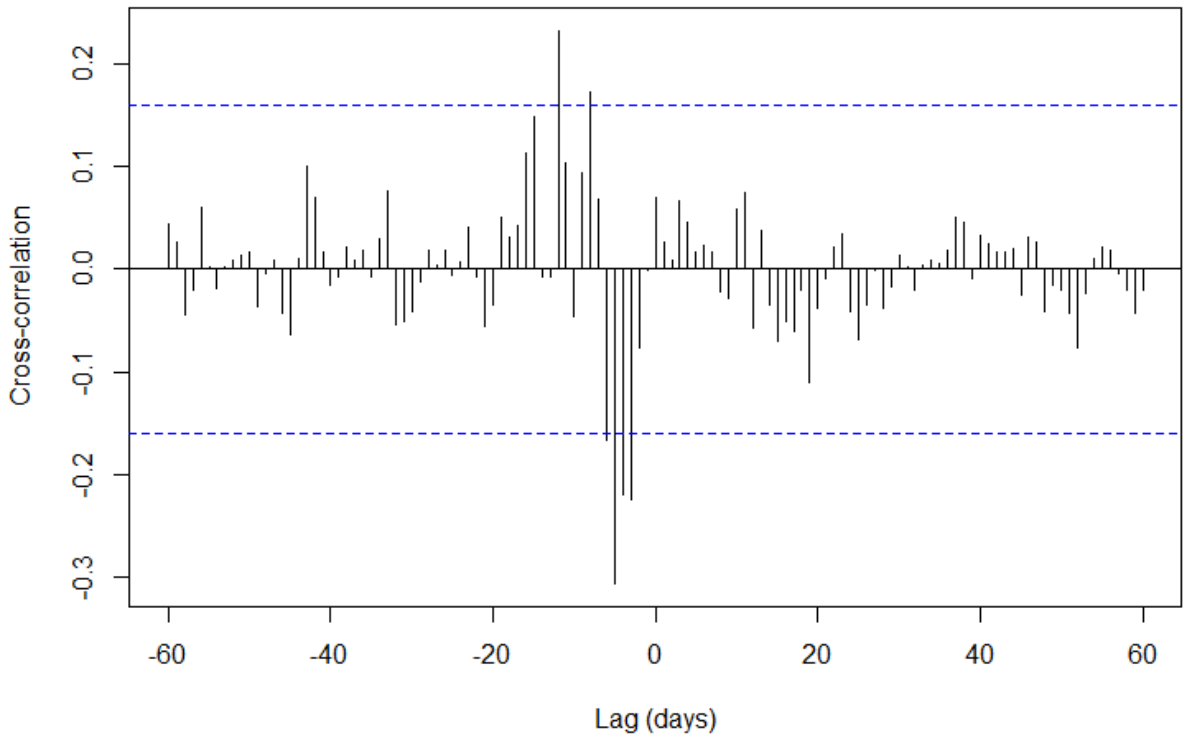

Figure 21: Pearson cross-correlation of snow melt and the Milk River flow balance (outflow minus inflow). Correlations extending outside the blue dotted line were statistically significant at the 0.95 significance level.

If the main source of TDS came from gauged surface flows, and the inflow waters (North and South Forks) mixed conservatively, the concentration of salt entering one of the downstream stations (town of Milk River or Hwy 880) should be equal to a weighted sum of salt concentrations from the North and South forks of the Milk River. A two-component mixing model was used to calculate the relative proportion of each source's (North and South forks) contribution of salt to the total under these assumptions (Table 2).

Table 2: Ion chemistry and mixing model results for the North Fork, South Fork, and Milk River mainstem. All concentrations are in mg/L. Data are from the specified locations, sampled on March 14, 2017. The proportions are calculated based on the outflow concentration given in parentheses in the first column. Percentages in the last row are the increase relative to concentrations from the town of Milk River.

Component	Location	Calcium	Magnesium	Sodium	Potassium	Alkalinity	Sulphate	Chloride
Inflow 1	North Fork	32	14	8.6	4	150	3	2.5
Inflow 2	South Fork	45	20	27	3	190	57	3.6
Outflow 1	Town of Milk River	58	26	37	3	250	74	4.6
Outflow 2	Hwy 880	59	33	73	6	280	160	7.6
Proportion Inflow 1 (Outflow 1)	North Fork/Milk River	-100%	-100%	-54%	0%	-150%	-31%	-91%
Proportion Inflow 2 (Outflow 1)	South Fork/ Milk River	200%	200%	154%	100%	250%	131%	191%
Proportion Inflow 1 (Outflow 2)	North Fork/ Hwy 880	-108%	-217%	-250%	300%	-225%	-191%	-364%
Proportion Inflow 2 (Outflow 2)	South Fork/ Hwy 880	208%	317%	350%	-200%	325%	291%	464%
Outflow 2 - Outflow 1	Hwy 880/ Milk River	1 (2%)	7 (27%)	36 (97%)	3 (100%)	30 (12%)	86 (116%)	3 (65%)

All the analytes except potassium showed a consistently increasing pattern with distance downstream from the confluence with the South Fork. Sodium, potassium, sulphate, and chloride had the largest percent increases between the town of Milk River and Hwy 880, though the high percent changes in potassium and chloride were likely due to the small initial concentrations. Importantly, ion concentrations at both the town of Milk River and at Hwy 880 (outflows) were larger than concentrations in either the North Fork or South Fork (inflows). This resulted in the estimated proportions from the mixing model of the North and South forks being either greater than one or less than zero. These proportions are not physically realistic and indicate the ion concentrations downstream of the confluence were not a simple weighted average of inputs from the two sources.

Upstream to downstream patterns in water quality along the Milk River were available during the open water season in 2012. There was an overall decrease in flow between April and August (see Figure B-1). However, the flow rates measured on the six days when water quality samples were taken did not follow a consistent pattern. Two main spatial patterns were apparent in the major ion data (see Figure B-2). Concentrations of calcium, magnesium, TDS, and to a lesser extent, bicarbonate increased from upstream to downstream. The chemistry of the Milk River during the open water season had a calcium carbonate content of 60-80% of TDS, similar to the St. Mary River. Concentrations also decreased with time, which matches the overall pattern in flow but not the flow on the specific days samples were taken.

Sodium and sulphate increased at the two stations furthest downstream (MST_C and MST_D) to a much larger extent than the two upstream stations. The two sets of stations (low concentrations at MST_A and MST_B, and high concentrations at MST_C and MST_D) group according to the predominant river substrate: the upstream stations are located in a primarily gravel-dominated area, while the downstream stations are in a sand-dominated area. The change in substrate type is linked to the erodability of the surficial rocks, which in turn may be related to the additional input of sodium and sulphate. The same pattern of increasing TDS concentration from upstream to downstream was also seen in winter (March) 2017, when surface water quality samples were taken from near the western boundary at Hwy 501 (270 mg/L), upstream of the town of Milk River (360 mg/L), and Hwy 880 (510 mg/L).

The geochemistry of winter Milk River samples taken at the Hwy 880 bridge are presented in a Piper plot (Figure 22). In the cation triangle (left portion of figure), most of the samples were clustered in an area between 50-70% calcium, 30% magnesium, and 30-50% sodium plus potassium. Some samples had a smaller proportion of calcium and magnesium (40% and 20%, respectively) and a correspondingly higher proportion of sodium plus potassium (60%). Variability in anion concentrations were also observed (right portion of figure). Samples were predominantly between 50-70% bicarbonate plus carbonate, 30-50% sulphate, and <10% chloride plus fluoride.

When the cation and anion proportions were projected into the central diamond, they formed a relatively tight cluster with the middle near the 60% calcium plus magnesium/60% bicarbonate plus carbonate intersection. The similarity in proportions suggests that much of the (Ca + Mg) is associated with carbonates, such as limestone (calcium carbonate, $CaCO_3$) or dolomite [calcium magnesium carbonate, $CaMg(CO_3)_2$].

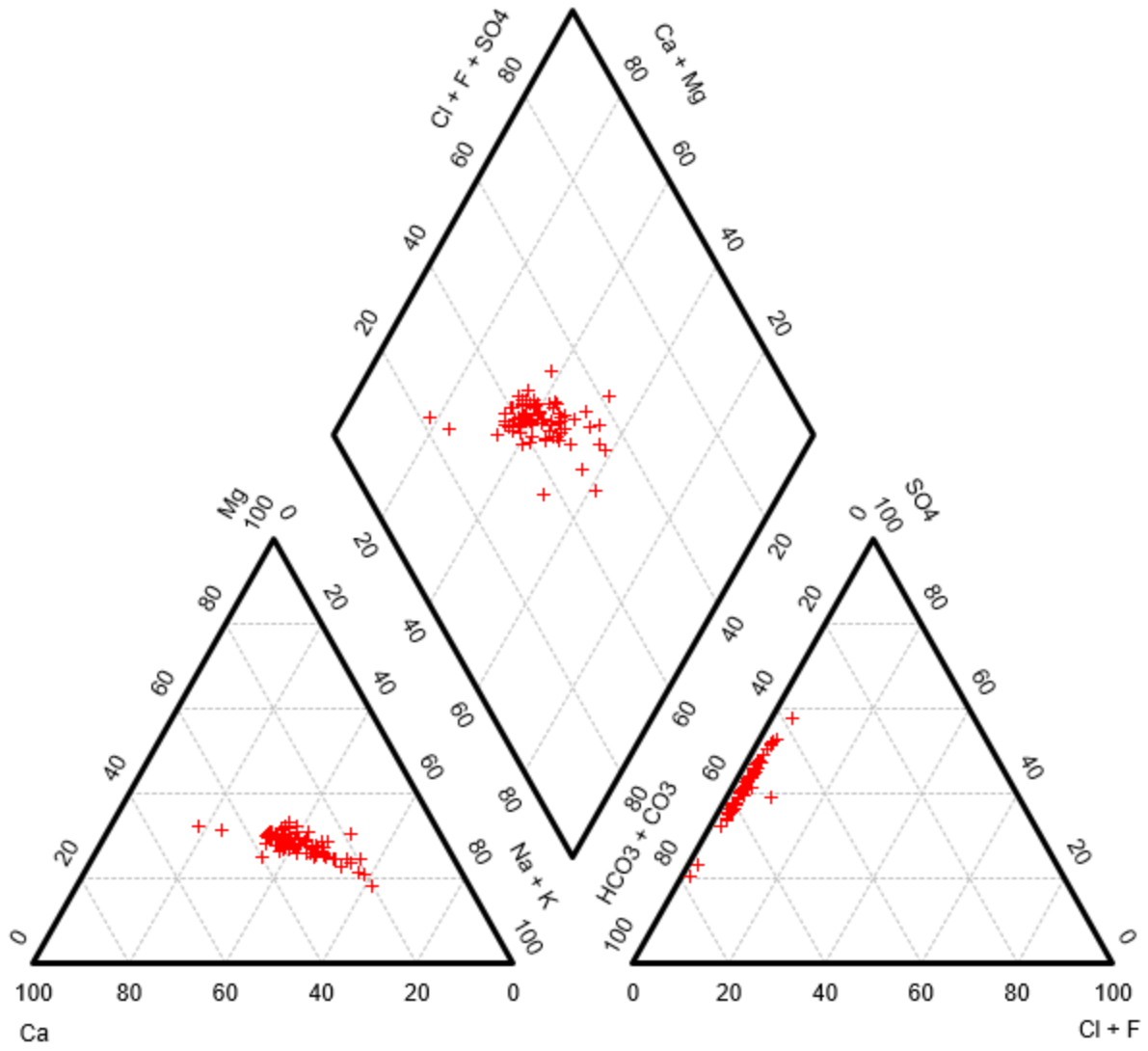

Figure 22: Piper plot for surface waters collected during the winter at the Hwy 880 bridge. Left figure is the "cation" triangle; right figure is the "anion" triangle; central figure is the "diamond." Monthly (winter) samples, 2003-2017, plus 1986-1988. Ion proportions based on equivalents.

Ion ratios were used to infer potential source rocks for TDS in the Milk River. Detailed examinations of the ion ratios are provided in Appendix B (see Figure A-23 to B-13); the results are summarized here. The alkalinity to silica ratio was very high (alkalinity was much higher than silica), suggesting that most of the source material was carbonate rock and not silicates (clay). Almost all of the samples had a ratio of alkalinity to (SO_4 + Cl) of one or above, implying at least half of the cation content likely came from carbonate sources.

This result matches the Piper plot, as the anion triangle ranged between 50-70% bicarbonate plus carbonate. Carbonates could account for most of the calcium and magnesium input. The magnitude of the excess (Ca + Mg) compared to alkalinity (up to 20%) matches the calcium to magnesium ratio, indicating a non-carbonate source of calcium. The median alkalinity to (SO_4 + Cl) ratio was near 1.5, and alludes to a significant amount of sulphate being added to the Milk River. The sodium to chloride ratio was well above one, which is strong evidence of a non-halite (NaCl) source of sodium. The overall low silica concentrations indicate that the sodium source was probably not from silicate (clay) dissolution. The (Na - Cl) to sulphate ratio was very close to one, suggesting the process(es) that added sulphate to the Milk River was linked to the process(es) adding sodium. This agrees with the Piper plot results that samples with higher sodium content tended to have higher proportions of sulphate. At low concentrations of non-halite sodium, the main cations (calcium and magnesium) were balanced by the main anions (carbonate and sulphate). As non-halite sodium increased, the ion balance shifted in favor of the anions. In particular, calcium and alkalinity concentrations decreased as sodium concentrations increased, while sulphate concentrations increased.

A Piper plot of the groundwater samples showed that each groundwater well had a relatively distinct geochemical fingerprint (Figure 23). Variation in chemistry among different wells was higher than among samples from a single well. Unlike the Milk River, there was little change in the ion proportions between the open water and winter seasons within each well (Figure 24). No notable changes in groundwater chemistry were identified over time in Milk River Aquifer wells (AGRA 1998).

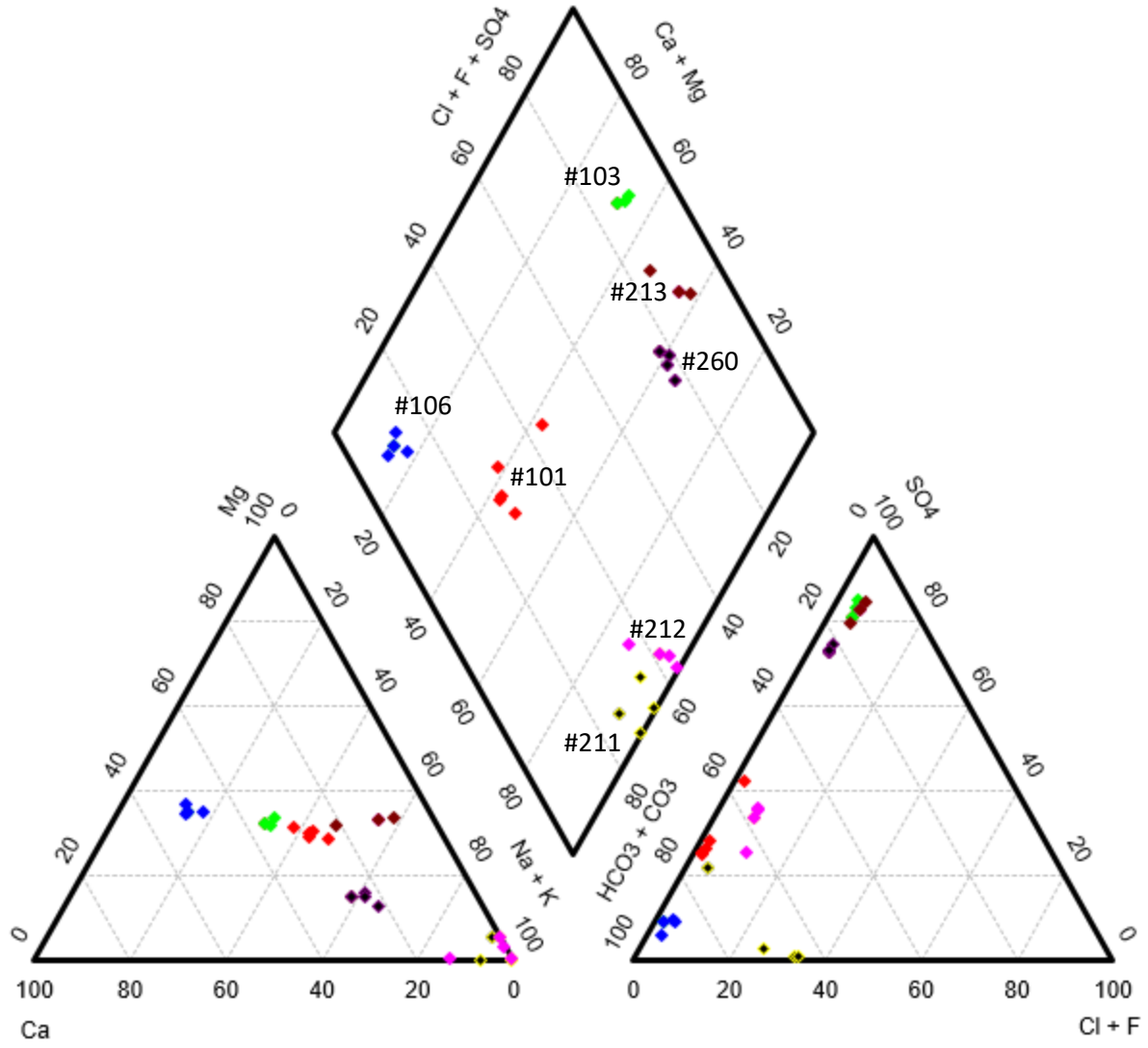

Figure 23: Piper plot of groundwater chemistry from the Groundwater Observation Well Network (GOWN). GOWN ID numbers are placed near their respective clusters, which are colored. See Figure 4 for locations of the wells. Ion proportions based on equivalents.

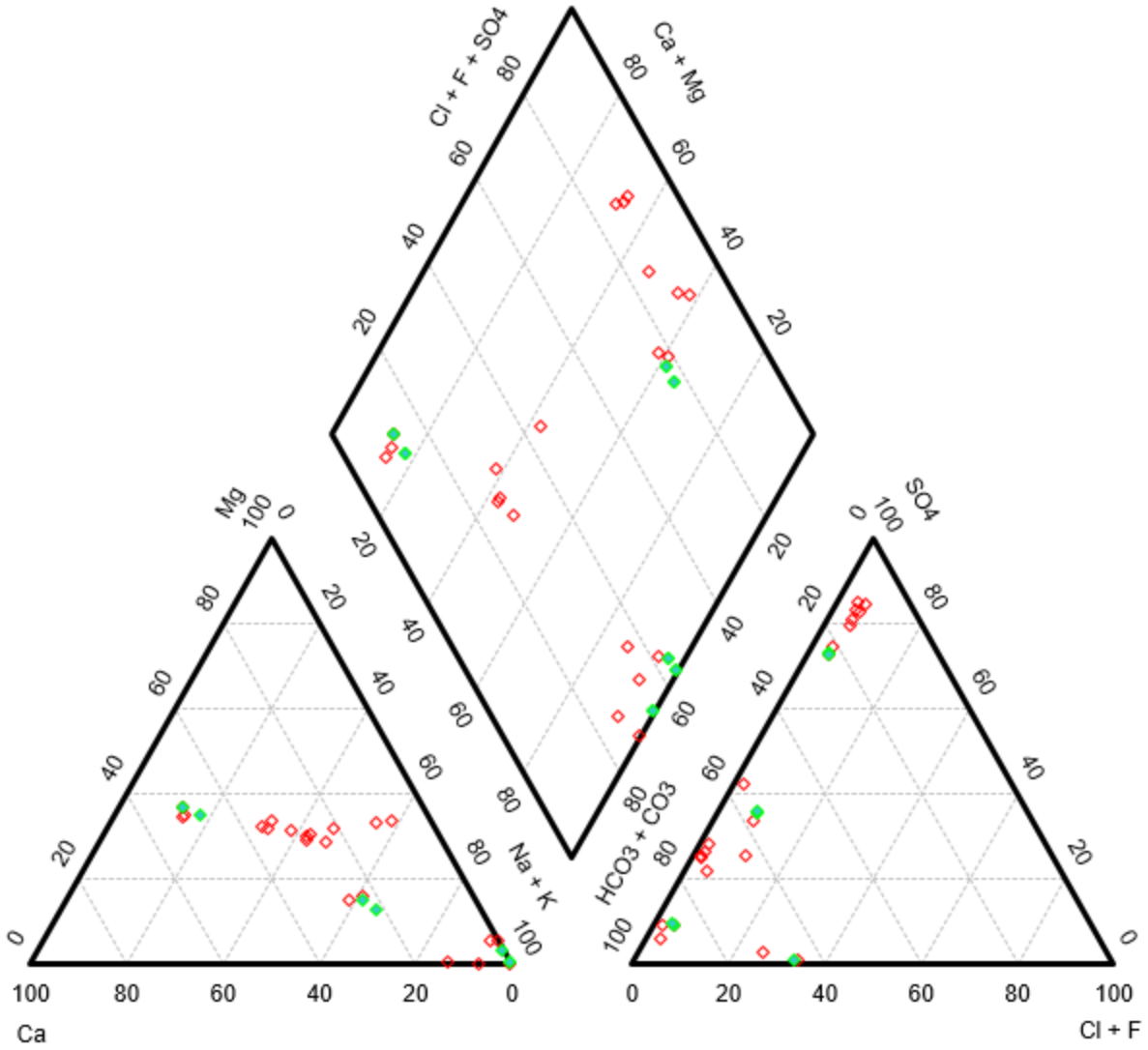

Figure 24: Piper plot of groundwater chemistry from the Groundwater Observation Well Network (GOWN). Green diamonds = open water; red diamonds = winter. Ion proportions based on equivalents.

GOWN Well #106 was located around Cypress Hills. This is a known area of groundwater recharge, and lies north of the Milk River. The geochemistry is strongly calcium-carbonate, with some magnesium. This site represents relatively fresh groundwater that has undergone minimal amounts of processing.

GOWN Well #103 was positioned near the calcium-sulphate endmember. The proportion of calcium decreased by 15% relative to Well #106, with the difference made up by an increase in sodium. The high calcium-sulphate content suggests the influence of anhydrite/gypsum in the water. Wells #213 and #260 also had very high proportions (80-90%) of sulphate, which may be related to all three wells being located on the north side of the Milk River. Well #103 and #213 were at similar surface locations and depth; although there was a notable shift from a calcium-magnesium to sodium-potassium water, these two wells were still the most similar based on the Piper plot. Well #260 was deeper, which may explain the continued trend towards a sodium/potassium-dominated cation chemistry. Although Well #103 was located within 70 m of GOWN Well #212, they had very different chemistry. Well #103 was primarily

calcium-sulphate, while Well #212 was a sodium-carbonate-sulphate (with notable chloride content). Well #212 was substantially deeper than Well #103 (60 m compared to 10 m), suggesting the difference in chemistry is due to a different groundwater source. GOWN Well #212 was located in the subcropping area of the Milk River Formation, while Well #213 was in a gravel bed (Pétré and Rivera 2015).

GOWN Well #101 was the only well in this study on the south side of the Milk River, and had a large production range. The geochemistry was mainly calcium and magnesium carbonates with a substantial proportion (~40%) of sodium plus potassium. The sample from Well #101 with relatively high sulphate concentrations was noted as having free gas, suggesting sulphides were present.

Infiltration and exfiltration of Milk River water in the alluvium during and after the diversion (respectively) could influence the groundwater well chemistry. Both processes may be linked to how much groundwater is withdrawn. This was evaluated by looking at the change in water depth at Well #101 at Del Bonita, Well #103 near Milk River, and Well #260 (also near Milk River) from the GOWN network. Annual median well depths during the summer (June, July, August) 1988-2001 were lower than the subsequent annual median well depths in the winter (November, December, January) of the same year (Figure 25). This is consistent with water withdrawals during the season, and not with infiltration of Milk River (St. Mary River diversion) water into the groundwater during high flow periods. Both median water depths as well as the variability in water depth was highest at Well #101 (Del Bonita), which was the only station south of the Milk River. The seasonal variability in median depth was approximately 13% of the annual well depth for Well #101, 1% for Well #260, and 8% for Well # 103. The annual seasonal differences in water level at Well #101 for years when chemistry was available (see Table B-2) ranged from -0.85 m to +0.77 m, and hence represent conditions when both the summer water level was greater than the winter water level, as well as the reverse. Both conditions were also observed at Well #260; annual seasonal differences ranged from -0.09 m to +1.63 m when water chemistry was available. The annual seasonal differences were all negative (winter depth greater than summer depth) at Well #103.

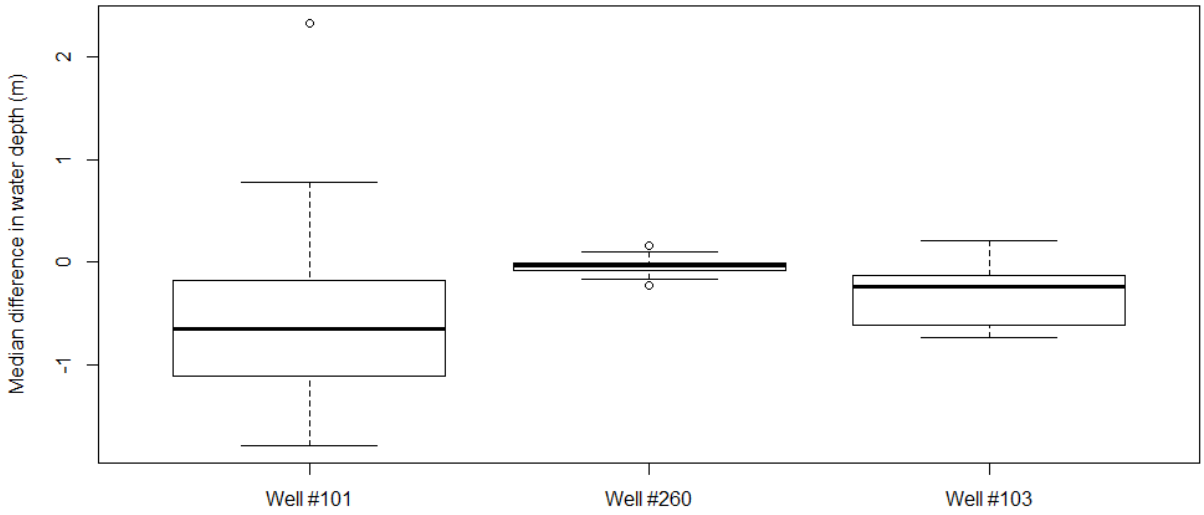

Figure 25: Annual seasonal median differences in well water depth. For each year in the well record, median well depth in the summer (June, July, August) were subtracted from the median well depth in the following winter (November, December, January). The boxes summarize the distribution of the annual median differences from 1988 to 2001, when data were available from all the wells.

A three-component mixing model was created to explore whether TDS concentrations at Hwy 880 could be explained by the conservative mixing of water from the North Fork, South Fork, and groundwater. The results of the mixing model included proportions >100% and <0%, and were not reasonable (Table 3).

Table 3: Results of the mass balance calculation. The values are the proportion (out of 100%) that are coming from each source.

Source	Milk River at Milk River	Milk River at Hwy 880
North Fork	131%	-662%
South Fork	-60%	1014%
Groundwater	44%	-172%

3.3.2 Discussion

Thompson (1986) calculated an average increase in water volume in the Milk River from 1910-1916 between the upstream and downstream crossing of the border between Alberta and Montana, before the St. Mary River diversion had begun. A 2007 study completed once diversion flow stopped also identified a consistent increase in flow from upstream to downstream of a similar magnitude (MacCulloch and Wagner-Watchel 2010, 2011). In those studies, flow was added at a rate of 0.002 m^3/s per km. The additional flow was attributed to discharge into the Milk River from alluvium (Thompson 1986). In the current flow balance, there was approximately 165 km of river that could contribute to additional flow: 88 km along the North Fork, 39 km along the South Fork, and 38 km between the confluence of the North and South forks and the town of Milk River. An ungauged source of flow contributing 0.002 m^3/s per km could add 0.33 m^3/s of flow, which is equal to both the most common value for the flow balance (Figure 16). The increase in open water ion concentrations observed in the Milk River at the two furthest downstream stations supplies further evidence of an ungauged source of ions (see **Error! Reference source not found.**).

One potential source of ungauged flow is from snowmelt downstream of the North and South Fork gauging stations. Since the gauging stations are located near the international border, there is a large catchment area that could accumulate snow and not be captured by the gauging stations. Based on a snowmelt rate of 1 cm per day, the ungauged flow (0.6 m^3/s) could be met with a snow cover of 52 km^2. As a rough approximation, the watershed that contributes to flow at the town of Milk River is around 1000 km^2. Only 5% of the snowmelt in the catchment area would be required to create the required ungauged flow. This calculation suggests that snowmelt has the potential to provide substantial amounts of water to the Milk River during chinooks. However, the consistently low correlation between the snowmelt and flow balance, coupled with a (weak) negative correlation when accounting for a lag, indicates snowmelt is unlikely to be the source of ungauged flow to the Milk River in the winter predicted by the flow balance.

In southern Alberta, snow accumulation is strongly controlled by sublimation (Dixon et al. 2014; MacDonald et al. 2018). When snow sublimates, the water frozen in the snow converts to a gas directly rather than forming a liquid. Sublimating snow would appear as a loss of the snow depth with no associated overland flow. Chinook winds are associated with both higher temperature as well as a lower humidity; the latter contributes to sublimation. Snow blown by high winds, which often occur in southern Alberta during chinooks, also has a higher sublimation rate (MacDonald et al. 2018). Soil moisture did not change over the course of three winter chinooks occurring in southern Alberta (MacDonald et al. 2018), further suggesting changes in the snow pack were not contributing to surface flows in the Milk River.

The tributaries of the Milk River usually have low to zero flow (Thompson 1986), though data are limited. When the tributaries are flowing in the winter, flow rates are ~1% of the mainstem of the Milk River. They can, however, have relatively large flows during the winter due to snowmelt during a chinook. For the purposes of this assessment, the role of tributaries on total flow does not specify the sources of flow to

the tributaries (e.g., snowmelt or groundwater). Winter tributary data were not available to directly evaluate the role of tributaries in the context of where the water in the tributaries came from.

Concentrations of TDS in the Milk River tributaries downstream of the town of Milk River, especially Verdigris Coulee, can be extremely high (hundreds to thousands of mg/L; Saffran 1998). When Verdigris Coulee had flow, specific conductance in the Milk River downstream of the coulee mouth increased by 100 µS/cm (≈40 mg/L TDS), though it only made up 6% of the total TDS load of the Milk River (Saffran 1998). During the 2016 open water season, the specific conductance of Red Creek (which is not affected by the St. Mary River diversion) ranged from 2290 to 3450 µS/cm, or around 1460 to 2200 mg/L TDS (Palliser 2017), which would have the potential to add substantial amounts of TDS if winter flows were sufficient to link Red Creek to the Milk River mainstem. The high TDS concentrations in Red Creek are linked to groundwater (MRWCC 2013). Unfortunately, data are not available to know for certain whether the tributaries upstream of the town of Milk River actively contributed to the flow or mass balance. However, the ephemeral nature of the tributaries make them an unlikely source to provide additional flow or TDS to the Milk River throughout the winter each year.

The input of groundwater is another potential source of ungauged flow to the Milk River in the winter. The Milk River basin has features that indicate extensive groundwater effects, including springs and soil piping. Groundwater could come from a variety of sources, including recent infiltration of snowmelt, or transport of groundwater through the Milk River Aquifer, Whiskey Valley Aquifer, or overlying till. Salts in groundwater come primarily from aerosols, salts dissolved in recharge water, and/or from mineral dissolution (Salama 1999). The latter is often the most important.

The hydrologic budget presented in Rivera et al. (2017) estimates groundwater discharge from the Milk River Aquifer to the Milk River at 0.3 m^3/s, which is in good alignment with the additional flow observed at the town of Milk River. Thompson (1986) also observed an increase in flow and specific conductance in the Milk River after diversion from the St. Mary River was shut off, and attributed the additional water and salt to discharge from the alluvium.

The Milk River at Hwy 880 Piper plot and ion ratio results suggest the following:

- Most of the weathering reactions producing TDS comes from carbonates, with additional material from sulphates. Relatively little TDS appears to be associated with silicate weathering.

- The calcium and magnesium content is primarily from the weathering of carbonates, such as calcite ($CaCO_3$) and dolomite [$CaMg(CO_3)_2$]. An additional source of calcium is likely present at certain times.

- There is a large source of sulphate. The addition of sulphate occurs with the addition of sodium, and the removal of calcium. The sulphate source may be from calcium sulphates (anhydrite/gypsum), but likely includes a calcium-sodium exchange reaction that reduces calcium concentrations when high sodium concentrations are present. Sulphate may also be added through sulphide oxidation.

- The source of sodium is unlikely to be halite (NaCl) or silicate weathering, and appears to be linked to ion exchange reactions with calcium.

The following specific reactions are suggested as driving the winter surface water chemistry in the Milk River:

- Dissolution of calcite: $CaCO_3 \leftrightarrow Ca^{2+} + CO_3^{2-}$
- Dissolution of dolomite: $CaMg(CO_3)_2 \leftrightarrow Ca^{2+} + Mg^{2+} + 2CO_3^{2-}$
- Dissolution of anhydrite: $CaSO_4 \leftrightarrow Ca^{2+} + SO_4^{2-}$

- Calcium/sodium ion exchange: Na-clay + Ca^{2+} ↔ Ca-clay + $2Na^{+}$

In these reactions, the carbonate would actually be present as bicarbonate.

These combinations of reactions are sufficient to explain the distribution of samples in the Piper plot (Figure 22). Most samples had a cation composition 60% Ca - 30% Mg - 40% Na + K. More extreme points formed a line pointing towards the 100% Na + K corner of the cation triangle. Based on the ion ratio results, the trend in the cation triangle is interpreted as the relative degree of calcium to sodium ion exchange, with samples closer to the 100% Na + K corner having undergone more extensive cation exchange. Ion exchange between sodium and calcium/magnesium was invoked to explain the high proportion of sodium in groundwaters from the Milk River Aquifer (Schwartz and Muelhenbach 1979). Two patterns in strontium and strontium/calcium ion ratios, corresponding to more and less aged groundwaters, were associated with flow paths through glacial till and the Milk River Aquifer, respectively (Armstrong et al. 1998). The variability in ion ratios at the Hwy 880 site could be related to the relative proportions of groundwater originating from different areas/formations.

Samples in the anion triangle were distributed between the bicarbonate plus carbonate and sulphate corners. The proportion of TDS consisting of sodium increased linearly with the proportion of TDS consisting of sulphate. The linear nature of the relationship suggests a common factor controlling the proportions, though the reaction equations did not contain a mineral that directly linked sulphate and sodium production. Rather, this pattern is interpreted as two independent processes that are linked through a third, mainly the travel time from a groundwater recharge area to when the water enters the Milk River. A longer travel time could result in more extensive ion exchange and more dissolution of anhydrite/gypsum, or sulphide oxidation. The correlation between sodium and sulphate could be linked to the weathering of sodium clays, whereby sulphur oxidation and associated acid generation increases the concentration of free sodium (Grasby et al. 2010; Huff 2014), though the overall low silica concentration is problematic for this explanation. Sulphate produced from sulphide oxidation could also be precipitated as gypsum (Van Stempvoort et al. 1994), which would push both the calcium to sodium and sulphate to sodium ratios towards one to one (the median Ca : Na ratio is 0.84; median SO_4 : Na ratio is 1.02). A similar list of processes that could explain the prevailing spatial trends in ion chemistry is provided by Pétré et al. (2016).

Geochemical modeling of pore water in the glacial till of southern Saskatchewan indicated that major ions consisted of both free ions as well as dissolved complexes such as $CaSO_4$ and $NaSO_4^-$ (Hendry and Wassenaar 2000). It is worth noting that since the measured ion concentrations from the Hwy 880 station are totals (i.e., particulate plus dissolved), interpretations of the ion ratios may be incorrect if the proportion of ion complexes is high.

Groundwater chemistry compiled by Pétré et al. (2016) identified six water types located throughout the Milk River Aquifer. The Hwy 880 samples match their Group 1, which were calcium-magnesium-carbonates originating from the Sweet Grass Hills recharge area. Immediately to the north (i.e., along the groundwater flow path leading to the Milk River), the chemistry changed to sodium-carbonate-sulphate (their Group 4); much of the calcium plus magnesium was replaced by sodium with the relative proportion of sulphate remaining similar between groups. This signifies that part of the evolution of groundwater in the Milk River Aquifer is the replacement of calcium with sodium as the dominant cation. Evaporites in Alberta soils are limited to gypsum, bassanite (also a calcium sulphate mineral), and calcite; these minerals were highlighted as potentially important sources of calcium and sulphate (Salama 1999). The mineral sources and reactions likely occur naturally in the Milk River basin.

The Milk River Aquifer flows from the south to the north, with water originating (recharging) in the Sweet Grass Hills and Cut Bank areas, and the Milk River intercepting northern flow (Pétré and Rivera 2015). The aquifer continues on the north side of the river, though the water there is substantially older. As described in Pétré and Rivera (2015), the primary source of groundwater recharge to the Milk River

Aquifer (the Virgelle sandstone) is from the infiltration of precipitation. Water closer to the recharge areas have more calcium-magnesium-carbonate chemistry, with increasing proportions of sulphate and sodium as water moves away from the recharge area. Sulphur isotope composition in sulphate measured in groundwater in the Milk River basin indicated an identical source of sulphur in glacial till and recharge waters (Drimmie et al. 1991; Grasby et al. 2010). Strontium isotope ratios and strontium to calcium ratios in pore waters near the Sweet Grass Hills recharge area confirmed that the groundwater was influenced by glacial till (Armstrong et al. 1998). The strontium to calcium ratios also revealed ion exchange reactions are important in the Milk River Aquifer. Soils in the Milk River area are often Solonetzic, which have high concentrations of exchangeable sodium (Miller and Brierley 2011). Calcium to sodium ion exchange was noted in oxidized depth profiles of glacial till in southern Saskatchewan, as well as the oxidation of pyrite producing elevated sulphate concentrations (Hendry and Wassenaar 2000).

Winter surface samples at Hwy 880 aligned with groundwater samples from GOWN Well #101 (**Error! Reference source not found.**), though the Hwy 880 samples generally had a higher portion of ($Cl + F + SO_4$) than Well #101. Well #101 was on the south side of the Milk River, at a depth consistent with glacial till. The chemistry of surface waters at Hwy 880 indicate a groundwater source that is within the glacial till and has undergone some modification (e.g., ion exchange and sulphate addition). Water from Wells #101 and #106 were relatively close to the recharge areas; Well #106 was in the Cypress Hills recharge area, and Well #101 was on the South side of the Milk River and potentially fed by the Cut Bank and Sweet Grass Hills recharge zones. Both wells #101 and #106 had primarily calcium-magnesium-carbonate chemistry, likely originating from relatively “fresh” glacial till. Similar chemistry is expected from surface water-groundwater interactions related to the Whiskey Valley Aquifer, a small sand and gravel aquifer located under the Milk River and above the Milk River Aquifer (Golder Associates 2004).

The failure of the two-component mixing model challenges the assumption that only the North and South forks contribute to the Hwy 880 TDS concentration, but rather suggests an additional source of ions contributed to the total load. A similar unknown source was identified by Saffran (1998) when upstream and downstream loads of sodium were compared along the Milk River. The failure of the three-component mixing model that included a groundwater source suggests that the surface water concentrations do not result from simple conservative mixing, at least not using these sources and analytes. Alternatively, the groundwater chemistry from the Well #101 November 2012 sample may not be related closely enough with the surface chemistry data from March 2017. Concentrations of sodium, sulphate, and chloride were notably higher in Well #101 for November 2012 compared to the other years with data at the same location (see Table B-3).The flow balance for this particular day (March 14, 2017) was also negative (more inflow than outflow) by 1.2 m^3/s, and had deficit of 20.7 m^3/s the following day. The high, negative flow imbalance suggests that the dataset used in the three component mixing model may not be suitable. Unfortunately, this dataset had the only combination of surface water chemistry from all three sources (North Fork, South Fork, and downstream receiving environment).

Changes in both absolute concentrations of major ions as well as analyte ratios occurred from upstream to downstream. In particular, the downstream stations had a lower content of calcium and magnesium, and an increase in sulphate. The reduction in calcium and gain in sulphate matches the change in ion composition that occurred between fresh and aged groundwater. However, the absolute values of the ion ratios were similar to values from GOWN Well #106, in the Cypress Hills recharge area, rather than modified groundwater. A diffuse source like groundwater could intercept the Milk River from either bank, and/or the riverbed. A bank source corresponds to water traveling through glacial till or the Milk River Aquifer, while the Whiskey Valley Aquifer underlies the Milk River in an ancestral streambed (Pétré et al. 2016). As surface water in the Milk River travels downstream, it could continually pick up additional TDS from these sources. The prediction that groundwater input results in a constant increase in TDS and associated concentrations with distance traveled downstream (assuming the rate and type of groundwater addition does not vary over the river reach) was observed during the open water measurements along the western portion of the Milk River.

The geological impacts on Milk River water chemistry could be altered by human activities, including road salting, discharge from the town of Milk River, groundwater usage, or industry. Road salts often consist of halite (NaCl) and their addition could affect the proportion of sodium and chloride in the Milk River. The sodium to chloride ratio was well above the one to one ratio predicted if halite addition was a major source of sodium to the Milk River. Chloride concentrations could be partly driven by road salt additions. However, the proportion of chloride was small (<10%) compared to carbonate and sulphate, meaning the potential addition of road salt would not have a large impact on the water quality of the Milk River. The quantity of road salt applied is likely insignificant in the Milk River basin (Ryan Leuzinger, pers. comm.). A high ratio of calcium to chloride and low percentage chloride also indicate calcium chloride ($CaCl_2$) salt addition would only have only a minor effect on winter concentrations of TDS in the Milk River.

Total dissolved solids could be added to the Milk River directly by the town of Milk River. For instance, the municipality uses copper sulphate as part of their water treatment (http://www.milkriver.ca/water-treatment-distribution/Personal communication); a leak in the sedimentation basin could potentially result in elevated concentrations of sulphate. Drinking water in the town of Milk River is treated with fluoride, which could unintentionally enter the Milk River. A leak in the sewage lagoon could also discharge a variety of materials into the Milk River. Unfortunately, no data were available upstream or downstream of the town of Milk River during the same year to directly examine potential influences of the town. Winter TDS concentrations downstream of the town of Milk River measured in the late 1980's were around 430 mg/L and usually did not exceed the SWQMF limit, suggesting discharge from the municipality is not the primary driver of the SWQMF limit exceedances. However, these data may be too old to reflect current impacts of the town of Milk River.

The land directly adjacent to the Milk River is mainly agricultural. The small and inconsistent seasonal changes in well depths indicate that TDS concentrations in the Milk River are unlikely to change as a result of potential infiltration of Milk River (St. Mary River) water into the alluvium during diversion, or through current groundwater usage. There is no active coal mining occurring near the Milk River. Only a couple of petroleum and natural gas processing facilities operate south of Lethbridge (https://www.energy.alberta.ca/AU/Services/Pages/PDF-Maps.aspx). However, there was a cluster of active natural gas wells along the Milk River approximately 10 km upstream of the Hwy 880 sampling location. Data were available from November 2006 to directly compare winter concentrations of salts measured at Writing-on-Stone Provincial Park (upstream of the wells) to Hwy 880 (downstream of the wells). This comparison showed that two potential indicators of gas extraction activity, chloride and fluoride concentrations, changed by 10% and 6% respectively from upstream to downstream. This is a smaller percent change than any of the other major ions making up TDS except for carbonate, and indicates that industrial activity is likely not having a major influence on TDS concentrations at Hwy 880. Additional potential indicators of extraction activity (e.g., total organic carbon, specific organic compounds, metals) were not available from the Writing-on-Stone Provincial park location.

The literature review identified eight processes that could contribute TDS to the Milk River (see Section 1.4). Processes that have not yet been considered in this report include ice scouring, non-erosional overland flow, and erosional overland flow. These three processes are episodic: ice scouring can only occur when ice is present and moving, and overland flow during the winter relies on snowmelt. Chinooks are episodic, and could potentially drive the changes in ice and overland flow required by these three processes. Although TDS concentrations do vary during the winter and the variability could be linked to chinook-driven processes, none of the three processes can explain the high concentrations of TDS that occur during the majority of the winter. Chinook conditions (warmer air temperatures) are less common during the winter than colder weather (when ice scouring and overland flow do not occur), so these TDS generating mechanisms would likely create peaks in TDS concentration, rather than the uniformly high TDS concentrations observed.

3.3.3 Question #2 Conclusion:

A flow balance identified a source of ungauged flow to the Milk River in winter, which could be due to tributary flow, snowmelt, or groundwater. Data were not available to directly evaluate the role of tributary flow. Although sufficient water was available from snowmelt to create the extra flow, the lack of a robust relationship between snow melt and the flow balance, as well as the direction of the lagged correlation and high potential for snow sublimation, suggest that snowmelt is not a major contributor. In contrast, groundwater flow rates did match the ungauged flow rates.

Milk River chemistry at Hwy 880 in the winter was primarily calcium-magnesium-carbonate. Based on various ion ratios, the chemistry of the Milk River is hypothesized to be driven by calcium carbonate and calcium magnesium carbonate weathering, combined with ion exchanges between calcium and sodium, and the addition of sulphates from weathering and/or sulphide oxidation. Both ion exchange and sulphate production indicated more extensive processing, potentially linked to the residence time of the groundwater before it enters the Milk River.

A mixing model calculation demonstrated that the downstream TDS load was not met solely from the North Fork and South Fork. Unfortunately, a mixing model that also included a groundwater source produced uninterpretable results. However, the surface water at Hwy 880 did match the chemistry of a groundwater well sample south of the Milk River. Downstream patterns in Milk River water chemistry were consistent with the input of modified groundwater.

The combination of these analyses, plus previously published literature regarding the influence of groundwater and the Milk River, and signs of surface expressions of groundwater behavior such as springs and soil piping, provides a weight of evidence that groundwater is likely a primary source of TDS to the Milk River during the winter. Although data were generally not available to evaluate specific sources, it did not appear that road salt addition, discharge from the town of Milk River, or petroleum/natural gas extraction were major contributors to the TDS concentration in the Milk River.

3.4 Investigation Question #3: What are the main processes controlling variability in total dissolved solids concentrations during the winter?

3.4.1 Results

The median seasonal (open water to winter) change in TDS concentrations – which is due to the dilution of TDS by the input of diverted St. Mary River water — was 428 mg/L (160 mg/L during open water, and 588 mg/L during the winter). The annual range of winter TDS concentrations varied from 250 mg to 910 mg/L (Figure 266). The observed variability during a single season (winter) is approximately the same as the amount of seasonal variability. Moreover, the variability between subsequent monthly samples (e.g., change between November 2013 and December 2013) was as high as 680 mg/L (Figure 27), though the median change was 180 mg/L.

Changes in TDS concentrations of ≈400 mg/L were observed over a period of two weeks, and changes of ≈100 mg/L occurred regularly over a few days. Although the time-series from the different datasonde deployments produced different records, there were three attributes consistent among all of the winter time-series (see Figure C-1 to C-4):

- Large peaks in TDS were relatively symmetrical
- Changes in TDS were generally smooth; there were few large jumps in concentration
- The time-series of TDS exhibited fine structure, specifically small dips that occurred daily

In addition to the magnitude of the changes in TDS, these characteristics of the datasonde time-series need to be represented by the process responsible for changing the overall TDS concentrations during the winter. A time-series from January 2 to January 12, 2012 was examined in more depth (Figure 28).

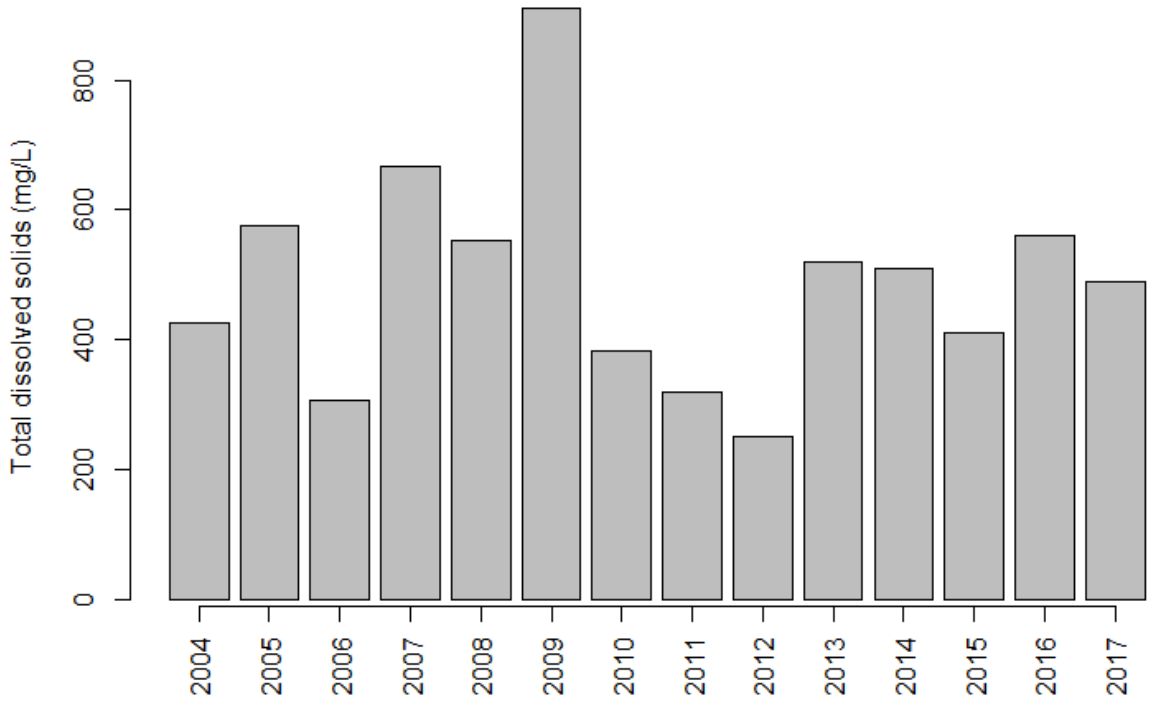

Figure 26: Annual range of winter total dissolved solids concentration (maximum monthly TDS- minimum monthly TDS); 2004-2017 from the Milk River at Hwy 880. A full year of TDS data was not available before 2004.

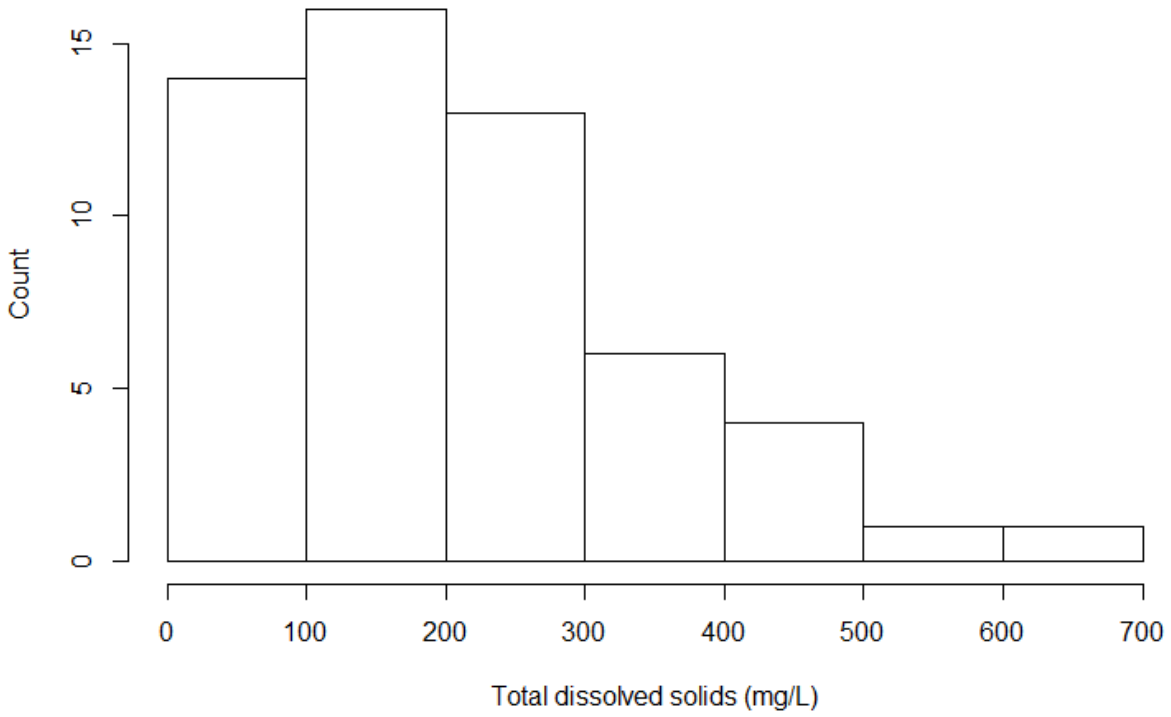

Figure 27: Absolute value of the difference in total dissolved solids concentrations between subsequent winter months, Milk River at Hwy 880, 2003-2017. For example, the TDS concentration decreased from 778 to 621 mg/L between January and February 2004. The difference (February - January) is -157; the absolute difference is 157, and the absolute difference is included in the bar extending between 100 and 200 mg/L. November 2006 had two measurements that were averaged for this calculation.

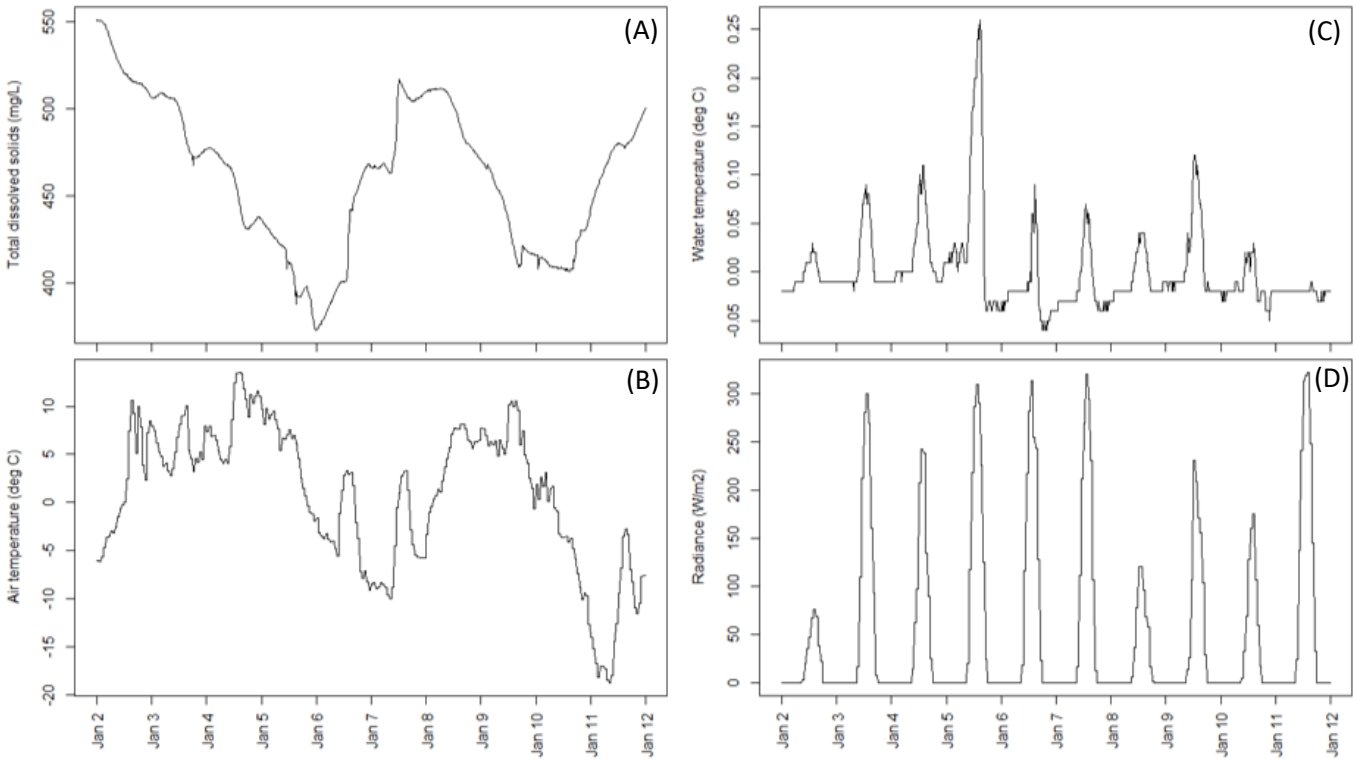

*Figure 28: Ten days of data used to test the hypothesis that salt exclusion affects TDS concentrations. All data are from January 2 to January 12, 2012. Total dissolved solids was converted from specific conductance measured by a datasonde at the Hwy 880 bridge using the formula: TDS (mg/L) = 0.66 *specific conductance (uS/cm) - 25.6 (see* Figure 5*). Air temperature and radiance are from an Agriculture Canada meteorological station at the town of Milk River. Water temperature was measured by the same datasonde as specific conductance.*

The time-series of TDS (Figure 28, A) began with a 150 mg/L decrease in concentration, punctuated by daily depressions in the TDS concentration. This occurred from around January 2 to January 5. During this time, air temperature (B) fluctuated twice daily with daily minimums three to ten degrees above 0°C. Water temperature (C) peaked once per day during the middle of the day, with nighttime minimums slightly below 0°C. The timing of the water temperature peaks corresponded with the peaks in radiance (D), though the magnitude of the peaks in water temperature did not scale with radiance. The timing of the daily depressions in TDS concentration aligned with the peaks in water temperature and radiance.

There was no fixed relationship between TDS concentrations and air temperature (Figure 29). In part, the lack of structure may be due to the distance between the meteorology station at the town of Milk River and the Hwy 880 sampling site (≈60 km). However, the combination of the qualitative relationship between air temperature and TDS concentration, and the alignment of the daily dips in TDS concentration with water temperature and radiance suggests that salt exclusion is a viable process to explain the observed short-term variations in TDS concentration. This was confirmed using a physics-based ice volume model developed for the Milk River as part of this investigation.

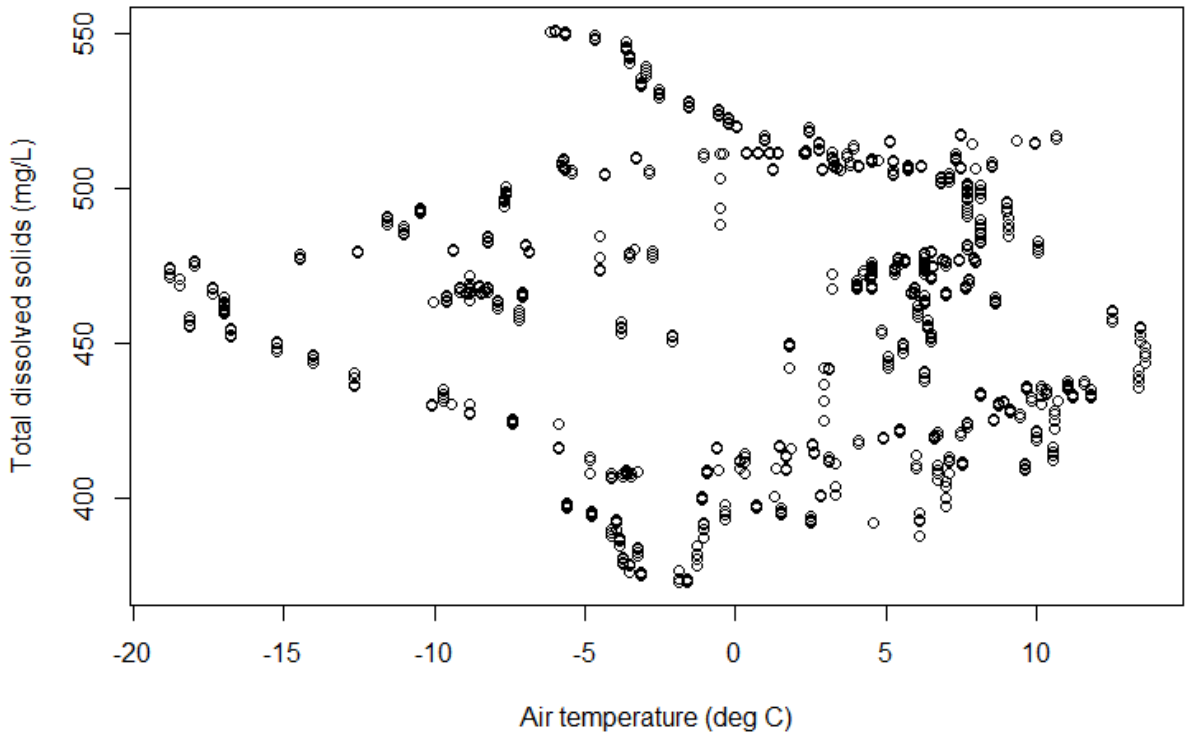

*Figure 29: Relationship between air temperature (measured at the town of Milk River) and total dissolved solids concentration (measured as specific conductance in the Milk River by a datasonde at the Hwy 880 bridge). Concentrations of total dissolved solids were calculated from the specific conductance reported by the datasonde using the formula: TDS (mg/L) = 0.66 *specific conductance (uS/cm) - 25.6 (see Figure 5).*

The calibrated ice volume model successfully recreated the range and main features of the observed water temperature (Figure 30) and TDS concentrations (Figure 31). The overall pattern was driven by the accumulation and loss of ice, which in turn was controlled by the amount of energy transferred between the air and water based on the temperature differential. The small, daily dips in TDS concentration (and ice volume) were a result of radiative heating that was independent of the air temperature.

There was a significant trend in the residuals (predicted results minus observed results), with the model increasingly overestimating the observed results at higher specific conductivities and underestimating observed results at higher temperatures (Figure 32). Although statistically significant (p<0.05), the strength of the trends in the residuals were very low (r^2 = 0.05-0.08).

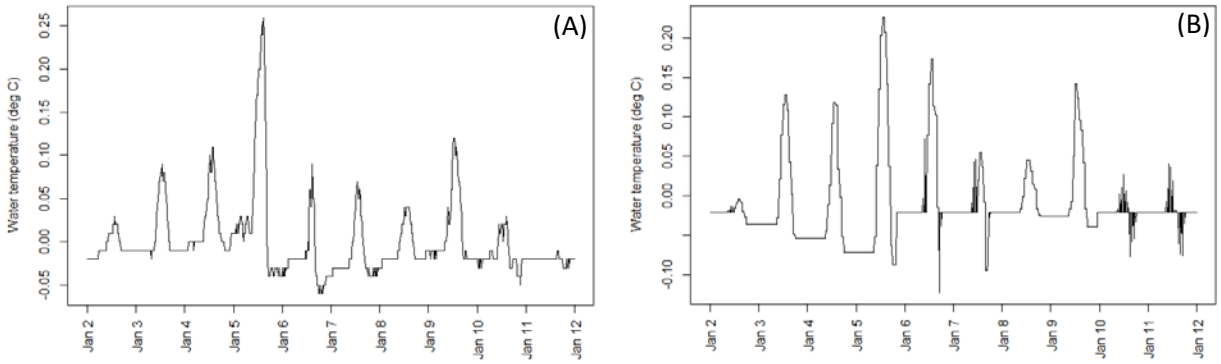

*Figure 30: Observed (A) and modeled (B) water temperature at the Hwy 880 bridge, January 2 through 11, 2012. Modeled = 0.89(±0.03) * Observed - 0.011(±0.001); r^2=0.57; p<0.01; n=960.*

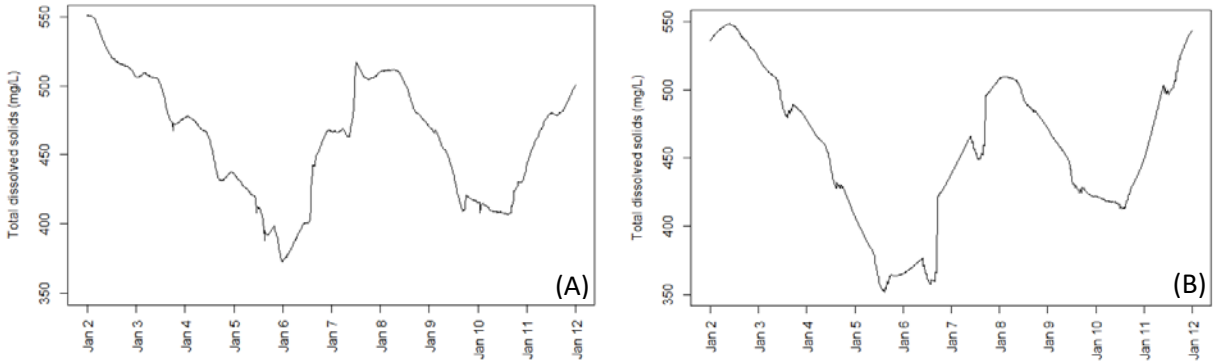

*Figure 31: Observed (A) and modeled (B) total dissolved solids concentrations from a datasonde at the Hwy 880 bridge, January 2 through 11, 2012. Total dissolved solids concentrations (observed and modeled) were calculated from specific conductance using the equation TDS (mg/L) = 0.66 *specific conductance (uS/cm) - 25.6 (see* Figure 5*). Modeled TDS = 1.15(±0.02)*Observed TDS - 74.9(±7.5); r^2=0.84; p<0.01; n=960.*

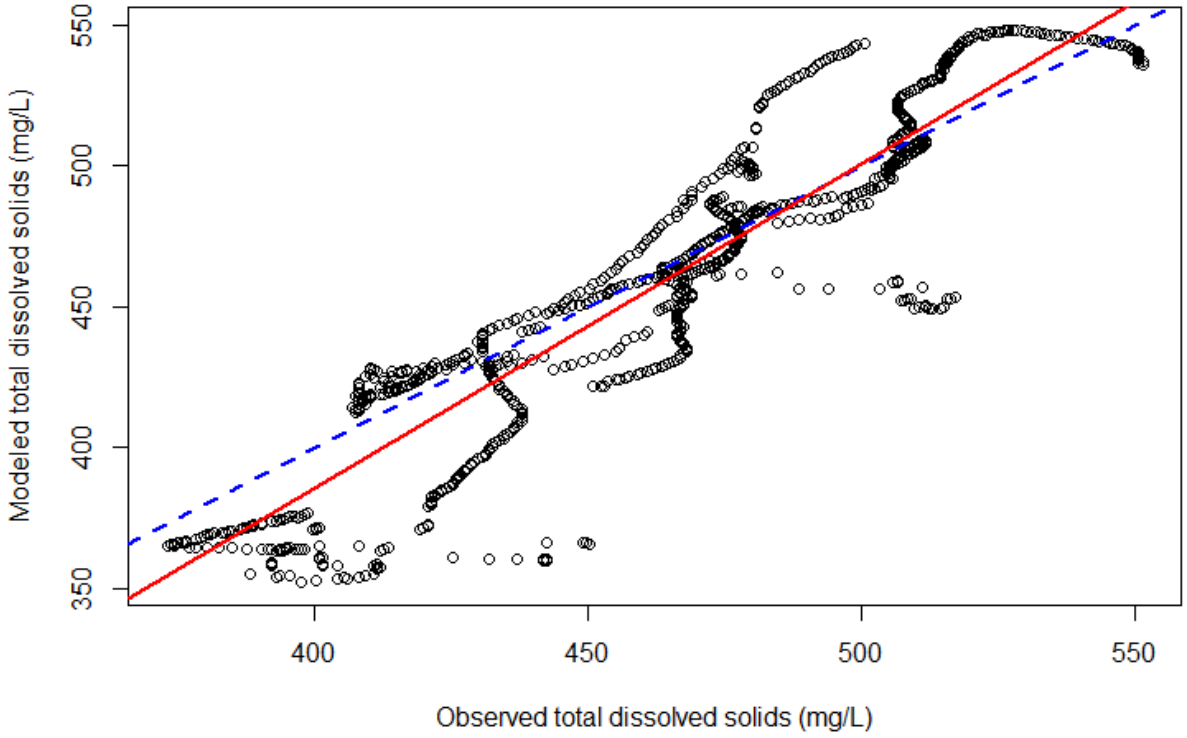

*Figure 32: Observed and modeled total dissolved solids concentrations from a datasonde at the Hwy 880 bridge, January 2-11, 2012. Total dissolved solids concentrations were calculated from specific conductance using the equation TDS (mg/L) = 0.66 *specific conductance (uS/cm) - 25.6 (see Figure 5). Dashed blue line indicates a perfect match between predicted and modeled results. Red line is the linear regression results: Modeled TDS = 1.15(±0.02)*Observed TDS - 74.9(±7.5); r2=0.84; p<0.01; n=960.*

3.4.2 Discussion

The process causing the variability in winter TDS concentrations had to explain three features noted in the datasonde time-series of specific conductance: large, symmetrical peaks; smooth changes; and small, daily dips. One process that meets the three criteria is salt exclusion, also known as brine rejection. During the formation of ice, the crystal lattice of the ice rejects salt ions. The salt ions can become concentrated in the remaining unfrozen solution. This process implies a positive correlation between the amount of ice and the TDS concentration, since higher ice volumes would result in more salt exclusion and greater concentration in the solution. However, the relationship may not be well-structured:

- the purity of the ice depends on the concentration of salts in the solution the ice is being formed from; water that begins with a high TDS concentration may not exclude as many ions
- Ice formation and melting depends on the air temperature, water temperature, radiance absorbance, ice thickness, and potentially other factors

Although the model created an accurate hindcast of TDS concentrations, the validity of the model is contingent on a few assumptions:

1) The relative volumes of air and water participating in energy exchange are reasonable and constant. In the model, the relative volumes are based on the relative densities: the volume of water is 1000 times that of the volume of air, and corresponds to the number of molecules available to participate in energy exchange.

2) Two model parameters control the impact of radiant energy on water and ice, and perform the role of controlling the albedo (reflectivity). The ratio of the two model parameters (water to ice) is 9, and is similar to expected ratios of the albedo of ice/snow (≈0.8) to the albedo of water (≈0.08).

3) There is a proportional relationship between changes in ice volume and specific conductance/TDS concentrations. The model predicts a relative ice volume, which was linearly scaled to convert the range of ice volumes to specific conductance/TDS concentrations.

4) Changes in ice volume occur in parallel among different areas of the Milk River. The model does not require the same amount of ice everywhere along the river, but the relatively proportions of ice are assumed to be constant everywhere. This assumption is required to keep the relationship between ice volume and salt exclusion constant.

5) Flow rates are constant over time. When flow rates are constant, the volume of water being sampled is affected by processes (including salt exclusion) acting a fixed distance upstream. If the flow rates increase (decrease), the water being sampled reflects processes acting over a larger (smaller) area. Flow rates varied by 1.2 m^3/s (approximately 0.09 m/s) at the town of Milk River over the modeled period, which equates to an extra 80 m of the river contributing to salt exclusion. The weak trends observed in the model residuals with air temperature and specific conductance are consistent with mild violations of this assumption.

The ice model indicates that TDS concentrations are related to ice volume and melting. This relationship suggests that other processes linked to ice and snow melt, including ice scouring, non-erosional overland flow, and erosional overland flow (see Section 1.4) may also contribute to changes in winter TDS concentration. Ice and overland flow would likely have the largest (positive) impact on TDS concentration during snow and ice melt, and hence a positive relationship between temperature and TDS concentration. The model results indicate that increasing air temperatures generally decreases the TDS concentrations. The actual air temperature-TDS concentration relationship is not well structured, and the opposing directions of salt exclusion versus ice scouring and overland flow on TDS concentration may contribute to the scatter. However, the overall negative relationship between TDS concentration and air temperature predicted by the model indicates salt exclusion is more important than ice scouring, non-erosional overland flow, and erosional overland flow in controlling short-term variability in TDS concentration.

3.4.3 Question #3 Conclusion:

Winter concentrations of TDS varied from year to year by hundreds of milligrams per litre. The same range of variability was observed in winter both from month to month within a single year as well as within a single week. Observed air temperature and radiance was used to model the volume of ice within the Milk River. During the formation of ice, the crystal lattice rejects salt ions. The salt ions can become concentrated in the remaining unfrozen solution, elevating the TDS concentration. The main process controlling variability in TDS concentrations occurring on short time scales (days to weeks) during the winter can be adequately explained by salt exclusion from the formation and melting of ice within the Milk River. The same process also explains the range of month-to-month variability in TDS, which would be linked to the large temperature changes associated with chinooks.

4 Overall Conclusions

Monthly measurements of water quality in the Milk River at the Hwy 880 bridge exceeded the Surface Water Quality Management Framework (SWQMF) limits for TDS in the winter (November to March) in 2015/2016, 2016/2017, 2017/2018 and 2018/2019 as well as specific conductance in the winter in 2017/2018 and 2018/2019. An investigation was initiated that focused on three questions:

- Why do the SWQMF exceedances for TDS in the Milk River at Hwy 880 only occur in the winter (November to March)?
- What is the primary source(s) of TDS to the Milk River during the winter?
- What are the main processes controlling variability in TDS during the winter?

The investigation included an extensive literature review and data analysis on surface water and groundwater quality of the Milk River and surroundings. The results of the investigation suggest the following:

- Seasonal variability (open water versus winter) was primarily controlled by the input of relatively dilute water from the St. Mary River into the Milk River. During the open water season when diversion from the St. Mary River was active, TDS concentrations and composition matched the St. Mary River. In the winter, when the St. Mary River did not contribute to the Milk River flow, TDS concentrations and composition changed to reflect a different (high TDS) source.
- Framework exceedances in the Milk River did not occur in the open water season because the St. Mary River, which made up 94% of the North Milk River flow during the open water season, has relatively low TDS concentrations.
- A primary source of TDS to the Milk River in the winter was likely from groundwater input. This is suggested from: increasing downstream flows with no apparent surface water input, a match between nearby groundwater chemistry with Milk River chemistry during the winter, the alignment of these results with previously established literature regarding the interaction of groundwater and the Milk River, and evidence of surface expressions of groundwater behavior such as springs and soil piping.
- Although data were generally not available to evaluate specific sources, road salt application, discharge from the town of Milk River, and petroleum/natural gas extraction did not appear to be major contributors to the TDS concentration in the Milk River.
- The range of variability in winter TDS concentrations in the Milk River was similar at both monthly and weekly scales. High resolution measures of specific conductance indicated that changes in salt concentration were related to changes in the volume of ice through the exclusion of salt ions. The viability of salt exclusion controlling winter concentrations of TDS in the Milk River was confirmed using a physics-based ice volume model.

Data were generally not available to exclude specific human activities from impacting the surface water quality. However, with the exception of the influence of the St. Mary River diversion, the investigation did not find evidence of anthropogenic impacts on the concentration or variability of TDS concentrations. The cause of the framework exceedances could be explained through a combination of the seasonal diversion of the St. Mary River and natural processes (e.g., salt exclusion).

A major limitation of the investigation was the lack of concurrent data from different locations along the Milk River and its tributaries. Similarly, groundwater chemistry was not available at the same time as

surface water quality samples. This limited the ability to do some types of analyses, such as a mass balance across different potential sources, or identify longitudinal (upstream to downstream) changes in TDS concentrations along the Milk River in the winter.

5 Recommendations

- Look at understanding the risk current conditions pose for aquatic life, other winter water uses and soil stability. The limit for total dissolved solids is based on an irrigation guideline, but since the exceedances happen during the winter period, anticipated risk is low. A more detailed risk assessment should be conducted for confirmation that no irrigators are using water during the low flow (higher salinity) months. The limit for specific conductance is based on soil stability and an assessment should be completed to determine the risk to soil stability on any irrigated lands.
- Evaluate developing site-specific water quality objectives for the parameters that exceeded their limits at this station.
- Adjust the seasons at this station to reflect low flow and the timing of the water diverted from the St Mary River.
- Evaluate any future applications to discharge to the Milk River for the potential to further increase salinity in the Milk River.
- Identify further management actions to mitigate any environmental impacts.
- Complete trend assessments on a regular basis (no less than every 5 years) to ensure that TDS and specific conductance are not developing undesirable trends over time.

6 References

6.1 Literature

Alberta Environment. 2006. Aquatic ecosystems field sampling protocols. Edmonton AB: Alberta Environment https://open.alberta.ca/publications/077855080x

Alberta Environment and Sustainable Resource Development (AESRD). 2014. South Saskatchewan Region Surface Water Quality Management Framework: for the Mainstem Bow, Milk, Oldman and South Saskatchewan Rivers (Alberta). Government of Alberta. ISBN: 978-1-4601-1860-3 (Print); 978-1-4601-1861-0 (PDF). Available at: https://open.alberta.ca/ publications/9781460118603

Alberta Environment and Parks (AEP). 2017a. South Saskatchewan Region Status of Management Response for Environmental Management Frameworks as of May 2016. Government of Alberta. ISBN: 978-1-4601-3457-3 (PDF). Available at: https://open.alberta.ca/ publications/9781460134573.

Alberta Environment and Parks (AEP). 2017b. Status of Water Quality South Saskatchewan Region, Alberta for April 2014 – March 2015. Government of Alberta. ISBN: 978-1-4601-3068-1. Available at: https://open.alberta.ca/ publications/9781460130681

Alberta Environment and Parks (AEP). 2018. South Saskatchewan Region Status of Management Response for Environmental Management Frameworks as of October 2017. Government of Alberta. ISBN: 978-1-4601-3678-2. Available at: https://open.alberta.ca/ publications/9781460136782

Alberta Environment and Parks (AEP). 2020a. South Saskatchewan Region Status of Management Response for Environmental Management Frameworks as of October 2018. Government of Alberta. ISBN: 978-1-4601-4703-0 (PDF). In Press

Alberta Environment and Parks (AEP). 2020b. South Saskatchewan Region Status of Management Response for Environmental Management Frameworks, as of October 2019. Government of Alberta. In Press

AGRA Earth and Environmental Limited (AGRA). 1998. Evaluation of depletion of the Milk River Aquifer. Submitted to County of Forty Mile No. 8, Rural Water Development Task Force. Report EG18038. 31pp.

Akyurt, M., Zaki, G., and Habeebullah, B. 2002. Freezing phenomena in ice-water systems. Energy and conversion Management 43: 1773-1789.

AMEC Earth and Environmental (AMEC). 2008. Study of erosion and sedimentation on the Milk River. Submitted to Milk River Watershed Council Canada. Report CW2020. 135pp.

American Public Health Association (APHA). 1999. Standard Methods for the Examination of Water and Wastewater. American Public Health Association, Washington D.C.

Armstrong, S. C., Sturchio, N. C., and Hendry, M J. 1998. Strontium isotopic evidence on the chemical evolution of pore waters in the Milk River Aquifer, Alberta, Canada. Applied Geochemistry 13(4): 463-475.

Barendregt, R.W., and Ongley, E.D. 1977. Piping in the Milk River Canyon, southeastern Alberta: A contemporary dryland geomorphic process. In: Erosion and Soil Matter Transport in Inland Waters – Symposium. Publication 122, Paris: International Association of Hydrological Sciences.

Beaney, C.L. 2002. Tunnel channels in southeast Alberta, Canada: evidence for catastrophic channelized drainage. Quaternary International 90: 67-74.

Beaty, C.B. 1990. Milk River in Southern Alberta: A classic underfit stream. The Canadian Geographer 34(2): 171-174.

Bennett, D.R., and Entz, T. 1990. Irrigation suitability of solonetzic soils in the County of Newell, Alberta. Canadian Journal of Soil Science 70: 705-715.

Bennett, D.R., Hecker, F.J., Entz, T., and Greenlee, G.M. 2000. Salinity and sodicity of irrigated Solonetzic and Chernozemic soils in east-central Alberta. Canadian Journal of Soil Science 80: 117-125.

Bieroza, M.Z., Heathwaite, A.L., Bechmann, M., Kyllmar, K., and Jordan, P. 2018. The concentration-discharge slope as a tool for water quality management. Science of the Total Environment 630: 738-749.

Capesius, J.P., and Stephens, V.C., 2009. Regional Regression Equations for Estimation of Natural Streamflow Statistics in Colorado: U.S. Geological Survey Scientific Investigations Report 2009–5136, 46 p. https://pubs.usgs.gov/sir/2009/5136/pdf/SIR09-5136.pdf

Chang, C., Kozub, G.C., and Mackay, D.C. 1985. Soil salinity status and its relation to some of the soil and land properties of three irrigation districts in southern Alberta. Canadian Journal of Soil Science 65: 187-193.

Cheung, K., Klassen, P., Mayer, B., Goodarzi, F., and Aravena, R. 2010. Major ion and isotope geochemistry of fluids and gases from coalbed methane and shallow groundwater wells in Alberta, Canada. Applied Geochemistry 25: 1307-1329.

Chung, C., Zhu, D., Kromrey, N. and Kerr, J. 2019. 2017-2018 Status of Surface Water Quality South Saskatchewan Region, Alberta for April 2017 – March 2018. Government of Alberta, Environment and Parks. ISBN: 978-1-4601-4164-9. Available at: https://open.alberta. ca/ publications/9781460141649

Dixon, D., Boom, S., and Silins, U. 2014. Watershed-scale controls on snow accumulation in a small montane watershed, southwestern Alberta, Canada. Hydrological Processes 28: 1294-1306.

Drimmie, R.J., Aravena, R., Wassenaar, L.I., Fritz, P., Hendry, M.J., and Hut, G. 1991. Radiocarbon and stable isotopes in water and dissolved constituents, Milk River aquifer, Alberta, Canada. Applied Geochemistry 6: 381-392.

Alberta Environment and Sustainable Resource Development (ESRD). 2014. South Saskatchewan region surface water quality management framework for the mainstem Bow, Milk, Oldman and South Saskatchewan rivers (Alberta). Edmonton, AB. 71 pp.

Florinsky, I.V., Eilers, R.G., and Lelyk, G.W. 2000. Prediction of soil salinity risk by digital terrain modelling in the Canadian prairies. Canadian Journal of Soil Sciences 80: 455-463.

Golder Associates (Golder). 2004. Report on development of a management/protection plan for the Whisky Valley Aquifer, County of Warner, Alberta. Milk River West Water User's Co-op, Milk River, AB. 72pp. plus appendices.

Grasby, S.E., and Hutcheon, I. 2000. Chemical dynamics and weathering rates of a carbonate basin Bow River, southern Alberta. Applied Geochemistry 15: 67-77.

Grasby, S.E., Hutcheon, I., and Krouse, H.R. 1997. Application of the stable isotope composition of SO4 to tracing anomalous TDS in Nose Creek, southern Alberta, Canada. Applied Geochemistry 12: 567-575.

Grasby, S.E., Hutcheon, I., and McFarland, L. 1999. Surface-water – Groundwater interaction and the influence of ion exchange reactions on river chemistry. Geology 27(3): 223-226.

Grasby, S.E., Osborn, J., Chen, Z., and Wozniak, P.R.J. 2010. Influence of till provenance on regional groundwater geochemistry. Chemical Geology 273: 225-237.

Godsey, S.E., Kirchner, J.W., and Clow, D.W. 2009. Concentration-discharge relationships reflect chemostatic characteristics of US catchments. Hydrological Processes 23: 1844-1864.

Hao, X., and Chang, C. 2003. Does long-term heavy cattle manure application increase salinity of a clay loam soil in semi-arid southern Alberta? Agriculture, Ecosystems and Environment 94: 89-103.

Hendry, M.J., Schwartz, F.W., and Robertson, C. 1991. Hydrogeology and hydrochemistry of the Milk River aquifer system, Alberta, Canada: a review. Applied Geochemistry 6: 369-380.

Hendry, M.J., and Wassenaar, L.I. 2000. Controls on the distribution of major ions in pore waters of a thick surficial aquitard. Water Resources Research 36(2): 503-513.

Hounslow, A.W. 1995. Water Quality Interpretation In *Water quality data: analysis and interpretation*. Boca Raton, Florida: Lewis Publishers (CRC Press).

Huff, G.F. 2014. Chemical weathering of smectitic sulphide-mineral-bearing unconsolidated surficial sediments in south-central Alberta, Canada. Aquatic Geochemistry 20: 381-403.

Iwanyshyn, M., Ryan, M.C., and Chu, A. 2009. Cost-effective approach for continuous major ion and nutrient concentration estimation in a river. Journal of Environmental Engineering 135(4): 218-224.

JMP®, Version 15.1.0. SAS Institute Inc., Cary, NC, 1989-2019.

Kerr, J.G. 2017. Multiple land use activities drive riverine salinization in a large, semi-arid river basin in western Canada. Limnology and Oceanography 62: 1331-1345.

Kerr, J., Kromrey, N., and Abbasi, S. 2018a. Status of Surface Water Quality South Saskatchewan Region, Alberta for April 2015 – March 2016. Government of Alberta, Environment and Parks. ISBN: 978-1-4601-3582-2. Available at: https://open.alberta.ca/publications/9781460135822.

Kerr, J., Kromrey, N., and Abbasi, S. 2018b. Status of Surface Water Quality South Saskatchewan Region, Alberta for April 2016 – March 2017. Government of Alberta, Environment and Parks.ISBN: 978-1-4601-3583-9. Available at: https://open.alberta.ca/publications/978146013583-9.

Lal, A.M.W., and Shen, H.T. 1993. A mathematical model for river ice processes. US Army Corps of Engineers, Cold Regions Research and Engineering Laboratory. CRREL Report 93-4. 87pp.

Linsley R.K., 1975. Hydrology for Engineers. McGraw-Hill Inc.,US

MacCulloch, G., and Wagner-Watchel, J. 2010. Milk River main channel: Channel losses and gains assessment. Field study 2007. Environment Canada, Meteorological Service of Canada. Submitted to the Milk River Technical Working Group. 69pp.

MacCulloch, G., and Wagner-Watchel, J. 2011. Milk River main channel: Channel losses and gains assessment. Field study 2007, supplementary report. Environment Canada, Meteorological Service of Canada. Submitted to the Milk River Technical Working Group. 39pp.

MacDonald, M.K., Pomeroy, J.W., and Essery, R.L.H. 2018. Water and energy fluxes over northern prairies as affected by chinook winds and winter precipitation. Agricultural and Forest Meteorology 248: 372-385.

McLean, D.G., and Beckstead, G.R. 1985. Long term effects of a river diversion on the regime of the Milk River. Alberta Research Council Contribution Series No. 1054. 21pp.

Menke, W., and Menke, J. 2016. Environmental Data Analysis With Matlab. 2016. Academic Press, Inc. Orlando, Florida. ISBN:978-0-12-804488-9

Milk River Watershed Council Canada (MRWCC). 2013. Milk River transboundary state of the watershed report, 2nd edition. Compiled by Palliser Environmental Services Ltd. And prepared for Milk River Watershed Council Canada (Alberta) in collaboration with the Milk River Watershed Alliance (Montana). Milk River, Alberta. 238pp.

Miller, J.J., and Brierley, J.A. 2011. Solonetzic soils of Canada: Genesis, distribution, and classification. Canadian Journal of Soil Science 91: 889-902.

Palliser Environmental Services Ltd (Palliser). 2017. Milk River watershed water monitoring report 2016. Submitted to Milk River Watershed Council Canada. 26pp.

Pétré, M.-A., and Rivera, A. 2015. A synthesis of knowledge of the Milk River Transboundary Aquifer (Alberta, Canada-Montana, U.S.A.). Natural Resources Canada, Geological Survey of Canada Open File 7654, 109pp. doi:10.4095/295754

Pétré, M.-A., Rivera, A., Lefebvre, R., Hendry, M.J., and Folnagy, A.J.B. 2016. A unified hydrogeological conceptual model of the Milk River transboundary aquifer, traversing Alberta (Canada) and Montana (USA). Hydrogeological Journal 24: 1847-1871.

Rivera, A., Pétré, M.-A., Letourneau, F., and Audet-Gagnon, F. 2017. Groundwater atlas of the Milk River transboundary aquifer, Alberta, Canada and Montana, U.S.A. Natural Resources Canada, Geological Survey of Canada Open File 7867. 122pp.

Rose, L.A., Karwan, D.L., and Godsey, S.E. 2018. Concentration-discharge relationships describe solute and sediment mobilization, reaction, and transport at event and longer timescales. Hydrological Processes 32: 2829-2844.

Ryan Leuzinger. Personal communication, Chief Administrative Officer for the town of Milk River. Conversation on January 11, 2019.

Saffran, K.A. 1998. Impact of Verdigris Lake drain on the Milk River, 1997. Prepared for the Water Management, Prairie Region. Alberta Environmental Protection, Water Management Division, Water Sciences Branch. 21pp.

Salama, R.B., Otto, C.J., and Fitzpatrick, R.W. 1999. Contributions of groundwater conditions to soil and water salinization. Hydrogeology Journal 7: 46-64.

Schwartz, F.W., and Muehlenbachs, K. 1979. Isotope and ion geochemistry of groundwaters in the Milk River Aquifer, Alberta. Water Resources Research 15(2): 259-268.

Simpson, C.J., and Smith, D.G. 2001. The braided Milk River, northern Montana, fails the Leopold-Wolman discharge-gradient test. Geomorphology 41: 337-353.

Smith, D.G., and Pearce, C.M. 2002. Ice jam-caused fluvial gullies and scour holes on northern river flood plains. Geomorphology 42: 85-95.

Taube, N. and Kerr, J. 2020. 2018-2019 Status of Surface Water Quality, South Saskatchewan Region, Alberta for April 2018 – March 2019. Government of Alberta, Environment and Parks. In Press

Thompson Jr., R.E. 1986. Natural flow and water consumption in the Milk River basin, Montana and Alberta, Canada. U.S. Geological Survey, prepared in cooperation with Environment Canada. Water-Resources Investigations Report 86-4006. 45pp.

Van Stempvoort, D.R., Hendry, M.J., Schoenau, J.J., and Krouse, H.R. 1994. Sources and dynamics of sulphur in weathered till, Western glaciated plains of North America. Chemical Geology 11(1): 35-56.

Visconti, F., De Paz, J.M., and Rubio, J.L. 2010. Calcite and gypsum solubility products in water-saturated salt-affected soil samples at 25°C and at least up to 14dS m^{-1}. European Journal of Soil Science 61(2): 255-270.

6.2 Software

Nevada Water Science Center. PiperPlot-QW.xls. https://nevada.usgs.gov/tech/excelforhydrology/. Accessed September 18, 2018.

R Core Team. 2018. R: A language and environment for statistical computing. R Foundation for Statistical Computing, Vienna, Austria. URL https://www.R-project.org/

6.3 Websites

Alberta Agriculture and Forestry. Historical weather. https://agriculture.alberta.ca/acis/alberta-weather-data-viewer.jsp. Accessed October 5, 2018.

Alberta Energy website. https://www.energy.alberta.ca/AU/Services/Pages/PDF-Maps.aspx. Accessed April 5, 2019.

Alberta Groundwater Observation Well Network (GOWN). http://environment.alberta.ca/apps/GOWN/#. Accessed March 21, 2019.

Environment Canada historical flows. https://wateroffice.ec.gc.ca/search/historical_e.html. Accessed March 12, 2019.

Milk River water treatment website. http://www.milkriver.ca/water-treatment-distribution/Personal communication. Accessed April 4, 2019.

Ryan Leuzinger: Chief Administrative Officer, Town of Milk River, Alberta. Email correspondence, October 22, 2018.

Appendix A

Ancillary information for Investigation Question #1: Why do the Surface Water Quality Management Framework exceedances for total dissolved solids in the Milk River at Hwy 880 only occur in the winter (November to March)?

Table A-1: Dates when the St. Mary River diversion was active. Note that the dates are when flow control was initiated; some years may have more gradual changes in flow rates after the specified day. Information comes from Palliser (2017).

Year	Start Date	End Date
2006	March 5	September 24
2007	March 7	September 3
2008	March 17	September 12
2009	March 16	September 24
2010	March 21	September 3
2011	July 24	October 6
2012	April 9	September 15
2013	March 11	September 24
2014	May 13	September 10
2015	March 31	August 28
2016	March 22	September 10

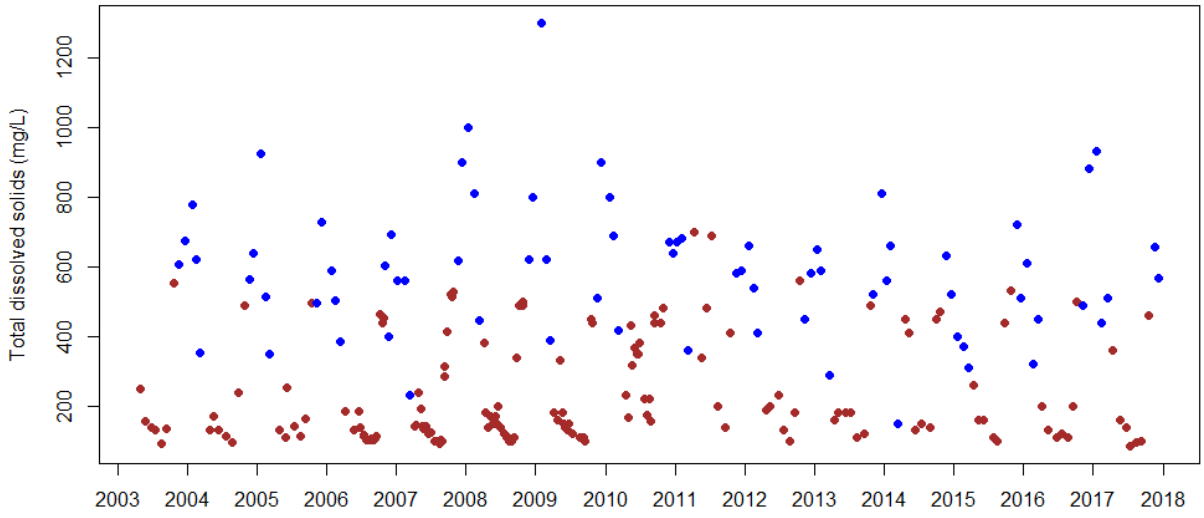

Figure A-1: Total dissolved solids concentrations observed in the Milk River at the Hwy 880 sampling station. Brown points are samples taken during the open water season (April to October); blue points were taken during the winter (November to March).

During the 2010 open water season, the median TDS concentration (350 mg/L) observed at the Hwy 880 monitoring station occurred in June during a particularly low flow period (Table A-1;Figure A-2;F-4). The maximum open water concentration for TDS (480 mg/L) was observed in October when the diversion was no longer active. Open water concentrations of TDS were above 300 mg/L in May through June, and

September through October. These are all periods when flow rates at the town of Milk River were low compared to the usual flow rates created by the St. Mary River diversion (for instance, in August 2010).

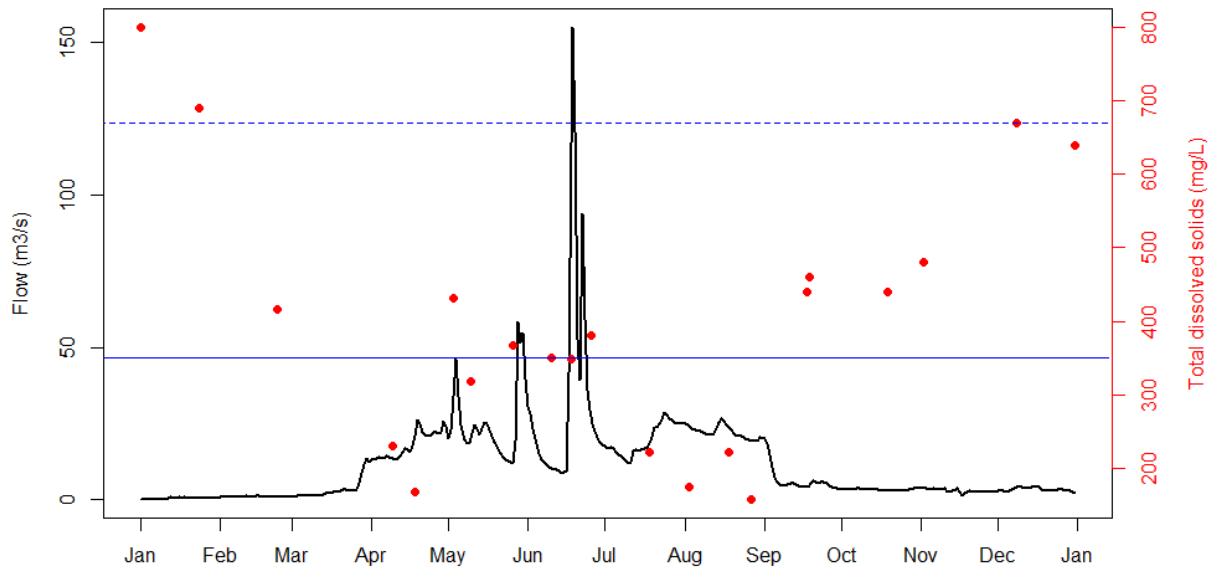

Figure A-2: Milk River flow rates and total dissolved solids (TDS) concentrations measured in 2010. Flow rates (left axis and black line) were observed at the town of Milk River (station EC 11AA005); TDS samples (right axis and red dots) were taken at the Hwy 880 monitoring station. The blue solid line indicates the median TDS concentration during the open water season; blue dashed line indicates the median TDS concentration during the winter.

In 2011, the diversion did not start until the end of July (Table A-1;Figure A-3;F-4). The median pre-diversion TDS concentration observed at the Hwy 880 monitoring station during open water (April to July) was 553 mg/L, which is close to the preceding winter median of 604 mg/L, and is higher than the median diversion period TDS concentration of 170 mg/L. In addition, the highest open water TDS measurement occurred in April (700 mg/L), before the St. Mary River diversion flow had started. The median TDS concentration for the open water season (410 mg/L) was observed in October, after the diversion had stopped.

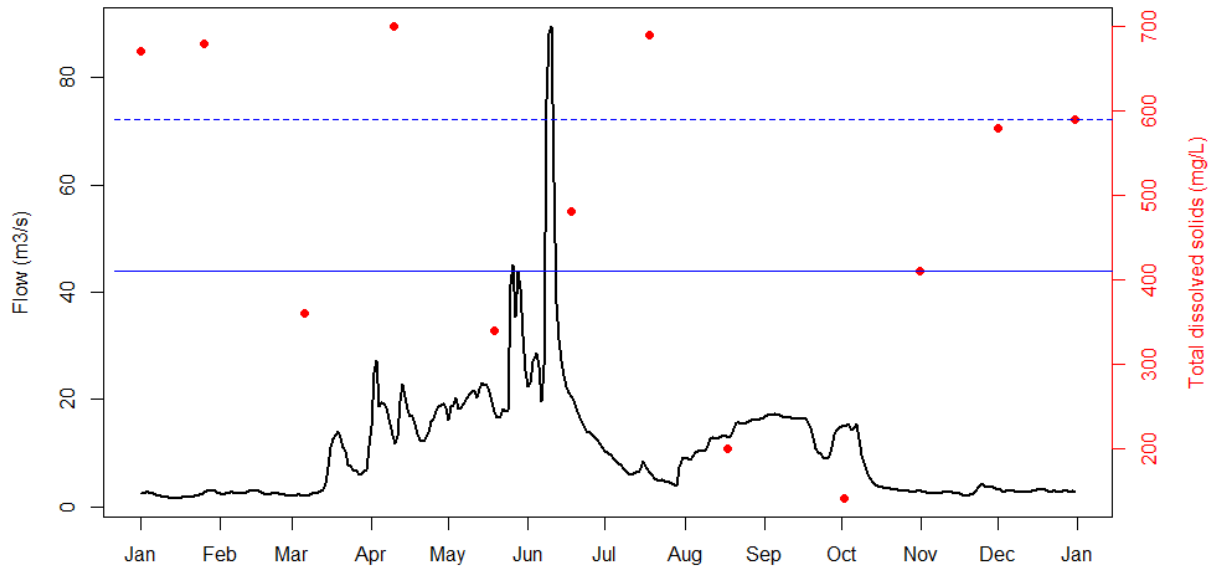

Figure A-3: Milk River flow rates and total dissolved solids (TDS) concentrations measured in 2011. Flow rates (left axis and black line) were observed at the town of Milk River (station EC 11AA005); TDS samples (right axis and red dots) were taken at the Hwy 880 monitoring station. The blue solid line indicates the median TDS concentration during the open water season; blue dashed line indicates the median TDS concentration during the winter.

The April, May, September, and October 2014 TDS samples were collected at the Hwy 880 monitoring station when there was no supplemental flow from the St. Mary River (Table A-1;Figure A-4;F-4). The median TDS concentration (410 mg/L) was observed in May 2014, before the diversion had started. Moreover, the median open water TDS concentration when the diversion was not active (450 mg/L) was closer to the 2014 winter median (400 mg/L) than the median open water concentration when the diversion was active (140 mg/L). The highest observed TDS concentration during the open water season was in October (470 mg/L), after the diversion ended.

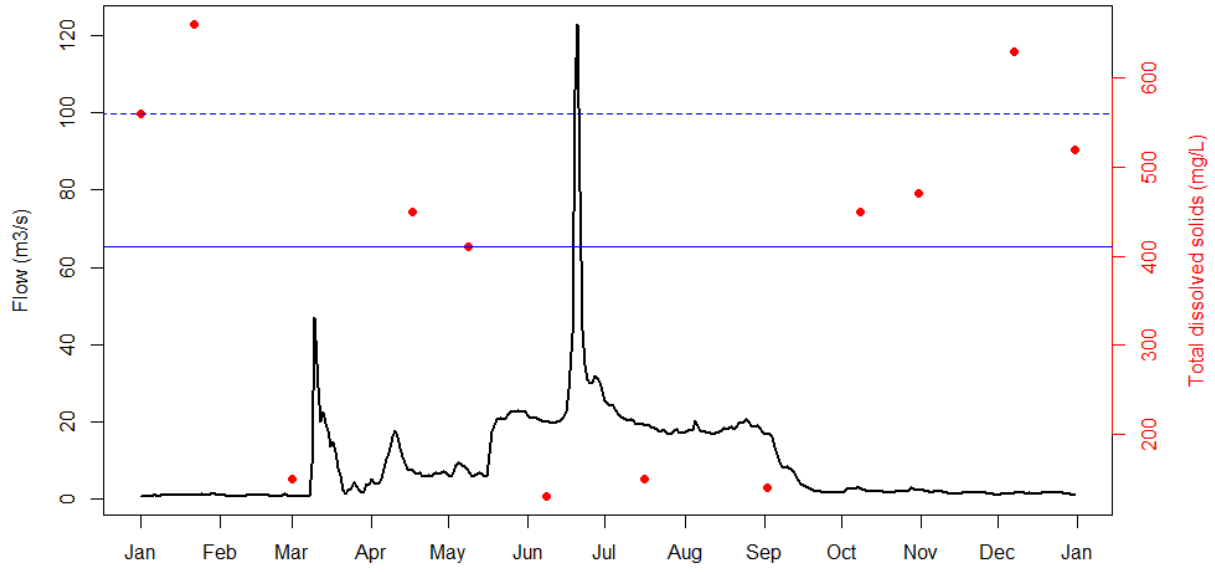

Figure A-4: Milk River flow rates and total dissolved solids (TDS) concentrations measured in 2014. Flow rates (left axis and black line) were observed at the town of Milk River (station EC 11AA005); TDS samples (right axis and red dots) were taken at the Hwy 880 monitoring station. The blue solid line indicates the median TDS concentration during the open water season; blue dashed line indicates the median TDS concentration during the winter.

Hydrographs from the North Fork, South Fork, and town of Milk River are presented in Figure A-5 to A-7. The two stations that receive inflow from the St. Mary River diversion – the North Fork ("North Milk Near Boundary"; Figure A-5) and the Milk River at Milk River (Figure A-7) – have much higher peak flows, as well as faster rising and falling limbs. The South Fork ("Milk River at West Crossing", Figure A-6) is not affected by the diversion. The increase in flow occurs around early March for all three stations, despite the diversion. Peak flows in the diversion-affected stations occurs in around June and do not reach baseline until October when the diversion flow is cut off, while peak flow in the South Fork (not affected by the diversion) occurs closer to April and reaches baseline by early September.

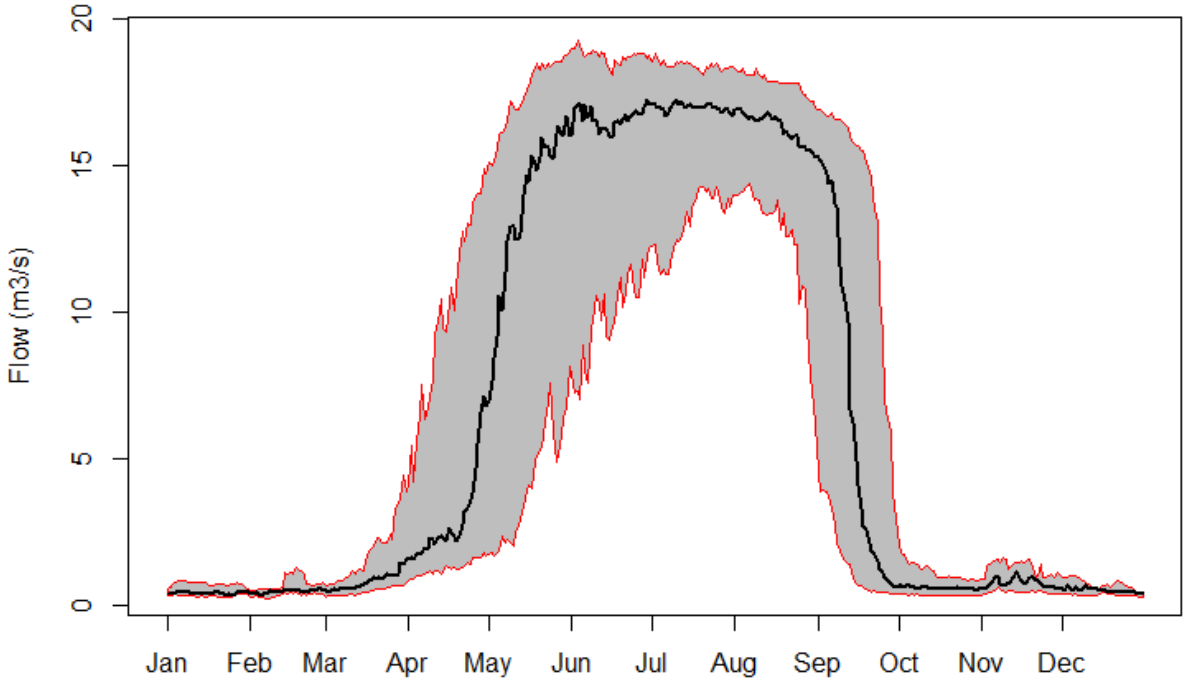

Figure A-5: Flow rates of the North Milk River (North Fork) from Environment Canada hydrometric station EC 11AA001, "North Milk Near Boundary." Black line is the median daily flow rate from 1909 to 2017; upper and lower red lines are the 75th and 25th percentile flow, respectively.

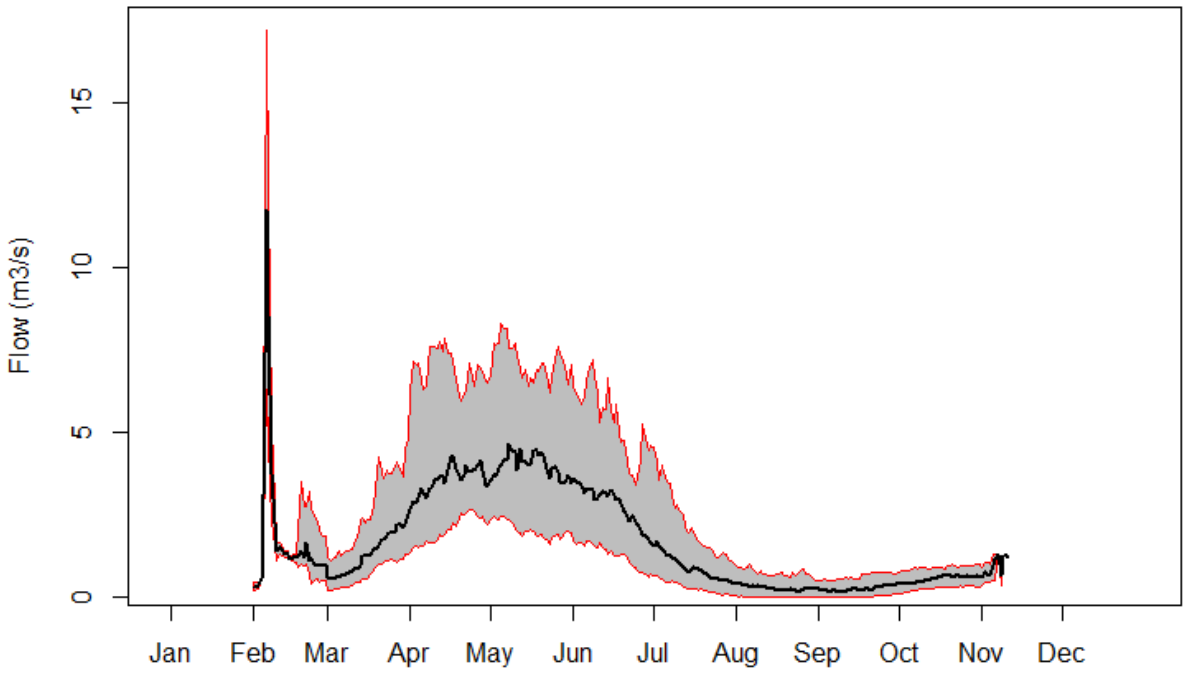

Figure A-6: Flow rates of the Milk River (South Fork) from Environment Canada hydrometric station EC 11AA025, "Milk River at West Crossing." Black line is the median daily flow rate from 1931 to 2017; upper and lower red lines are the 75th and 25th percentile flow, respectively. Flow rates were not available in January or December.

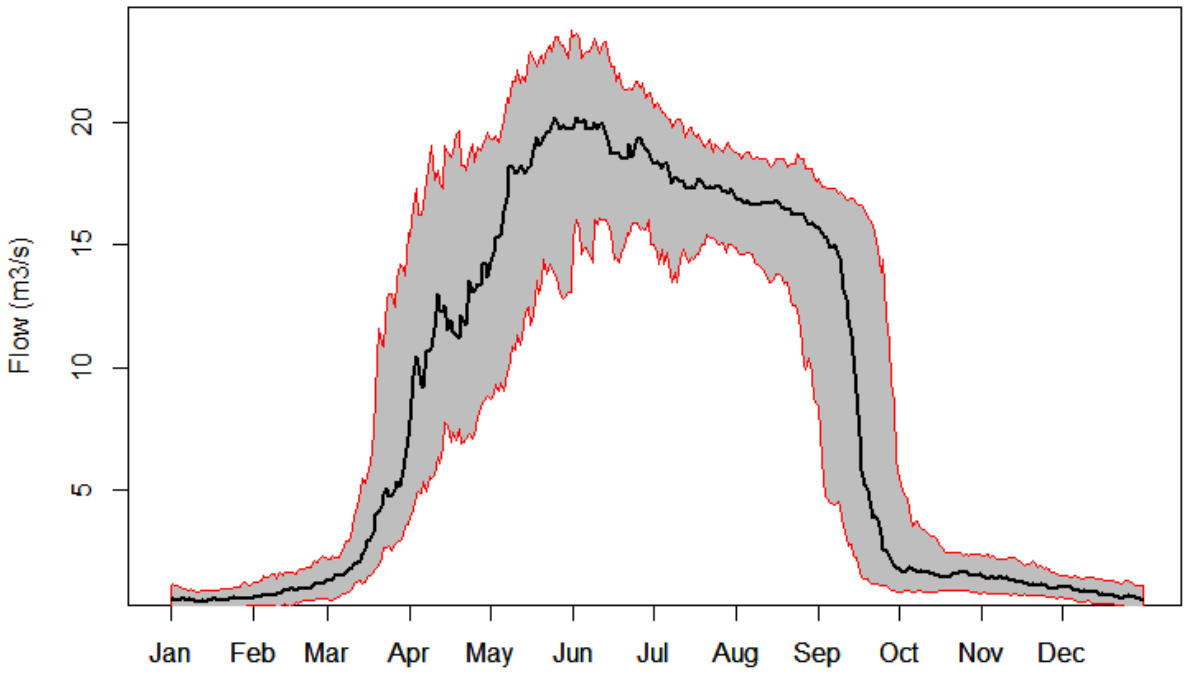

Figure A-7: Flow rates of the Milk River from Environment Canada hydrometric station EC 11AA005, "Milk River at Milk River." Black line is the median daily flow rate from 1909 to 2017; upper and lower red lines are the 75th and 25th percentile flow, respectively.

Appendix B

Ancillary information for Investigation Question #2: What is the primary source(s) of total dissolved solids to the Milk River during the winter?

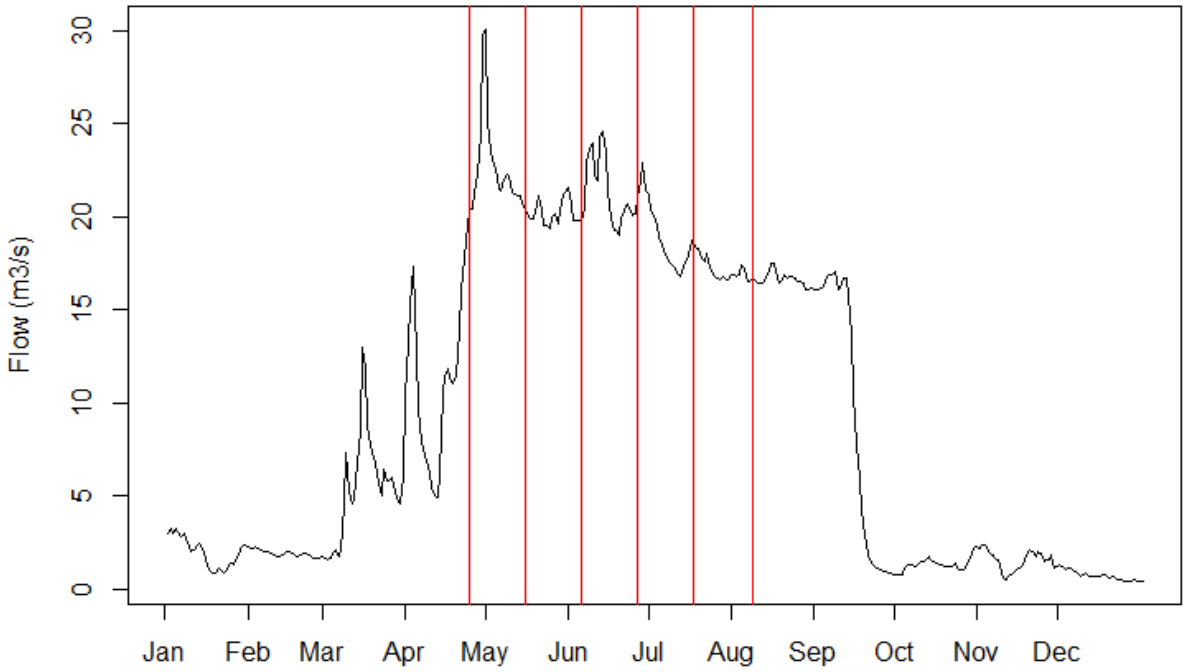

Figure B-1: Milk River flow rates measured at the town of Milk River in 2012. Red lines indicate the six days when water quality samples were taken.

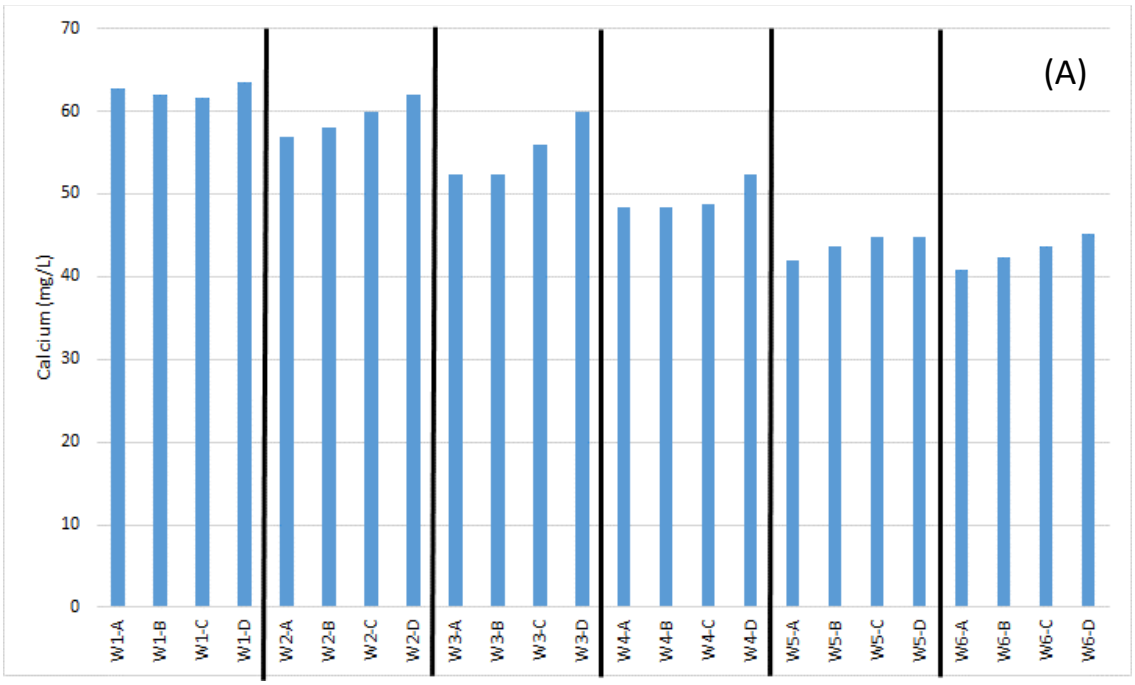
(A)
Calcium (mg/L)
70
60
50
40
30
20
10
0
W1-A
W1-B
W1-C
W1-D
W2-A
W2-B
W2-C
W2-D
W3-A
W3-B
W3-C
W3-D
W4-A
W4-B
W4-C
W4-D
W5-A
W5-B
W5-C
W5-D
W6-A
W6-B
W6-C
W6-D

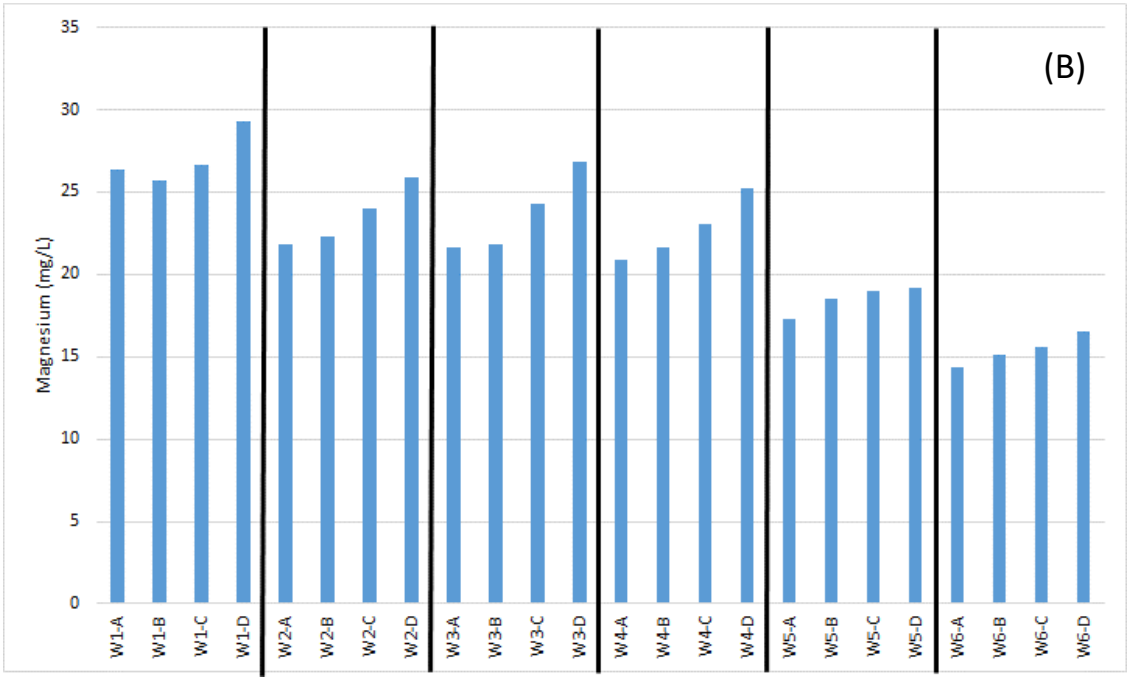
(B)
Magnesium (mg/L)
35
30
25
20
15
10
5
0
W1-A
W1-B
W1-C
W1-D
W2-A
W2-B
W2-C
W2-D
W3-A
W3-B
W3-C
W3-D
W4-A
W4-B
W4-C
W4-D
W5-A
W5-B
W5-C
W5-D
W6-A
W6-B
W6-C
W6-D

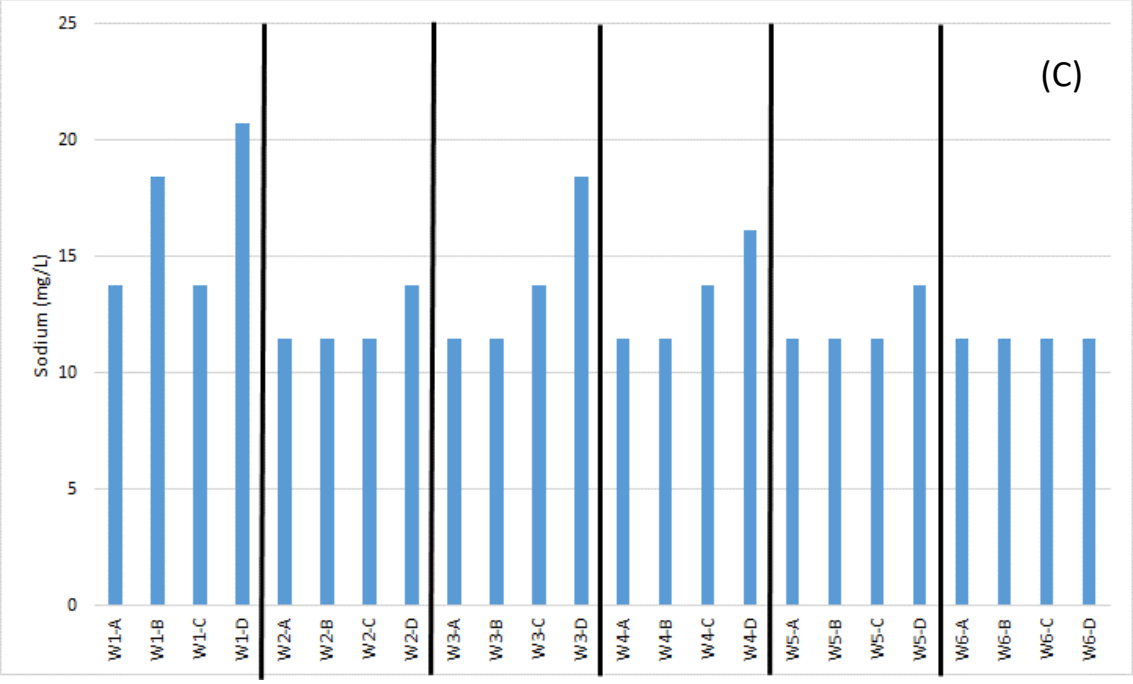
(C)
Sodium (mg/L)
25
20
15
10
5
0
W1-A
W1-B
W1-C
W1-D
W2-A
W2-B
W2-C
W2-D
W3-A
W3-B
W3-C
W3-D
W4-A
W4-B
W4-C
W4-D
W5-A
W5-B
W5-C
W5-D
W6-A
W6-B
W6-C
W6-D

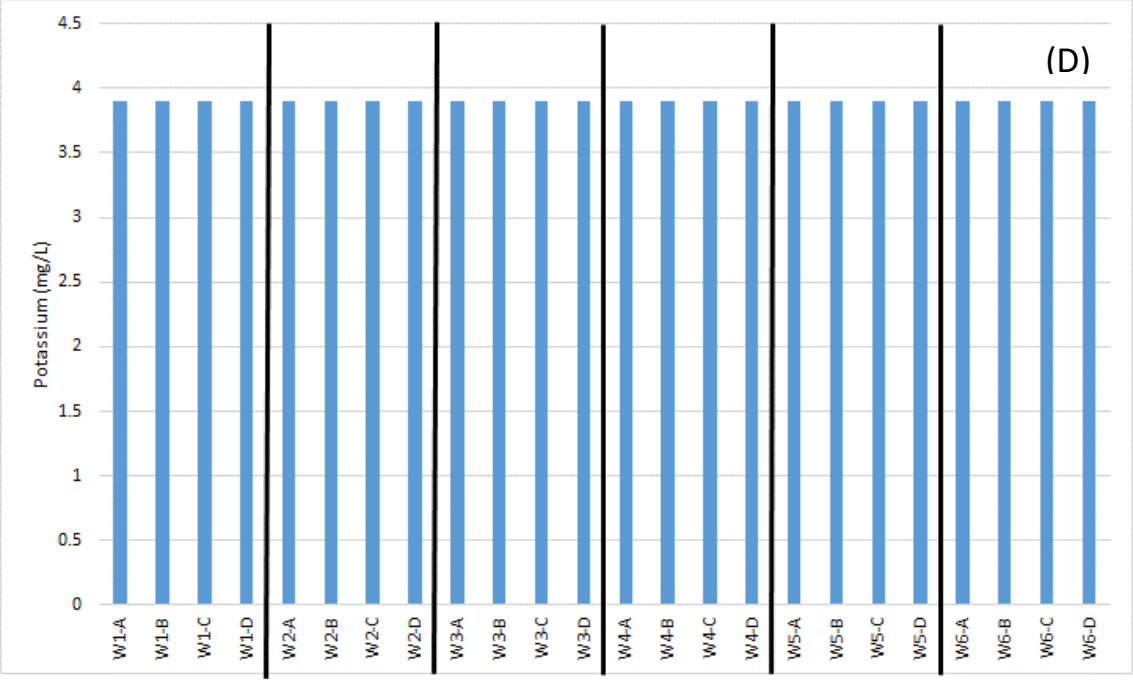
(D)
Potassium (mg/L)
4.5
4
3.5
3
2.5
2
1.5
1
0.5
0
W1-A
W1-B
W1-C
W1-D
W2-A
W2-B
W2-C
W2-D
W3-A
W3-B
W3-C
W3-D
W4-A
W4-B
W4-C
W4-D
W5-A
W5-B
W5-C
W5-D
W6-A
W6-B
W6-C
W6-D

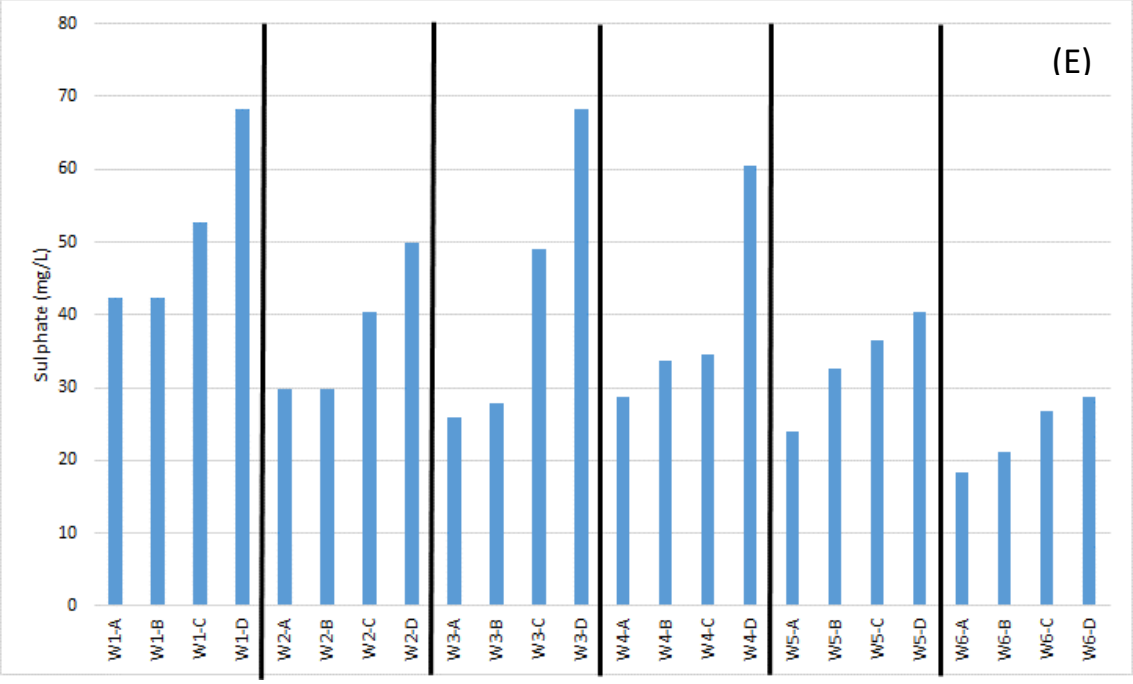
(E)
Sulphate (mg/L)
0
10
20
30
40
50
60
70
80
W1-A
W1-B
W1-C
W1-D
W2-A
W2-B
W2-C
W2-D
W3-A
W3-B
W3-C
W3-D
W4-A
W4-B
W4-C
W4-D
W5-A
W5-B
W5-C
W5-D
W6-A
W6-B
W6-C
W6-D

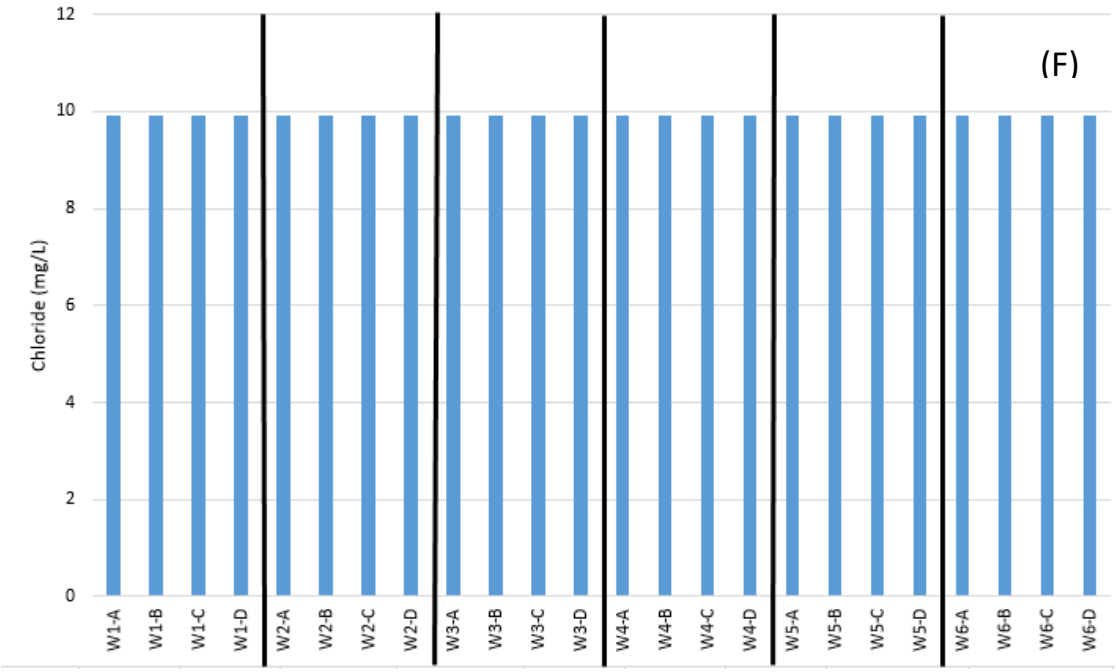
(F)
Chloride (mg/L)
0
2
4
6
8
10
12
W1-A
W1-B
W1-C
W1-D
W2-A
W2-B
W2-C
W2-D
W3-A
W3-B
W3-C
W3-D
W4-A
W4-B
W4-C
W4-D
W5-A
W5-B
W5-C
W5-D
W6-A
W6-B
W6-C
W6-D

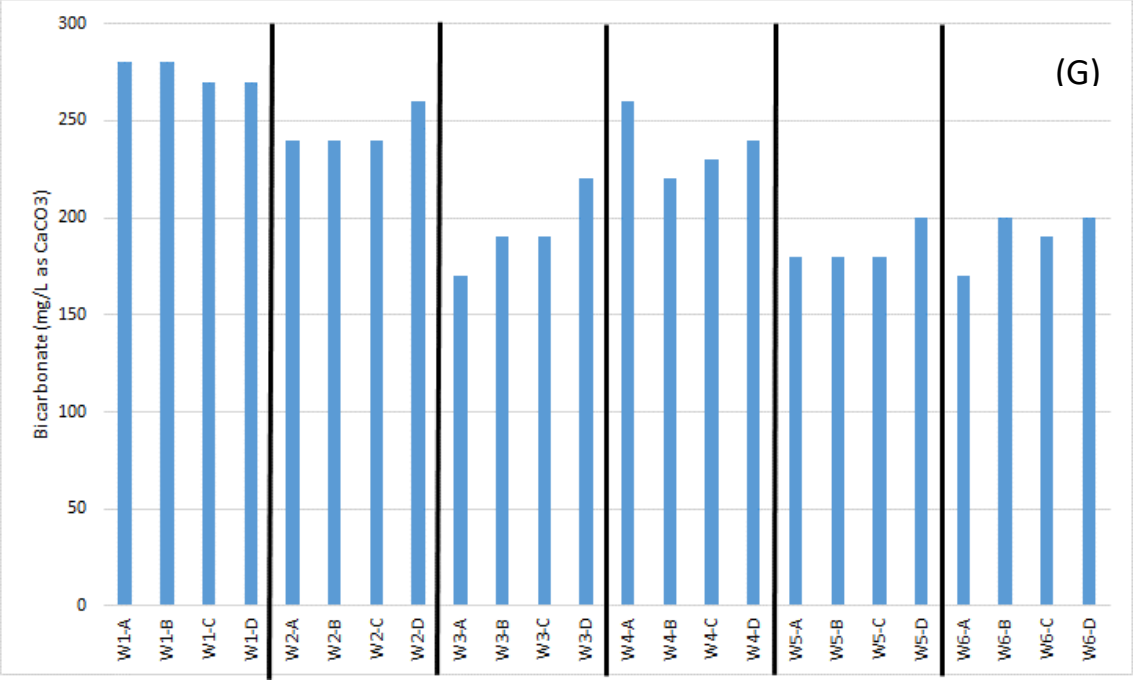
(G)
Bicarbonate (mg/L as CaCO3)
300
250
200
150
100
50
0
W1-A
W1-B
W1-C
W1-D
W2-A
W2-B
W2-C
W2-D
W3-A
W3-B
W3-C
W3-D
W4-A
W4-B
W4-C
W4-D
W5-A
W5-B
W5-C
W5-D
W6-A
W6-B
W6-C
W6-D

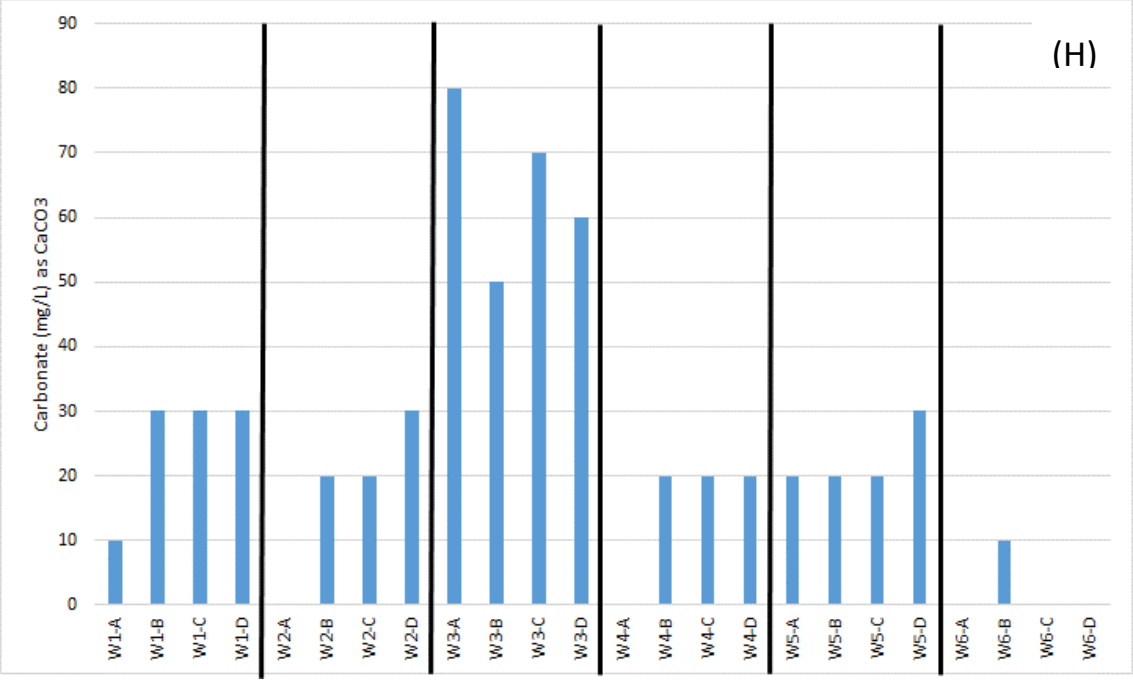
(H)
Carbonate (mg/L) as CaCO3
90
80
70
60
50
40
30
20
10
0
W1-A
W1-B
W1-C
W1-D
W2-A
W2-B
W2-C
W2-D
W3-A
W3-B
W3-C
W3-D
W4-A
W4-B
W4-C
W4-D
W5-A
W5-B
W5-C
W5-D
W6-A
W6-B
W6-C
W6-D

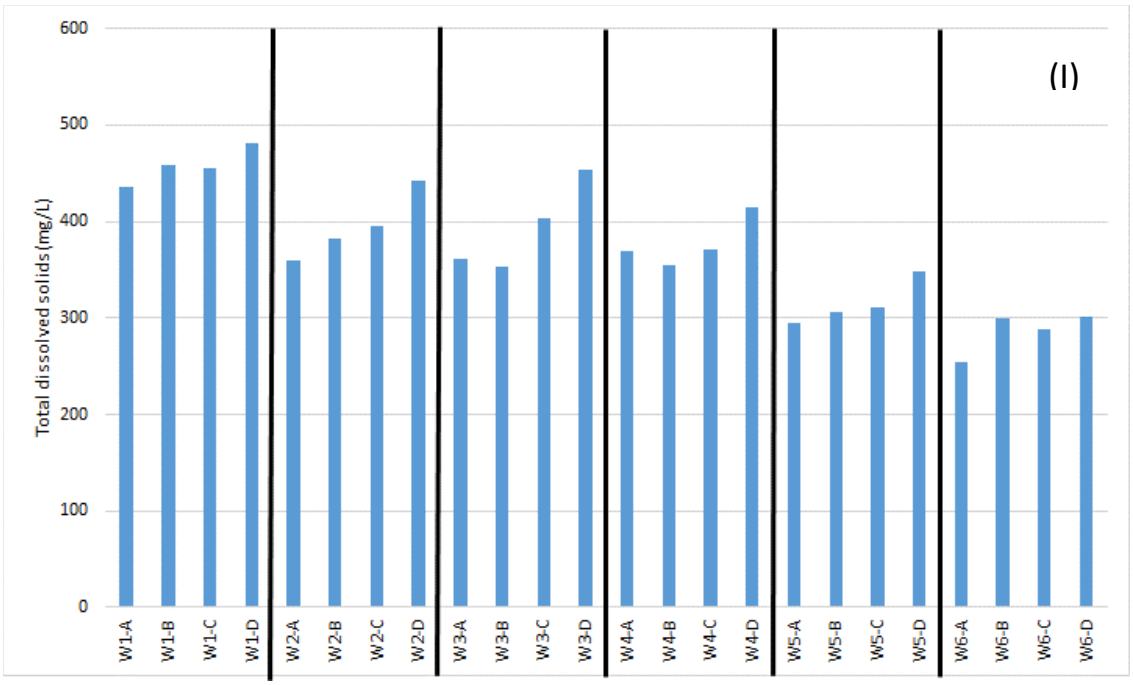
(I)
Total dissolved solids (mg/L)
600
500
400
300
200
100
0
W1-A
W1-B
W1-C
W1-D
W2-A
W2-B
W2-C
W2-D
W3-A
W3-B
W3-C
W3-D
W4-A
W4-B
W4-C
W4-D
W5-A
W5-B
W5-C
W5-D
W6-A
W6-B
W6-C
W6-D

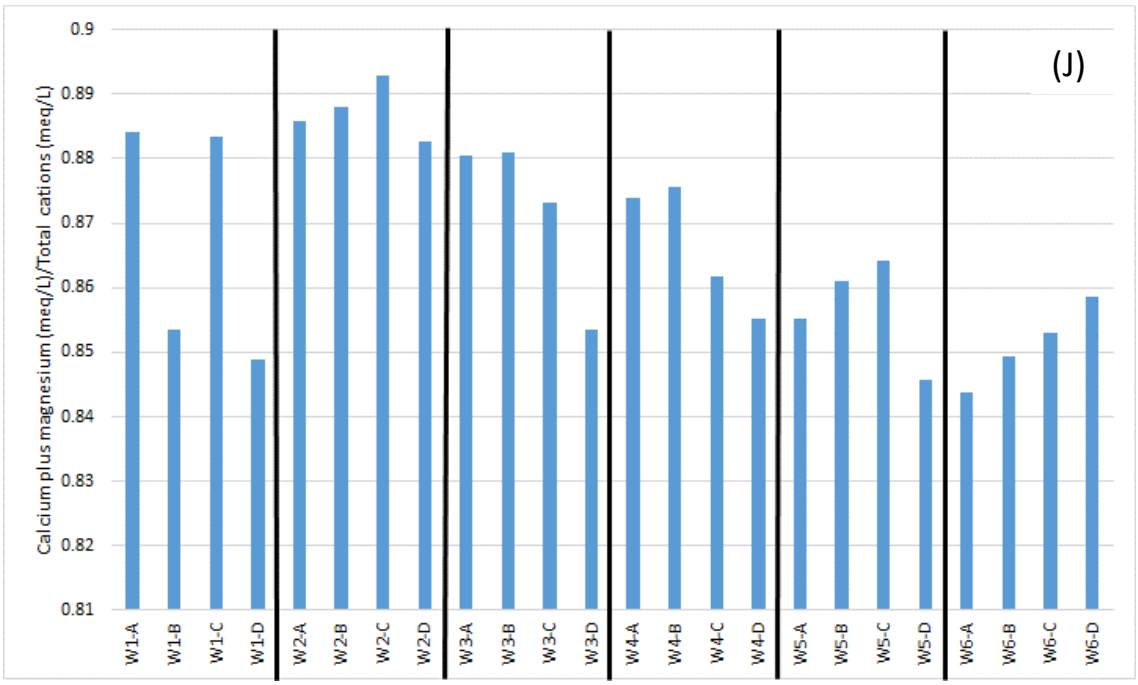
(J)
Calcium plus magnesium (meq/L)/Total cations (meq/L)
0.9
0.89
0.88
0.87
0.86
0.85
0.84
0.83
0.82
0.81
W1-A
W1-B
W1-C
W1-D
W2-A
W2-B
W2-C
W2-D
W3-A
W3-B
W3-C
W3-D
W4-A
W4-B
W4-C
W4-D
W5-A
W5-B
W5-C
W5-D
W6-A
W6-B
W6-C
W6-D

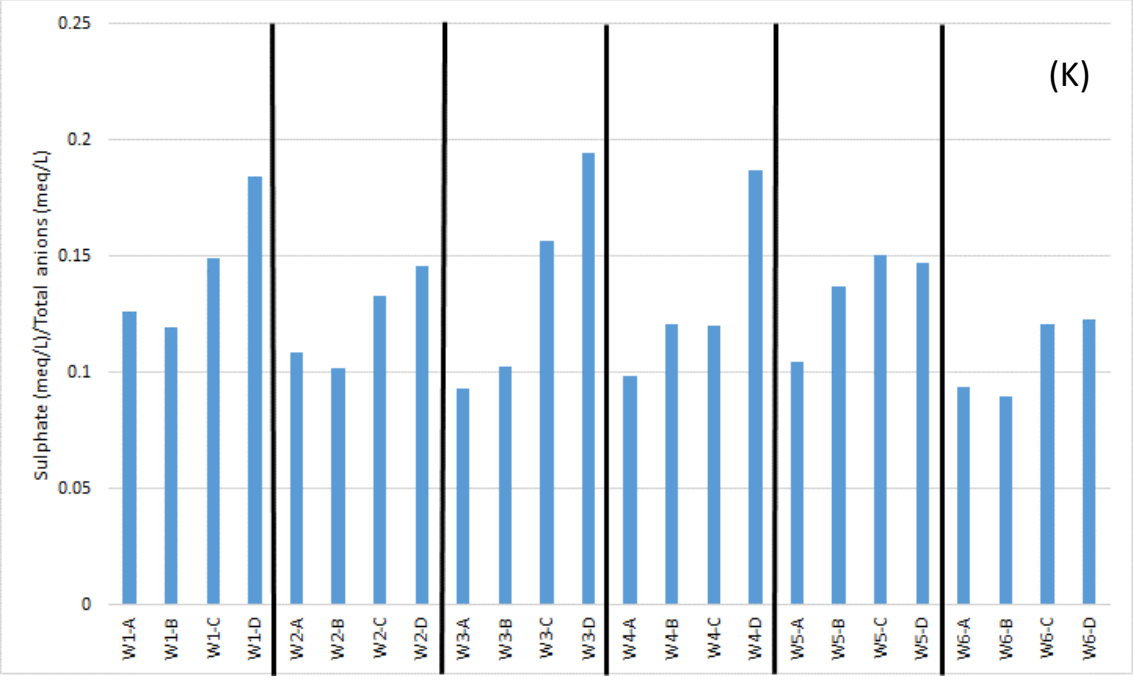

Figure B-2: Upstream to downstream changes in major ion content. Black lines and the number within the sample code denote different dates samples were taken; stations (hyphenated letter in the sample code, A through D) are ordered from upstream to downstream within each group. See Figure 4 for the locations of the stations. Samples W1-A, W2-A, W3-A, and W4-A were taken at AAF station MST_A (upstream of town of Milk River); the B series of samples were from station MST_B (just downstream of the town of Milk River), the C series from station MST_C (Writing-On-Stone Provincial Park), and the D series from station MST_D (Hwy 880 bridge). Plot letter A=calcium; B=magnesium; C=sodium; D=potassium; E=sulphate; F=chloride; G=bicarbonate; H=carbonate; I=total dissolved solids; J=(calcium + magnesium)/total cations; K=sulphate/total anions. Potassium (D) and chloride (F) concentrations were always below the detection limit; their concentrations are graphed at the detection limit. Data from Alberta Agriculture and Forestry (AAF).

The alkalinity to silica ratio was very high (alkalinity was much higher than silica), suggesting that most of the source material was carbonate rock and not silicates (clay) (**Error! Reference source not found.**). This is important since bentonite clays are very common around the Milk River.

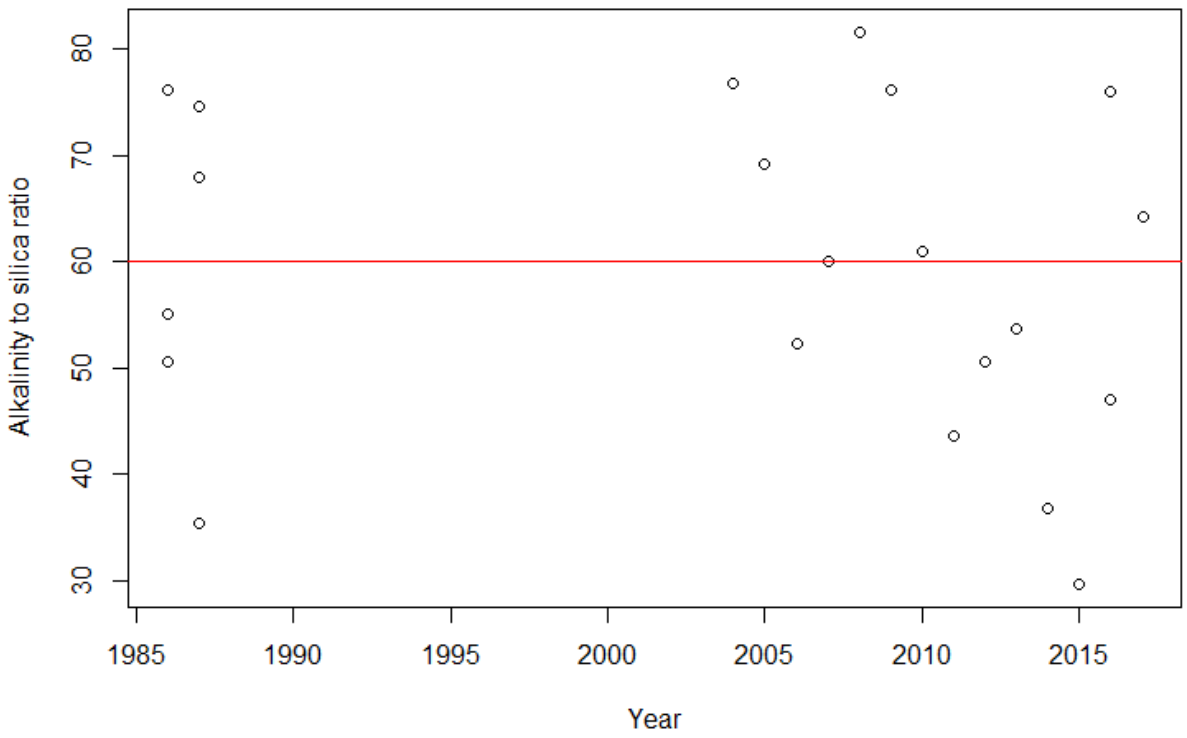

Figure B-3: Ratio of alkalinity (carbonates) to silica (clay) for winter samples taken at Hwy 880. Red line indicates the median ratio. Ratios based on equivalents.

Almost all of the samples had a ratio of alkalinity to (SO_4 + Cl) of one or above (**Error! Reference source not found.**). This implies that at least half of the cation content likely came from carbonate sources. This result matches the Piper plot, as the anion triangle ranged between 50-70% bicarbonate plus carbonate. Although carbonates may have been a dominant anion source, substantial amounts of non-carbonate anions (sulphate) were also present in the water. The relationship between alkalinity and sulphate (in equivalents) was positive and linear: Alkalinity = 1.01(±0.08) * Sulphate + 0.002(±0.0003) (r^2=0.68; *p*<0.01; n=82). The positive relationship suggests that biogeochemical processes adding sulphate also added alkalinity, which is unlikely to happen with anhydrite ($CaSO_4$) or gypsum ($CaSO_4 * H_2O$) dissolution but is consistent with sulphate and acid production through pyrite (FeS_2) oxidation and the subsequent weathering of carbonates or calcium clays (Huff 2014).

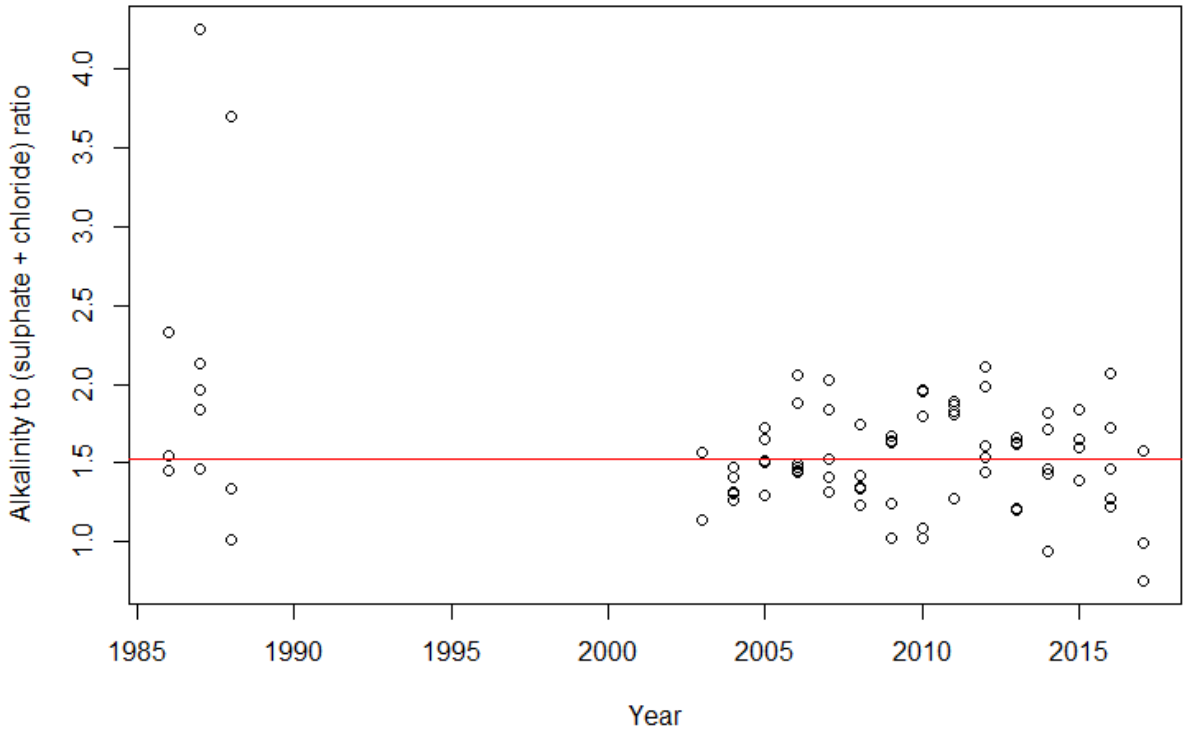

Figure B-4: Ratio of alkalinity (carbonates) to (SO_4 + Cl) for monthly winter samples taken at Hwy 880. Red line indicates the median ratio. Ratios based on equivalents.

Calcium and magnesium are often associated with carbonate rocks that create alkalinity. The ratio of (Ca + Mg) to alkalinity indicates the degree to which calcium and magnesium are potentially associated with carbonates. The observed ratio near one suggests that carbonates could account for most of the calcium and magnesium input (**Error! Reference source not found.**). There was an overall increasing trend in the (Ca + Mg) to alkalinity ratio (in equivalents) from 2003 to 2017 (r^2=0.27; *p*<0.01; n=71), as well as an increasing trend in the annual median ratios (r^2=0.54; *p*<0.01; n=15). In more recent years, there has been an excess of calcium and/or magnesium with respect to alkalinity, implying an additional source of calcium and/or magnesium.

Figure B-5: Ratio of (Ca + Mg) to alkalinity (carbonates) for monthly winter samples taken at Hwy 880. Red line indicates the median ratio. Ratios based on equivalents.

The median calcium to magnesium ratio was greater than one (**Error! Reference source not found.**). A stoichiometric ratio of 1 Ca : 1 Mg is expected if the primary source of both calcium and magnesium is from dolomite [$CaMg(CO_3)_2$]. The excess calcium with respect to magnesium indicates that a source of calcium additional to dolomite is required. The magnitude of the excess (Ca + Mg) compared to alkalinity (up to 20%) matches the excess calcium to magnesium ratio, indicating a non-carbonate source of calcium.

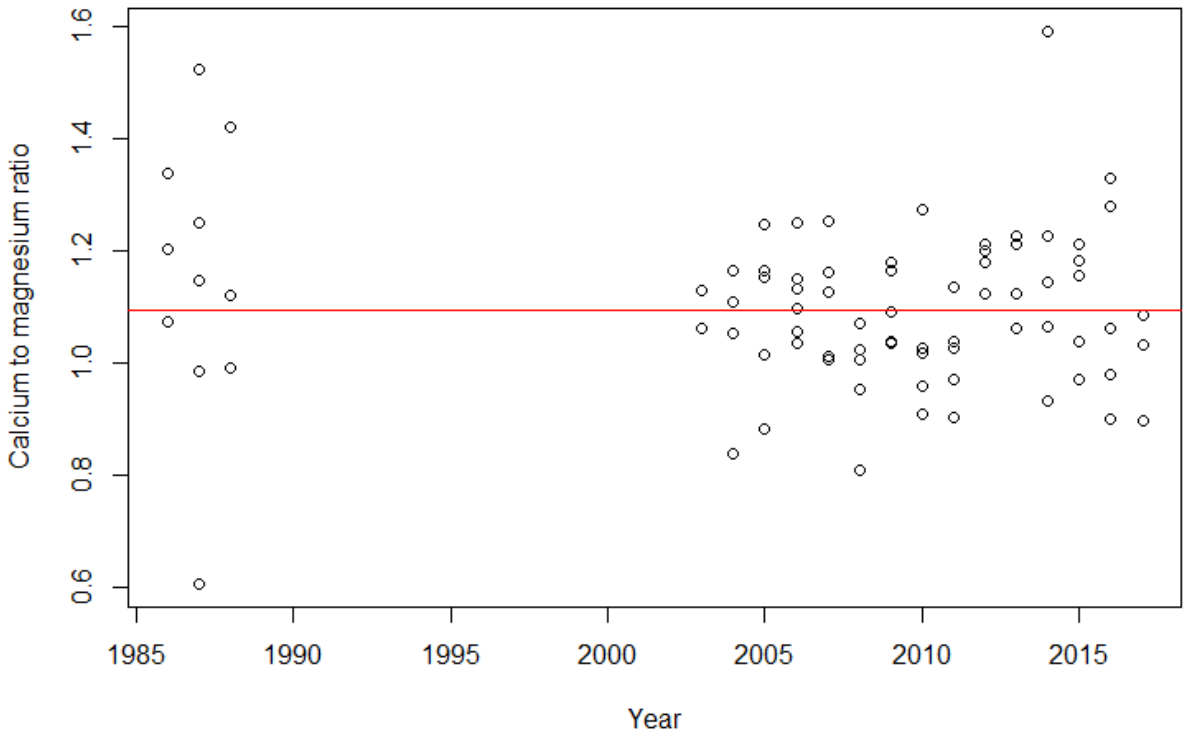

Figure B-6: Ratio of calcium to magnesium for monthly winter samples taken at Hwy 880. Red line indicates the median ratio. Ratios based on equivalents.

The alkalinity to (SO_4 + Cl) ratio alludes to a significant amount of sulphate being added to the Milk River (see **Error! Reference source not found.**). Two simple minerals that can supply sulphate are anhydrite ($CaSO_4$) and gypsum ($CaSO_4 * H_2O$). In addition, the observed excess calcium with respect to magnesium and alkalinity could be accounted for by anhydrite or gypsum dissolution. The stoichiometric ratio for both minerals is 1 Ca : 1 SO_4.

Substantial amounts of calcium are expected to be derived from carbonates (calcite, dolomite) based on the high proportion of bicarbonate anions. If so, concentrations of calcium should be higher than sulphate concentrations, as calcium could be contributed from calcite, dolomite, and anhydrite/gypsum, while sulphate is only added from the latter. However, the median calcium to sulphate ratio was below one (**Error! Reference source not found.**). Although the excess calcium (compared to alkalinity) may have come from calcium sulphate, there was an important second source of sulphate entering the Milk River. The Piper diagrams indicate that samples with higher proportions of sulphate were associated with higher proportions of sodium. The relatively low calcium concentrations compared to sulphate may be linked to a

sodium sulphate source, or through ion exchange between calcium and sodium. The latter process would allow the dissolution of calcium sulphate rocks to produce sulphate while reducing the overall calcium concentration. Ion exchange was identified as a process participating in the evolution of groundwater chemistry in the Milk River Aquifer (Schwartz and Muehlenbachs 1979), and occurs in shallow groundwater in southern Alberta (Grasby et al. 1999; Cheung et al. 2010).

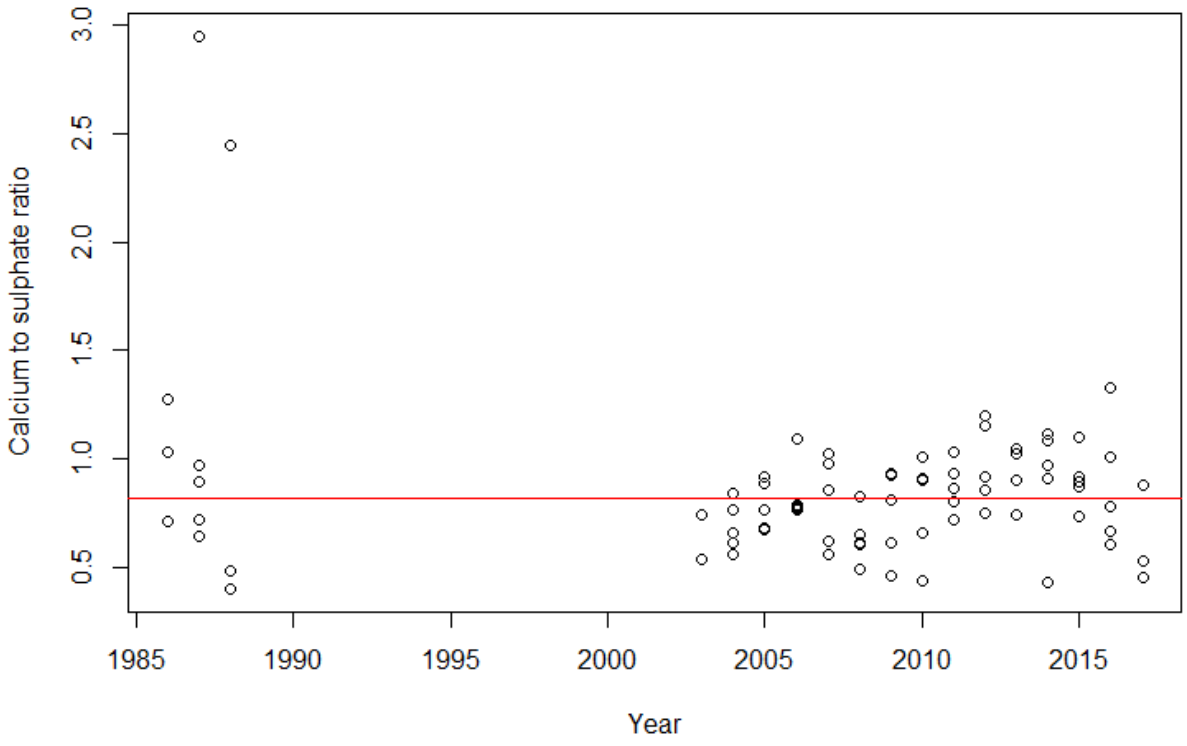

Figure B-7: Ratio of calcium to sulphate for monthly winter samples taken at Hwy 880. Red line indicates the median ratio. Ratios based on equivalents.

Calcite was supersaturated and gypsum undersaturated in winter samples taken at Hwy 880 (Table B-1). This result is consistent with the dissolution of gypsum occurring along a groundwater flow path, and carbonates forming the primary weathering product.

Table B-1: Mineral saturation index (SI) for calcite and gypsum for monthly water samples taken during the winter at the Hwy 880 bridge, 1986-1988 and 2003-2017. Negative SI indicates undersaturation; positive SI indicates supersaturation. Log(Ksp) for calcite was -8.4; log(Ksp) for gypsum was -4.6 (Visconti et al. 2010).

Summary Statistic	Saturation Index	
	Calcite ($CaCO_3$)	Gypsum ($CaSO4 * 2H_2O$)
Minimum	1.99	-2.15
Median	2.99	-0.94
Mean	2.96	-1.00
Maximum	3.45	-0.28

The sodium to chloride ratio was well above one, which is the ratio expected from primarily halite (NaCl) dissolution (**Error! Reference source not found.**). This is strong evidence of an additional source of sodium. The overall low silica concentrations indicate that the sodium source was probably not from silicate (clay) dissolution; the median non-halite sodium (Na - Cl) to silica ratio was ≈36 (**Error! Reference source not found.**).

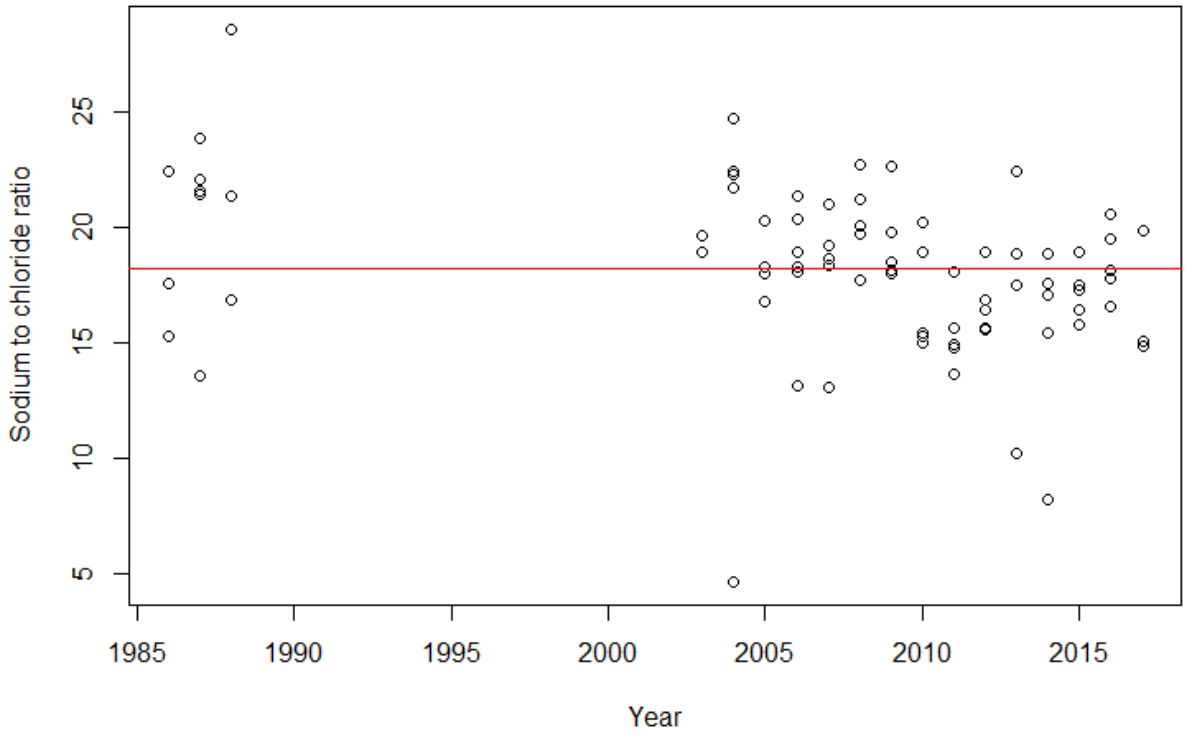

Figure B-8: Ratio of sodium to chloride for monthly winter samples taken at Hwy 880. Red line indicates the median ratio. Ratios based on equivalents.

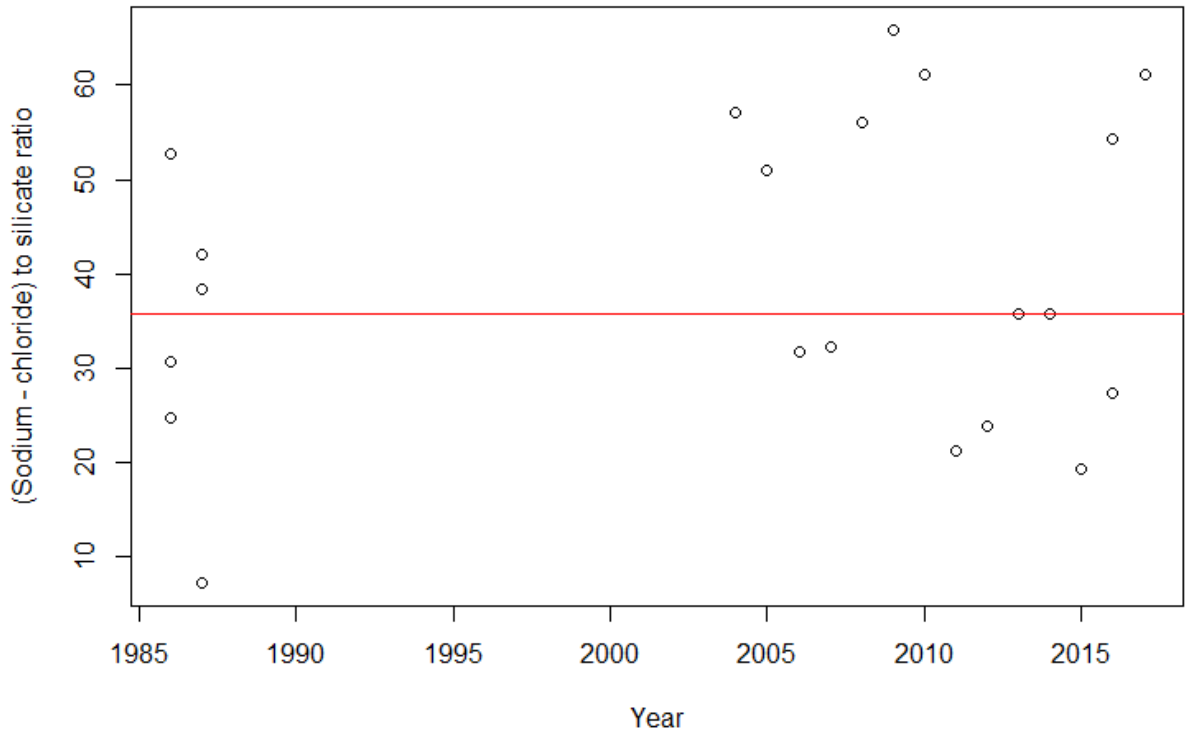

Figure B-9: Ratio of (Na - Cl) to silicate for monthly winter samples taken at Hwy 880. Red line indicates the median ratio. Ratios based on equivalents.

The (Na - Cl) to sulphate ratio was very close to one, suggesting the process(es) that added sulphate to the Milk River was linked to the process(es) adding sodium (**Error! Reference source not found.**). This agrees with the Piper plot results that samples with higher sodium content tended to have higher proportions of sulphate. However, the higher sodium and sulphate proportions do not suggest a direct mineral source as sodium sulphate (Na_2SO_4) has a sodium to sulphate ratio of 2 : 1, while the data were concentrated around a 1 : 1 ratio.

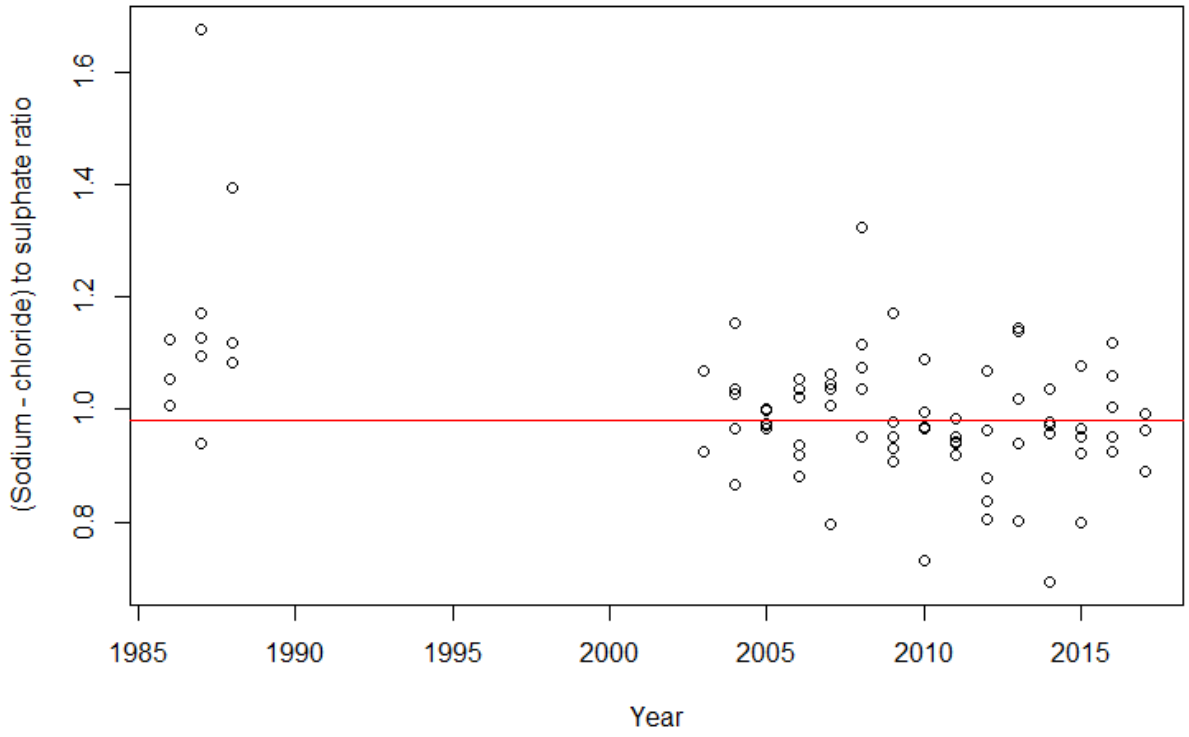

Figure B-10: Ratio of (Na - Cl) to sulphate for monthly winter samples taken at Hwy 880. Red line indicates the median ratio. Ratios based on equivalents.

At low concentrations of non-halite sodium, the main cations (calcium and magnesium) were balanced by the main anions (carbonate and sulphate) (**Error! Reference source not found.**). As non-halite sodium increased, the ion balance shifted in favor of the anions. In particular, calcium and alkalinity concentrations decreased as sodium concentrations increased (Figure B-12), while sulphate concentrations increased (Figure B-13). A potential set of geochemical processes that match these observations include the dissolution of a sulphate source (e.g., anhydrite or gypsum) coupled with ion exchange that swaps out calcium for sodium ions. The dissolution of e.g., gypsum would add sulphate. As the dissolution occurs, ion exchange reduces the calcium concentration and increases the sodium concentration. Sulphate could also be added through sulphide oxidation (Grasby et al. 1997), though this does not provide the surplus of calcium relative to carbonates that was observed. Laurentide glacial deposits are associated with sodium-sulphate waters through oxidation processes (Grasby et al. 2010; Huff 2014). The dissolution of sodium sulphate minerals (thenardite, Na_2SO_4; mirabilite, $Na_2SO_4 * 10H_2O$) is another potential source of sodium and sulphate, and are common in the glacial drift of saline areas (Miller and Brierley 2011). However, the dissolution of thenardite or mirabilite would produce a sodium to sulphate ratio of 2 : 1, whereas the observed ratio was 1 : 1.

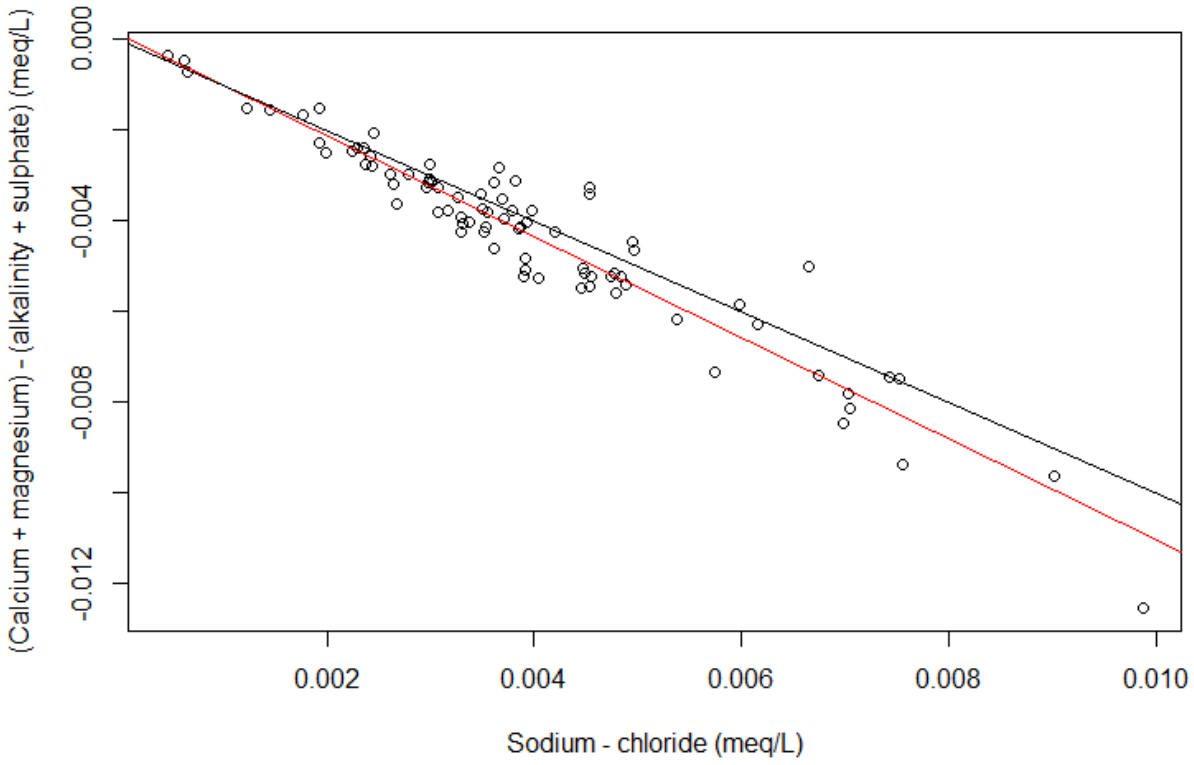

Figure B-11: Ion exchange plot. Black line = 1:1 ratio; red line = linear fit to data. Regression: Y = -1.11(±0.04)X; intercept not significant; r^2=0.91; p|<0.01; n=82.

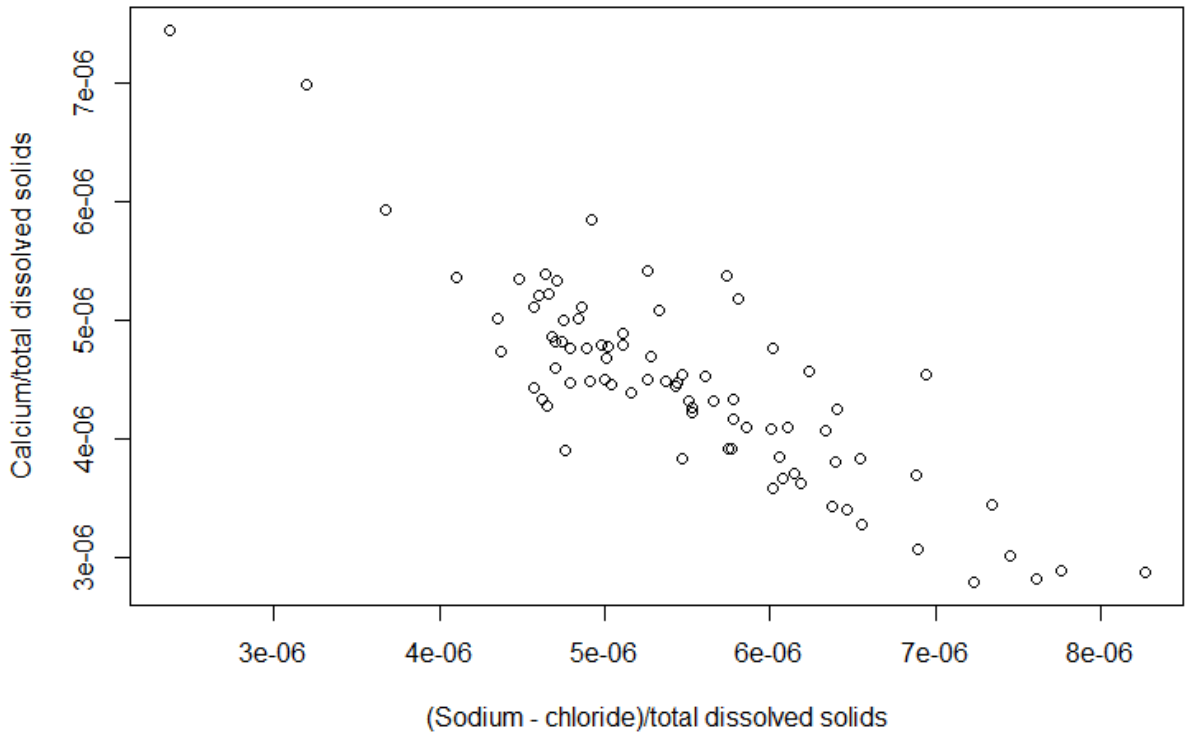

Figure B-12: Change in proportion of calcium with changes in non-halite sodium (Na - Cl). Ratios based on concentrations in mg/L.

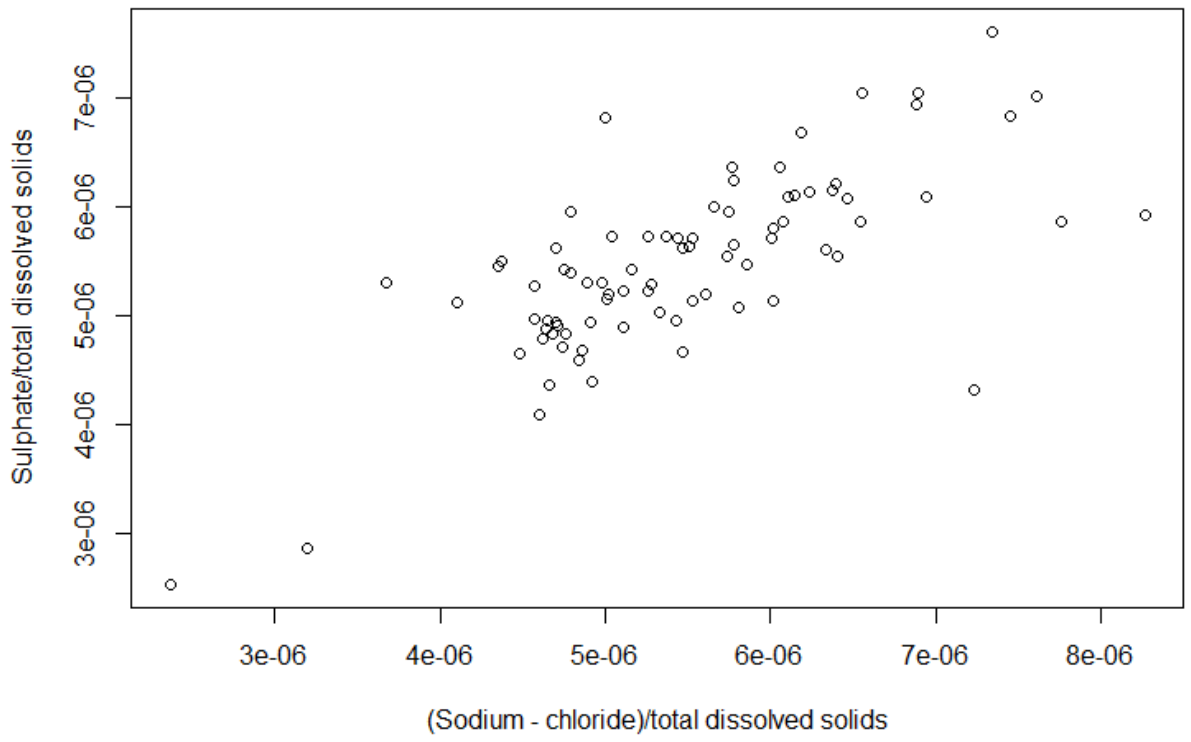

Figure B-13: Change in proportion of sulphate with changes in non-halite sodium (Na - Cl). Ratios based on concentrations in mg/L.

Table B-2: Properties of the Groundwater Observation Well Network (GOWN) sites near the Milk River.

GOWN Well ID	Sample Year	Well depth (m)	Cover
101	1989;1991;1994;2009;2012	26.5-73.2	Open
103	1989;1991;1994	7.6	Unknown
106	1989;1990;1994;2009	27-30	Screen
211	1987;1989;1992;2012	158.5-165.2	Screen
212	1986;1986;1990;2014	54.6-72.8	Open
213	1987;1988;1992	8.5-9.75	Screen
260	1988;1989;1993;2009	24.7-25.9	Screen

Table B-3: Major ion chemistry for GOWN Well #101. All concentrations are in mg/L (mg/L as CaCO3 for alkalinity).

Sampling Date	Calcium	Magnesium	Sodium	Potassium	Alkalinity	Sulphate	Chloride
Dec 1989	54.5	38	99	3.1	398.5	107	4.9
Nov 1991	55.8	36.8	97	3.2	386.8	107	4.7
Dec 1994	49	35	108	2.7	393	113	5.3
Jan 2009	65	41	94	3.1	410	130	6
Nov 2012	70.2	44.7	122	3.6	380	229	7.6

Appendix C

Ancillary information for Investigation Question #3: What are the main processes controlling variability in total dissolved solids concentrations during the winter?

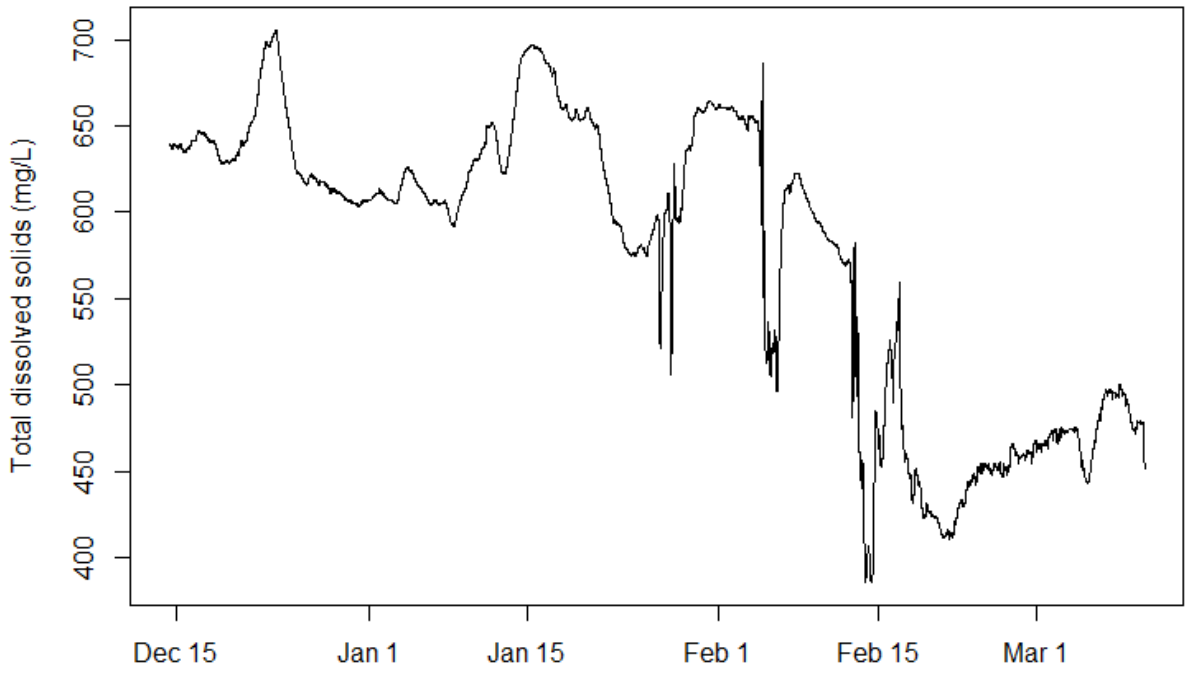

*Figure C-1: Datasonde time-series from Writing-on-Stone Provincial Park, from December 14, 2010 to March 11, 2011. 15 minute sampling frequency. Concentrations of total dissolved solids were calculated from the specific conductance reported by the datasonde using the formula: TDS (mg/L) = 0.66 *specific conductance (uS/cm) - 25.6 (see* Figure 5*).*

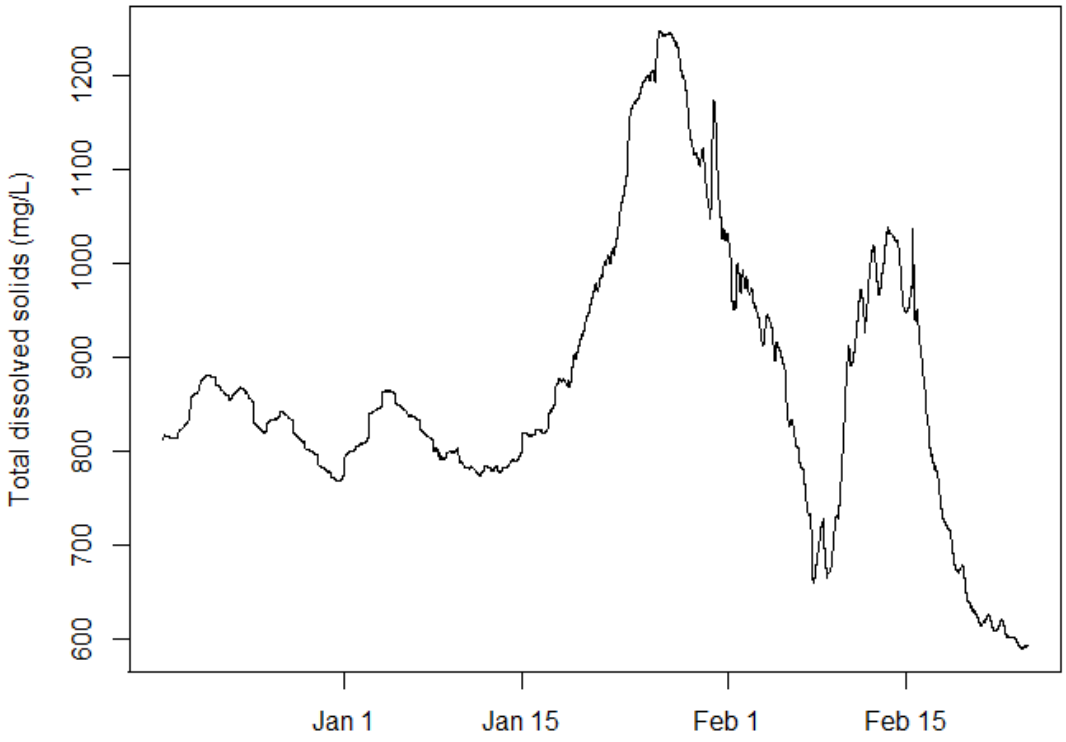

*Figure C-2: Datasonde time-series from Hwy 880, from December 18, 2008 to February 24, 2009. 15 minute sampling frequency. Concentrations of total dissolved solids were calculated from the specific conductance reported by the datasonde using the formula: TDS (mg/L) = 0.66 *specific conductance (uS/cm) - 25.6 (see* Figure 5*).*

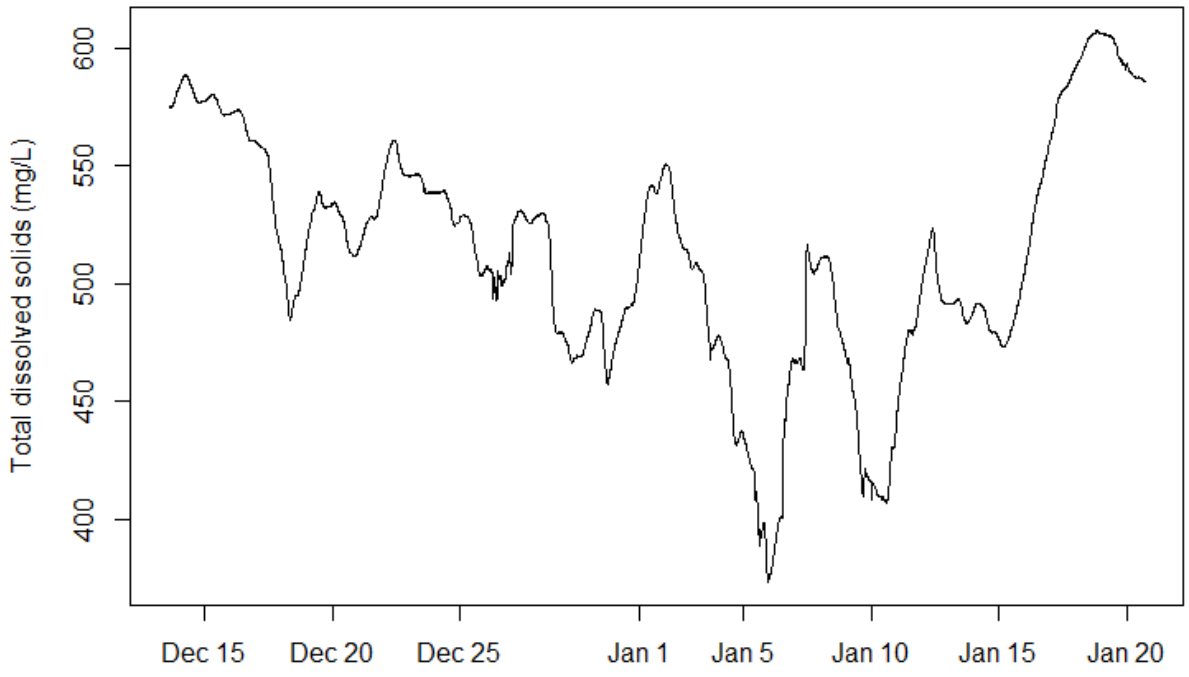

*Figure C-3: Datasonde time-series from Hwy 880, from December 13, 2011 to January 20, 2012. 15 minute sampling frequency. Concentrations of total dissolved solids were calculated from the specific conductance reported by the datasonde using the formula: TDS (mg/L) = 0.66 *specific conductance (uS/cm) - 25.6 (see* Figure 5*).*

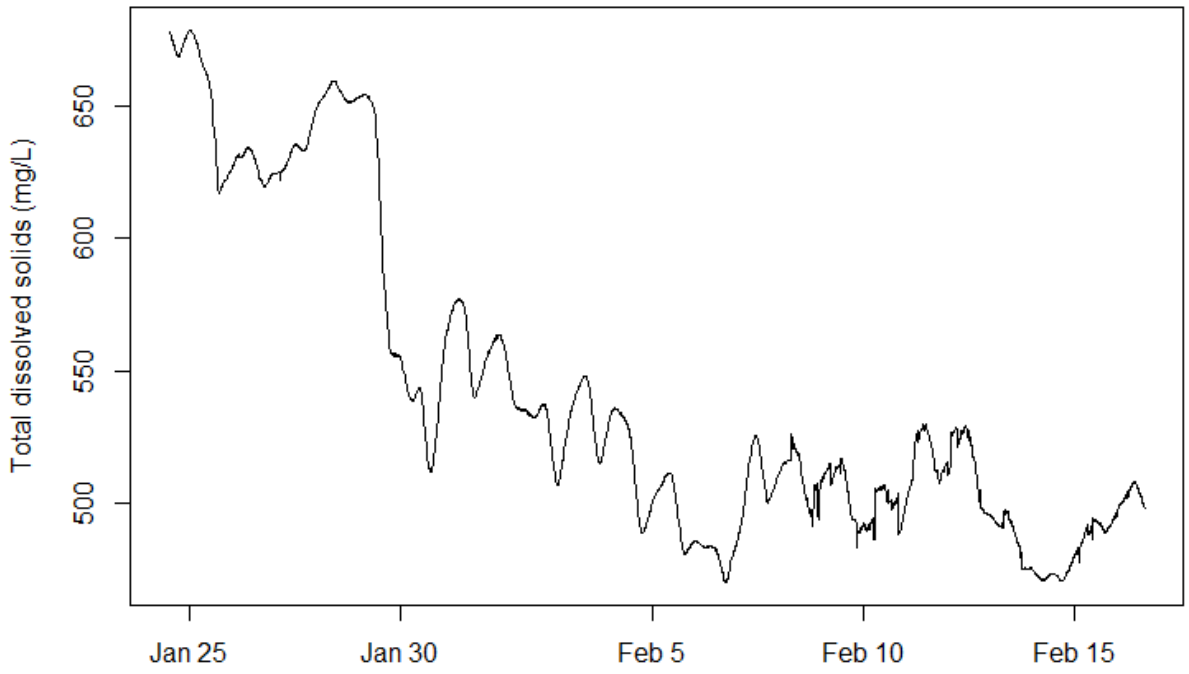

*Figure C-4: Datasonde time-series from Hwy 880, from January 24, 2012 to February 16, 2012. 15 minute sampling frequency. Concentrations of total dissolved solids were calculated from the specific conductance reported by the datasonde using the formula: TDS (mg/L) = 0.66 *specific conductance (uS/cm) - 25.6 (see* Figure 5*).*

Appendix D

Ice Volume Model

The ice volume model is effectively a two-component box model consisting of a water component and an ice component. Energy flows between these two boxes, with external inputs from a fixed time-series of air temperature and radiance. Energy transfer is balanced in the water and ice components, but is not balanced in the radiance or air components; these last two are strictly used to force changes in the model. The overall approach is similar to the ice growth and decay processes described in Lil and Shen (1993).

Model Overview

For each time step in the model, the following activities occur:

1) The amount of energy in the air and water components is calculated using the relevant volumes, temperatures, and specific heat capacities. Energy in the ice component is also calculated using the current ice volume and specific heat capacity of ice; the ice is assumed to be a constant temperature.

2) The temperature differential between the air and the water is calculated, and used to create a hypothetical equilibrium temperature based on the volumes, temperatures, and specific heat capacities of the air and water.

3) Energy is lost if the equilibrium temperature is less than the water temperature. First, the water temperature is reduced to the freezing point. Additional energy loss results in ice growth.

4) Energy is gained if the equilibrium temperature is greater than the water temperature. First, ice is melted. Addition energy gain results in increased water temperatures.

5) A portion of the radiant energy is directly used to melt ice (when present) and heat water, regardless of the air or water temperatures.

The calculated water temperatures and ice volumes were recorded between time steps and used in subsequent calculations. Observations of air temperature and radiance were applied at each time step but were not calculated by the model. Although observations of water temperature were available, the model used the calculated water temperature.

Model Constants

The model requires 12 constants to be defined. Of these, four are physical constants, one is defined using the water temperature time-series, and the others must be calibrated. The volume of water was set equal to one, under the assumptions that 1) changes in ice volume along different portions of the Milk River occurred proportionally to each other, and 2) flow rates remained constant. The volumes of air and ice are scaled relative to the volume of water.

- *Heat_capacity_air* = Isochoric heat capacity of air. Physical constant. Value taken from Engineeringtoolbox.com for temperature at 0°C

- *Heat_capacity_water* = Isochoric heat capacity of water. Physical constant. Value taken from Engineeringtoolbox.com for temperature at 0°C

- *Heat_capacity_ice* = Specific heat of ice. Physical constant. Value taken from Engineeringtoolbox.com for temperature at 0°C

- *Vol_air* = Volume of air (relative to water). Physical constant. The surface area participating in heat exchange between the air and water is the same for both components. Hence, the volume of air, relative to water, is interpreted as having the same ratio as the relative density of air to water. Value taken from Engineeringtoolbox.com

- *Vol_ice* = Volume of ice (relative to water). Calibrated parameter. This parameter was set to match the initial amount of total dissolved solids present in the Milk River.

- *Rad_water* = Radiative heating of water. Calibrated parameter. Controls addition of energy to water from radiance without adding heat. Calibrated using water temperature component with no ice formation.

- *Rad_ice* = Radiative heating of ice. Calibrated parameter. Controls addition of energy to ice from radiance without adding heat. The ratio (*Rad_ice / Rad_water*) is the relative albedo of the ice, compared to water. A representative ratio for non-colored water is (~0.8 / ~0.08) ≈ 10.

- *Ice_damp_coeff1 and Ice_damp_coeff2* = Ice dampening coefficients. Calibrated parameters. Ice does not conduct heat well (Akyurt et al. 2002; Lal and Shen 1993); this was used to adjust the absorbance of radiant energy by water depending on the amount of ice. The adjustment is linear: an increase in ice volume reduces the amount of energy transferred proportionally.

- *Min_energy* = Minimum energy level. Defined from the temperature where water freezes. Based on the datasonde information, minimum water temperatures were observed to be around -0.02°C. In the model, the water temperature was not allowed to decrease below this amount, and formed ice instead.

- *Cond_coeff1 and Cond_coeff2* = Conversion from ice volume to electrical conductance. Calibrated parameters. Used to convert the modeled ice volume to electrical conductance. The two parameters are part of a linear scaling.

Model Forcing

The model is forced using a time-series of air temperature (*Temp_air*) and radiance. These are direct meteorological observations. Observed air temperature (in degrees Celsius) is converted to degrees Kelvin to produce only positive temperature values. The change in observed radiance (*dRad*) is calculated as: $\text{radiance}_{(t+1)}$ - $\text{radiance}_{(t)}$. This calculation provides the increase/decrease in radiance between time steps.

Model Activities

The following is calculated for each time step of the model:

1) *Energy_air* = *Vol_air* * *Temp_air* * *Heat_capacity_air.* This is the amount of energy in the prescribed (constant) volume of air at the current time step. *Vol_air* and *Heat_capacity_air* are constants, and *Temp_air* is an observed value.

2) *Energy_water* = *Temp_water* * *Heat_capacity_water*. This is the amount of energy in the prescribed (constant) volume of water at the current time step. *Heat_capacity_water* is a constant, and *Temp_water* is either the initial water temperature, or the water temperature from

the end of the previous time step. The volume of water was assumed to be one (1.0).

3) *Energy_ice* = *Vol_ice* * *Temp_ice* * *Heat_capacity_ice*. This is the amount of energy in the current (variable) volume of ice at the current time step. *Temp_ice* and *Heat_capacity_ice* are constants.

4) *Equil_temp* = ((-*Heat_capacity_water* * *Temp_water*) - (*Vol_air* * *Heat_capacity_air* * *Temp_air*)) / ((-*Vol_air* * *Heat_capacity_air*) - (*Heat_capacity_water*)). This is the temperature that the air and water would reach if it could reach equilibrium. It is the reference point used to determine how much energy enters or leaves the water.

5) *Ice_damp* = 1 - ((*Vol_ice* - *Ice_damp_coeff1*) * *Ice_damp_coeff2*. This imposes a linearly decreasing amount of radiant energy available to heat water when ice is present; a large ice volume results in more dampening and less heating. *Ice_damp_coeff1* and *Ice_damp_coeff2* were determined during the calibration. There is no separate consideration for the extra insulating effect of snow on top of the ice (Lil and Shen 1993).

After the model parameters are calculated, one of four different scenarios were evaluated.

Scenario 1: *Temp_air* < *Temp_water* and *Energy_water* = *Min_energy*

In this scenario, there is more thermal energy in the water than in the air (*Temp_air* < *Temp_water*), and energy flow is out of the water. The amount of energy that needs to be lost is calculated as: *Excess_energy* = |*Vol_water* * *Heat_capacity_water* * (*Equil_temp* - *Temp_water*)|, which is based on the difference between the current water temperature and the temperature the water would have at equilibrium, ignoring ice formation. However, the stipulation that *Energy_water* = *Min_energy* implies that the water is already at a minimum temperature (and hence has a minimum amount of energy) and cannot lose heat/energy by lowering its temperature. Instead, all the *Excess_energy* is transferred to the ice component, minus some energy loss due to the effect of radiance directly on the ice: *Energy_ice* = *Energy_ice* + *Excess_energy* - (*dRad* * *Rad_ice*). The *dRad* and *Rad_ice* terms define the proportion of radiance (in W m^{-2}) that goes directly into melting ice; the loss of ice mass is equivalent to the loss of energy stored in the ice component. Similarly, the water gains energy from the direct radiative heating of the water (*dRad* * *Rad_water*) modified by the amount of ice present (*Ice_damp*): *Energy_water* = *Energy_water* + (*dRad* * *Rad_water* * *Ice_damp*)

Scenario 2: *Temp_air* < *Temp_water* and *Energy_water* > *Min_energy*

As in Scenario 1, there is more thermal energy in the water than in the air (*Temp_air* < *Temp_water*), and energy flow is out of the water. The amount of energy lost is calculated as: *Excess_energy* = |*Vol_water* * *Heat_capacity_water* * (*Equil_temp* - *Temp_water*)|, which is based on the difference between the current water temperature and the temperature the water would have at equilibrium, ignoring ice formation. In this scenario, the water is not at its minimum temperature (*Energy_water* > *Min_energy*), and some of the *Excess_energy* is shed as a temperature change of the water before any ice is formed: *Energy_water* = *Energy_water* - (*Energy_water* - *Min_energy*) + (*dRad* * *Rad_water* * *Ice_damp*). Some energy is added back into the water through radiative heating (*dRad* * *Rad_water* * *Ice_damp*) modified by the amount of ice present. The remaining *Excess_energy* (whatever was not accounted for by changing the water temperature) goes into ice formation, as modified by the input of radiative energy: *Energy_ice* = *Energy_ice* + *Excess_energy* - (*dRad* * *Rad_ice*). If the amount of energy to be lost does not reduce the *Temp_water* to the *Min_temp*, then the *Temp_water* is reduced by the appropriate amount and ice is not formed.

Scenario 3: *Temp_air* ≥ *Temp_water* and *Energy_ice* = 0

In this scenario, the air temperature is greater than the water temperature (*Temp_air* ≥ *Temp_water*), and there is no ice (*Energy_ice* = 0). The difference in energy due to the temperature difference is transferred from the air to the water: *Excess_energy* = |*Vol_water* * *Heat_capacity_water* * (*Equil_temp* - *Temp_water*)|. The energy heats the water, supplemented by the radiative energy: *Energy_water* = *Energy_water* + *Excess_energy* + (*dRad* * *Rad_water* * *Ice_damp*). Since there is no ice in this scenario, *Ice_damp* equals 1.

Scenario 4: *Temp_air* ≥ *Temp_water* and *Energy_ice* > 0

Here, the air temperature is greater than the water temperature (*Temp_air* ≥ *Temp_water*), but ice is also present (*Energy_ice* > 0). A positive *Energy_ice* is equivalent to a non-zero volume of ice, as the two are related through the heat capacity of ice. As before, an equilibrium temperature is calculated between the air and the water to determine the amount of energy that will be transferred: *Excess_energy* = |*Vol_water* * *Heat_capacity_water* * (*Equil_temp* - *Temp_water*)|. The energy difference, plus radiative energy, first goes into melting the existing ice. If all of the energy is used up in this process [*Energy_ice* ≥ *Excess_energy* + (*dRad* * *Rad_ice*)], the ice volume is changed but the water temperature is only affected by the radiance: *Energy_ice* = *Energy_ice* - *Excess_energy* - (*dRad* * *Rad_ice*); *Energy_water* = *Energy_water* + (*dRad* * *Rad_water* * *Ice_damp*). If all the ice is melted and there is still additional energy, the remaining energy and radiative energy goes into warming up the water: *Energy_ice* = 0; *Energy_water* = *Energy_water* + (*Excess_energy* - *Energy_ice*) + (*dRad* * *Rad_water* * *Ice_damp*).

After the appropriate scenario is resolved, the new amounts of energy in the water and ice components are converted to temperatures and volumes, respectively:

Temp_water = *Energy_water* / *Heat_capacity_water*. This is the temperature of the water at the end of the timestep.

Vol_ice = *Energy_ice* / (*Heat_capacity_ice* * *Temp_ice*). This is the volume of ice at the end of the timestep.

Pred_cond = *Vol_ice* * *Cond_coeff1* + *Cond_coeff2*. This is the predicted electrical conductance in the unfrozen water. It is a linear scaling of the ice volume.

Appendix E

Ice Volume Model R Code

```
#Set up model
Temp_air = Air_temp + 273.15 #temp in Kelvin so no negative numbers
Temp_water = Water_temp[1] + 273.15 #initial water temperature, converted to Kelvin
Temp_ice = 273.00 #ice temperature; constant
dRad = c(0, diff(Radiance)) #change in radiance; initial zero is to align time-series (occurs in the dark)

#create summary arrays to fill in during the model run
Energy_air_ts = vector(length=length(Temp_air),mode="numeric")
Energy_water_ts = vector(length=length(Temp_air),mode="numeric")
Energy_ice_ts = vector(length=length(Temp_air),mode="numeric")
Excess_energy_ts = vector(length=length(Temp_air),mode="numeric")
Temp_ice_ts = vector(length=length(Temp_air),mode="numeric")
Temp_water_ts = vector(length=length(Temp_air),mode="numeric")
Vol_ice_ts = vector(length=length(Temp_air),mode="numeric")
Rad_ts = vector(length=length(Temp_air),mode="numeric")
Ice_damp_ts = vector(length=length(Temp_air),mode="numeric")

#Assign model parameters
Heat_capacity_air = .72 #physical constant
Heat_capacity_water = 4.2 #physical constant
Heat_capacity_ice = 2.1 #physical constant
Vol_air = .001 #fixed; relative to water. Based on density difference with water (water = 1)
Vol_ice = .2 #variable; relative to water
Rad_water = 0.0045 #fixed; result of calibration
Rad_ice = 0.0005 #fixed; result of calibration
Ice_damp_coeff1 = 0.197
Ice_damp_coeff2 = 200
Min_energy = (-0.02 + 273.15) * Heat_capacity_water #energy of water when ice forms
Cond_coeff1 = 100 #converts ice volume to electrical conductance
```

```
Cond_coeff2 = -19.15 #converts ice volume to electrical conductance

for (index in 1:length(Temp_air)) { #loop for entire time-series

  #Calculate air, water, and ice energies

  Energy_air = Vol_air * Temp_air[index] * Heat_capacity_air

  Energy_water = Temp_water * Heat_capacity_water

  Energy_ice = Vol_ice * Temp_ice * Heat_capacity_ice

  Equil_temp = ((-Heat_capacity_water * Temp_water) - (Vol_air * Heat_capacity_air * Temp_air[index])) /
  ((-Vol_air * Heat_capacity_air) - (Heat_capacity_water))

  Ice_damp = 1 - ((Vol_ice - Ice_damp_coeff1) * Ice_damp_coeff2) # dampens ability of radiance to heat
  up water based on amount of ice


  #Scenario A: Air energy < Water energy

  if (Temp_air[index] < Temp_water) {#water needs to lose energy


    #Scenario A-1: Air energy < Water energy; water loses energy to ice formation

    if (Energy_water == Min_energy){ #water is at minimum energy level

      #excess water energy goes into ice formation

      Excess_energy = abs(Heat_capacity_water * (Equil_temp - Temp_water))

      Energy_ice = Energy_ice + Excess_energy - (dRad[index] * Rad_ice) #ice formation

      Energy_water = Energy_water + (dRad[index] * Rad_water * Ice_damp)

      #End A-1


      #Scenario A-2: Air energy < Water energy; water needs to lose heat before making ice

    }else{

      Excess_energy = abs(Heat_capacity_water * (Equil_temp - Temp_water))

      Energy_water = Energy_water - (Energy_water - Min_energy) + (dRad[index] * Rad_water *
     Ice_damp) #heat to lose

      Excess_energy = Excess_energy - (Energy_water - Min_energy) #residual heat goes to ice

      Energy_ice = Energy_ice + Excess_energy - (dRad[index] * Rad_ice) #ice formation

    }

    #End A-2
```

```
  #End Scenario A

}else{

  #Scenario B: Air energy > water energy
  #Scenario B-1: Air energy > water energy; no ice to melt
  if (Energy_ice==0) {#no ice volume = no energy; all energy goes into water temp
    Excess_energy = abs(Heat_capacity_water * (Equil_temp - Temp_water))
    Energy_water = Energy_water + Excess_energy + (dRad[index] * Rad_water * Ice_damp)
    #End B-1

  #Scenario B-2: Air energy > water energy; ice present
  }else{
    #melt ice
    Excess_energy = abs(Heat_capacity_water * (Equil_temp - Temp_water))
    if (Energy_ice >= (Excess_energy + (dRad[index] * Rad_ice))) { #all excess energy goes to melting
ice
      Energy_ice = Energy_ice - Excess_energy - (dRad[index] * Rad_ice) #remove ice
      Energy_water = Energy_water + (dRad[index] * Rad_water * Ice_damp)
    }else{ #melt ice then heat water
      Energy_ice = 0 #melt all ice
      Energy_water = Energy_water + (Excess_energy - Energy_ice) + (dRad[index] * Rad_water *
      Ice_damp)  #remainder goes into heating water
    }
  }
  #End B-2

}
#End Scenario B

#Summary
Energy_air_ts[index] = Energy_air
```

```
  Energy_water_ts[index] = Energy_water
  Energy_ice_ts[index] = Energy_ice
  Excess_energy_ts[index] = Excess_energy
  Temp_water = Energy_water / Heat_capacity_water
  Temp_water_ts[index] = Temp_water - 273.15
  Temp_ice_ts[index] = Temp_ice - 273.15
  Vol_ice = ((Energy_ice / (Heat_capacity_ice * Temp_ice)))
  Vol_ice_ts[index] = Vol_ice
  Ice_damp_ts[index] = Ice_damp
}
#End loop

#Ice_vol to Cond conversion
Pred_cond = Vol_ice_ts * Cond_coeff1 + Cond_coeff2
```

Appendix F

Appendix F-1 (Excel file): Raw datasonde and meteorology data

Appendix F-2 (Excel file): Raw flow rates

Appendix F-3 (Excel file): Raw groundwater well depths

Appendix F-4 (Excel file): Raw Milk River area water quality (AEP)

Appendix F-5 (Excel file): Raw Milk River water quality (AAF)

Appendix F-6 (Excel file): Raw St. Mary River water quality

These appendix files can be found as attachments within this PDF document, located under the paperclip icon tab in Adobe Acrobat (see example screenshot below).